# MODEL STUDIES OF OUTFALL SYSTEMS FOR DESALINATION PLANTS

## PART I

## FLUME STUDY OF THE MIXING CHARACTERISTICS OF DENSE JETS DISCHARGED INTO A FLOWING FLUID

Volume I

MAIN TEXT

APPENDIX A: NOTATION

APPENDIX B: CONDUCTIVITY PROBE CALIBRATION AND DATA REDUCTION

August 1971

PREFACE

The experimental investigation reported herein was conducted under Contract 14-30-2656 between the U. S. Department of the Interior and the U. S. Army Corps of Engineers. The study was conducted in the Hydraulics Division of the U. S. Army Engineer Waterways Experiment Station during the period June 1970 to July 1971 under the direction of Mr. E. P. Fortson and Mr. H. B. Simmons, Chiefs of the Hydraulics Division during this period, and Mr. T. E. Murphy, Chief of the Structures Branch. The tests were conducted by SP5 F. M. Holly, Jr., under the supervision of Mr. J. L. Grace, Jr., Chief of the Spillways and Conduits Section. This report was prepared by Messrs. Holly and Grace.

Messrs. Walter Rinne and C. L. Gransee of the Office of Saline Water, Professor R. O. Reid of Texas A&M University, and Dr. M. A. Zeitoun of Dow Chemical Company visited the Waterways Experiment Station during the investigation phase of the study to observe and discuss testing and the application of results.

COL Ernest D. Peixotto, CE, was Director of the Waterways Experiment Station during the conduct of the investigation and the preparation and publication of this report. Mr. F. R. Brown was Technical Director.

# TABLE OF CONTENTS

CONTENTS

v

# LIST OF TABLES

vi

# LIST OF FIGURES

# CONVERSION FACTORS, BRITISH TO METRIC UNITS OF MEASUREMENT

British units of measurement used in this report can be converted to metric units as follows:

| Multiply | By | To Obtain |
|---|---|---|
| inches | 2.54 | centimeters |
| feet | 0.3048 | meters |
| square feet | 0.092903 | square meters |
| cubic feet | 0.02831685 | cubic meters |
| feet per second | 0.3048 | meters per second* |
| cubic feet per second | 0.02831685 | cubic meters per second |
| feet per second per second | 0.3048 | meters per second per second |
| Fahrenheit degrees | 5/9 | Celsius or Kelvin degrees** |
| gallons (U. S.) | 3.785412 | cubic decimeters |
| square feet per second | 0.0930 | square meters per second |

---

\* To obtain velocity in knots, multiply velocity in feet per second (fps) by 1.689.

\*\* To obtain Celsius (C) temperature readings from Fahrenheit (F) readings, use the following formula:  $C = (5/9)(F - 32)$.  To obtain Kelvin (K) readings, use:  $K = (5/9)(F - 32) + 273.15$.

# SECTION I: INTRODUCTION .

## A. The Problem and Purpose of Study

In the planning and design of plants for desalination of salt water, a major consideration is the environmentally acceptable disposal of the waste brine--a warm, dense, highly salt-laden effluent whose concentrations of copper and other metallic ions are considered to be a threat to the marine ecology. Among the several alternatives for disposal of this brine is the economically attractive one of discharging the effluent back into the ocean or estuary from which it was withdrawn. However, a means of mixing the dense liquid with the ambient fluid sufficiently to dilute the concentration of various salts to safe levels is required.

The Office of Saline Water has been funding an ongoing research program through the Dow Chemical Company, in which Dr. M. A. Zeitoun of Dow Chemical Company and Professor R. O. Reid of Texas A&M University have been developing conceptual designs of desalination plant outfall systems and numerical models for prediction of their performance. The purpose of the present study was to utilize a physical model to evaluate the degree of mixing attainable through use of a diffuser located on the estuary floor or the ocean floor beyond the surf zone, from which the dense brine is discharged vertically through circular ports into a uniform and steady crosscurrent.

## B. Approach and Specific Objectives

Experiments at the U. S. Army Engineer Waterways Experiment Station (WES) were conducted in two areas: (1) tests of multiple-port diffusers in three distorted estuary models, to be reported under separate cover as Part II of this report, and (2) tests of single- and multiple-port diffusers at an undistorted scale of 1:20 in a flume having a level bottom and conveying uniform steady flow. The flume tests reported herein involved a study of the separate effects of the following variables on the distribution of brine downstream from a diffuser:

| Variable | Prototype Range |
| --- | --- |
| $U$ = ambient velocity | 0.1 to 1.0 knot |
| $V_o$ = port discharge velocity | 8 to 20 fps |
| $\Delta \rho_m$ = density difference between brine and ambient fluid | 0.0045 to 0.026 g/cc |
| $D_o$ = port diameter | 3, 6, and 9 in. |

Specifically, the objectives were as follows:

    1. To evaluate the effects of the above variables on the maximum

1

height of the upper boundary of an arcing plume, the lateral spread of the plume, and the downstream density distribution.

2. To determine whether single-port results can be superimposed to predict multiple-port mixing.

3. To determine whether or not heated brine has significantly different mixing characteristics as compared with nonheated brine.

4. To evaluate the mixing advantages of a multiple-port diffuser over a simple outfall pipe.

C. Qualitative Description of Jet Plume

While specific characteristics of the dense plumes will be evaluated as part of this report, it appears appropriate at the outset to describe qualitatively the general characteristics of dense jets discharged vertically into uniform ambient flow. At ambient flows only slightly above zero the jet rises nearly vertically in the longitudinal plane, arcing and falling relatively intact. Upon hitting the bottom, the brine forms rings that rapidly expand concentrically upstream and downstream in close proximity to the bottom. The effect appears to be one of gravity waves; any localized buildup of dense liquid on the bottom is unstable and must result in outward spreading to reach equilibrium.

As ambient flow is increased, the gravity wave effect is less dominant; rings form on the bottom and spread rapidly, but tend to move downstream with the ambient flow in distinct waves. At moderate ambient velocities the rings do not appear to form; the plume arcs to a peak, then flows downstream and spreads slightly as it slowly settles to the bottom.

The above discussion is descriptive of totally submerged jets. For cases in which the jet is discharged with sufficient energy to reach the surface, its characteristics are significantly altered. At low ambient velocities the plume boils and spreads concentrically along the surface; highly diluted brine then gradually falls toward the bottom. With higher ambient velocities the jet boils and spreads to an initially lesser degree than it does with low ambient velocities and is swept downstream as it spreads laterally and falls toward the bottom. However, the spread and dilution of a jet that reaches the surface are generally greater than for one totally submerged.

# SECTION II: SUMMARY AND CONCLUSIONS

Nearly 400 tests were run in a 1:20-scale, uniform flow flume to evaluate the effects of port diameter, brine flow rate, density differential, and ambient velocity on the geometry and mixing characteristics of a dense jet discharged vertically through a single port. Geometry data were taken through photographic and visual observations; dilution data were compiled using combined conductivity-temperature probes. The product of the ratio of ambient to port velocities and a port densimetric Froude number has been found to be the significant parameter in all aspects of the problem.

The maximum height of the upper boundary of a jet, $Z_m$, can be predicted with the following equations:

$$\frac{Z_m - D}{D_o} = C \mathbb{F}_D$$

$$C = 3.4 \times 10^{-0.148(U/V_o)\mathbb{F}_D}$$

where

   $D$ = outfall diameter, ft

$D_o$ = port diameter, ft

$\mathbb{F}_D$ = port densimetric Froude number

$U$ = ambient velocity, fps

$V_o$ = port velocity, fps

A correlation of the minimum dilution at a downstream station with relevant dimensionless flow parameters provides for prediction of the maximum concentrations to be expected for a given set of design/operating parameters, according to the following equation:

$$\epsilon_m = \left[ 31 \times 10^{0.4(U/V_o)\mathbb{F}_D} \right] \left( \frac{x}{x_o} \right)^{0.68}$$

where

   $x$ = distance downstream from diffuser, ft

$x_o$ = distance at which plume falls to bottom, ft

$\epsilon_m$ = minimum observed dilution

3

Correlations of lateral plume width with downstream distance led to the following equations for prediction of plume spread:

$$\frac{w}{w_o} = \left(\frac{x}{x_o}\right)^R$$

where

$w$ = total plume width, ft

$w_o$ = plume width at $x = x_o$ , ft

and

$$R = 3.02 \times 10^{-0.26(U/V_o)\mathbb{F}_D} \quad \text{for} \quad x \leq x_o$$

$$R = 0.61 \log_{10}\left(4 \frac{U}{V_o} \mathbb{F}_D\right) \quad \text{for} \quad x > x_o$$

The normalizing quantities $x_o$ and $w_o$ can be predicted by

$$x_o = 9.62 \, Z_m \log_{10}\left(2 \frac{U}{V_o} \mathbb{F}_D\right)$$

$$w_o = 1.51 \, Z_m \log_{10}\left(4.91 \frac{U}{V_o} \mathbb{F}_D\right)$$

Tests using a multiple-port diffuser verified that linear superposition of single-port results can be used to predict multiple-port mixing characteristics. Tests using heated brine indicated that the presence of a temperature differential of up to 10°C between the brine and ambient fluid has no significant effect on the plume mixing characteristics. A multiple-port diffuser was found to have a significant advantage over a simple outfall pipe in keeping high concentrations of dissolved metallic ions away from the ocean floor.

# SECTION III:  DESCRIPTION OF TEST FACILITY

## A.  Flume

In choosing a scale for the laboratory model, it was important to en-
sure that Reynolds numbers were kept high enough so that the flows could be
considered fully turbulent, as in prototype situations.  A 1:20 scale of
model to prototype was chosen and similitude based upon the Froudian cri-
terion dictates the following correspondence between geometric and kine-
matic parameters of the two systems:

|  | Prototype | Model |
|---|---|---|
| Length | 20 | 1 |
| Area | 400 | 1 |
| Volume | 8000 | 1 |
| Time | 4.4721 | 1 |
| Velocity | 4.4721 | 1 |
| Discharge | 1788.840 | 1 |
| $\mathbb{R}_p$ | $1.7 \times 10^5$ | $1.9 \times 10^3$ |
| $\mathbb{R}_c$ | $5.6 \times 10^5$ | $6.3 \times 10^3$ |

where

$$\mathbb{R}_p = \frac{V_o D_o}{\nu} \, , \ \mathbb{R}_c = \frac{UH}{\nu}$$

$\mathbb{R}_p$  = port Reynolds number

$\mathbb{R}_c$  = channel Reynolds number

$V_o$  = port discharge velocity

$D_o$  = port diameter

$\nu$  = kinematic viscosity of water

$U$  = ambient flow velocity

$H$  = ambient flow depth (40 ft used)

The above Reynolds numbers are representative of the minimum values simu-
lated and indicate that all flow situations investigated were of the fully
developed turbulent type.  At a scale of 1:20 the model reproduces a

5

section of level ocean floor 140 ft wide and 600 ft long, with a maximum water depth of 40 ft. Figs. 1 and 2 are photographs of the flume. The flume bottom was surrounded by 6- by 6-in. gutters that trapped dense fluid before it reflected off the flume walls. A sump area at the elevation of the gutters and a cutoff wall extending across the downstream end of the flume were built to provide an area from which excess brine could be pumped back into holding tanks. It was found during preliminary testing that it was impractical to reclaim the diluted brine, and the cutoff wall was removed. Water-surface elevations were regulated by means of a downstream gate. One wall of the flume was constructed of transparent plastic (1/2 in. and 3/4 in. thick) mounted in a wooden frame to provide for visual observations of dispersion throughout the full length of the flume. The opposite masonry wall was finished with plaster. The flume bottom was a smooth-troweled concrete slab with two coats of glossy white epoxy paint; 1.0-ft grids were painted on both vertical walls as well as on the bottom of the flume.

The experimental work reported by Dow Chemical Company[1] verified that in modeling a dense discharge it is the density difference between the effluent and the ambient fluid, rather than the overall level of density, which is important. Therefore, the WES flume was provided with a recirculating freshwater system to model the ocean current. Fresh water supplied by pumps and a constant head tank was discharged through either a 20- or a 6-in. supply line into an 8-ft-wide forebay that was separated from the main flume by flow-straightening tiles and a rock baffle. Venturi tubes on the two supply lines provided for accurate measurement of model discharges that ranged from 0.2 to 14 cfs.

## B. Brine Supply System

Two 8- by 7- by 3-ft tanks (fig. 2) were used to prepare and store brine solutions; sump pumps on the tank floor kept the solutions well mixed. Two 8-gpm centrifugal pumps with stainless steel rotors pumped from either tank through either of two Rotameters or a 1- by 1/2-in. venturi. A 2- by 2- by 1-ft tank with a point gage attached was used to calibrate volumetrically the venturi and Rotameters for model discharges ranging from 0.00014 to 0.012 cfs. The various calibrations were found to be essentially independent of the small brine density variations expected. All brine piping was 1-in. copper tubing with appropriate reducers for the pumps and Rotameters.

The model diffuser consisted of a length of pipe extending across the full width of the flume at sta 0+00. A threaded connection permitted installation of a number of different diffusers with discharge ports drilled vertically at the flume center line for most cases.

## C. Flume Velocity Distribution

Velocity measurements were made in the flume to establish the degree of uniform flow obtained. Fig. 3 is a plot of velocity contours, looking
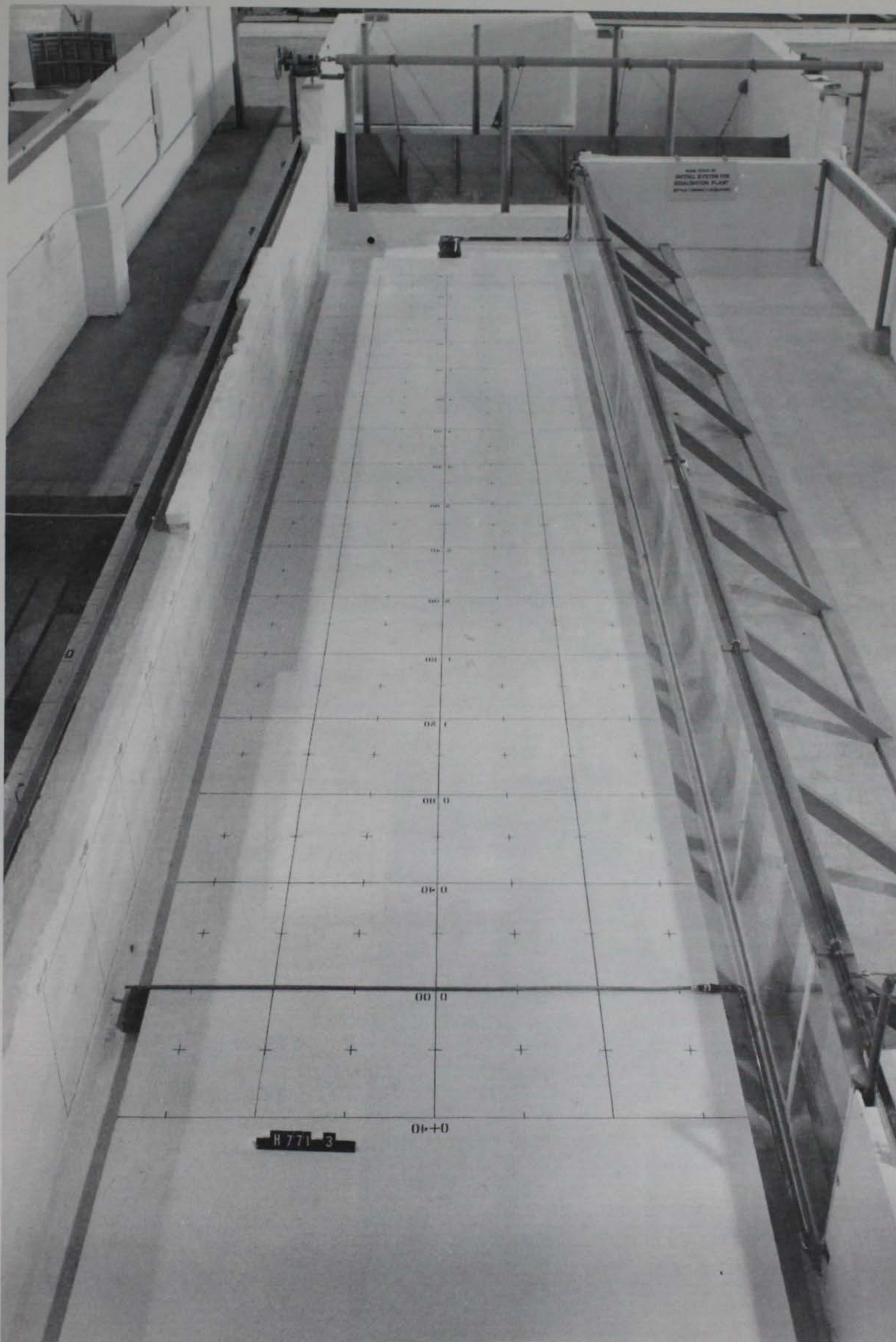
Fig. 1.  Uniform flow flume (looking downstream)
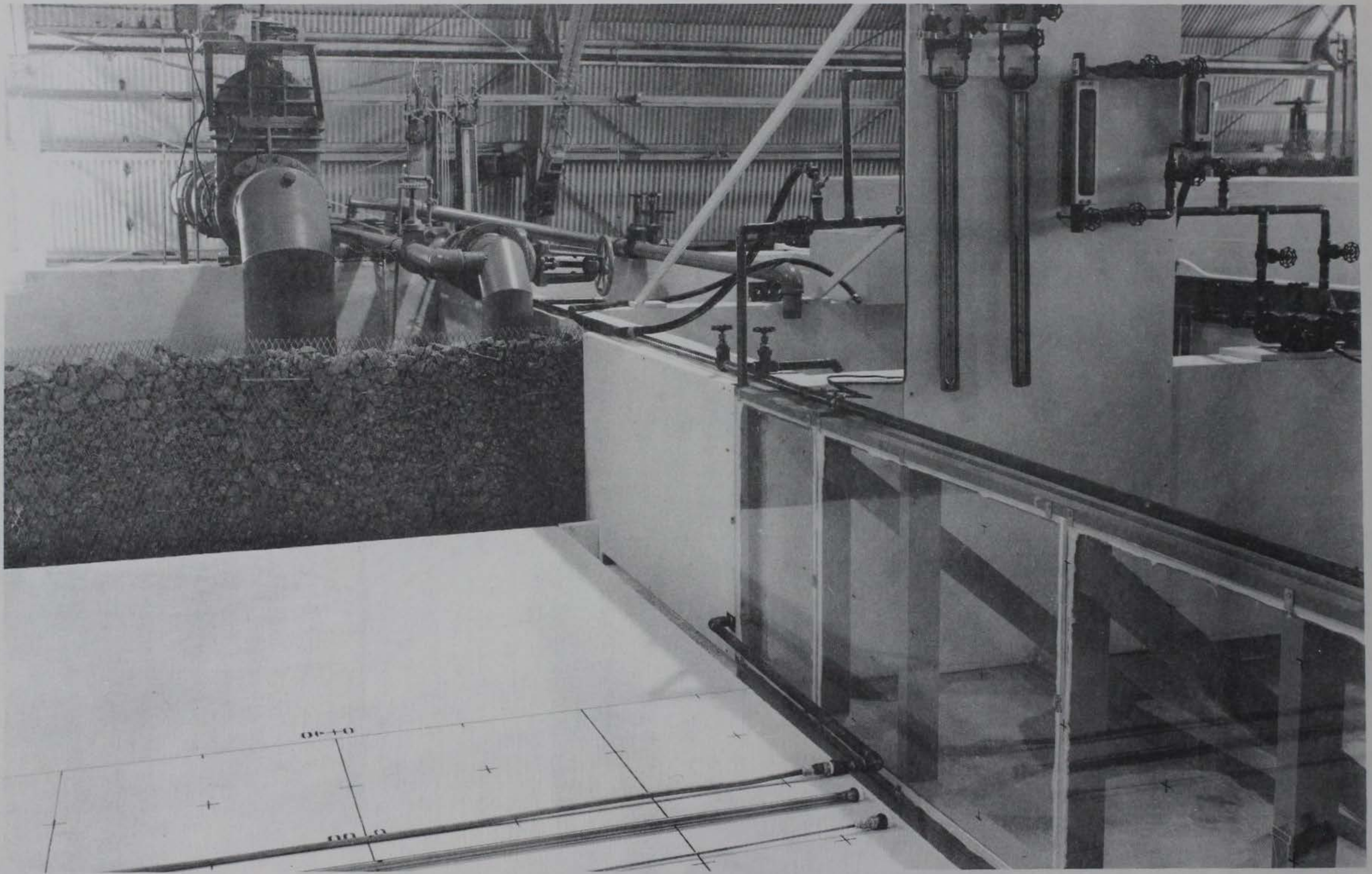
Fig. 2. Flume forebay and brine supply system (looking upstream)
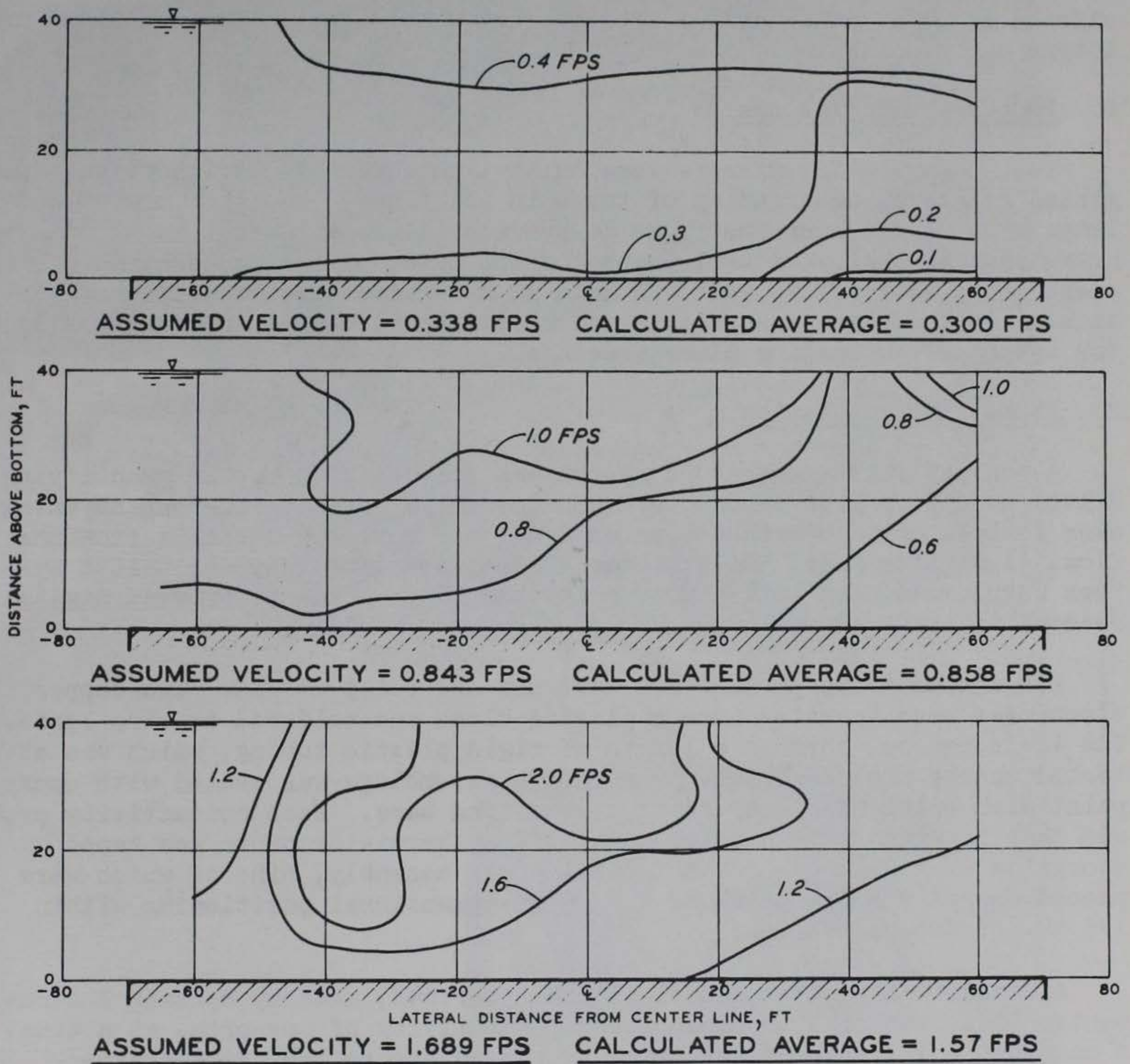
Fig. 3. Prototype velocity contours in flume (looking upstream) at x = -36 ft

upstream, determined at sta 0-36 (prototype) for assumed ambient velocities of 0.2, 0.5, and 1.0 knot (prototype). The irregular rock baffle, along with the nonsymmetrical water-supply situation, is responsible for the non-uniformity of the flow. However, the averaged velocity measurements agree well with the assumed velocities based on a discharge divided by cross-sectional area calculation; the deviations from uniform flow are not considered to be significantly different from what might be expected in a prototype ocean situation.

## D.  Photograph Provisions

Two 30- by 40-in. mirrors were built into a movable periscope that permitted eye-level observation of tests in the flume. Banks of photoflood lamps were placed over the flume to provide illumination for two 16-mm movie cameras that were used to photograph brine plumes through the periscope and plastic flume wall. A grid of known dimensions was placed vertically on the flume center line and photographed during initial testing for later use in scaling plume tracings.

## E.  Flume Instrumentation

A conductivity-temperature system was selected for use in quantifying dilution; the in situ probes were considered to have an inherent advantage over fluorescent dye methods, which require removal of a sample from the flow. A Digitec Model 501-N Digital Thermometer, made by the United Systems Corp., was used with remote probes on 50-ft leads to provide digital readout in degrees Centigrade.

The conductivity probes were designed and built at WES. Two copper electrodes were inserted into a plastic block and soldered to wire leads. The leads ran out through a length of rigid plastic tubing, which was attached to the plastic block. The entire assemblage was sealed with epoxy paint with only the electrode tips remaining bare. Each conductivity probe was then inserted into a point gage, and a thermistor probe was taped alongside it. Fig. 4 shows a typical probe assembly, nine of which were placed on rails over the flume for three-dimensional positioning within 1/2 in. of the boundaries.

A Conductivity Meter, Model R13x10-S58-P164K, made by Beckman Instruments, Inc., was used to measure the conductivity of one probe at a time. A constant resistance of 527 ohms was placed across the temperature-compensating circuit of the instrument and a 0-100 thousand ohm potentiometer was added to its bridge circuit so that the conductivity range could be varied. A 0- to 100-mv digital voltmeter and chart recorder were driven by a linearizing circuit in the conductivity meter, providing a linear record of conductivity variations. As testing proceeded it was necessary to add a so-called integrating circuit in which a capacitor accumulates voltage proportional to conductivity so that a time-averaged conductivity could be obtained.
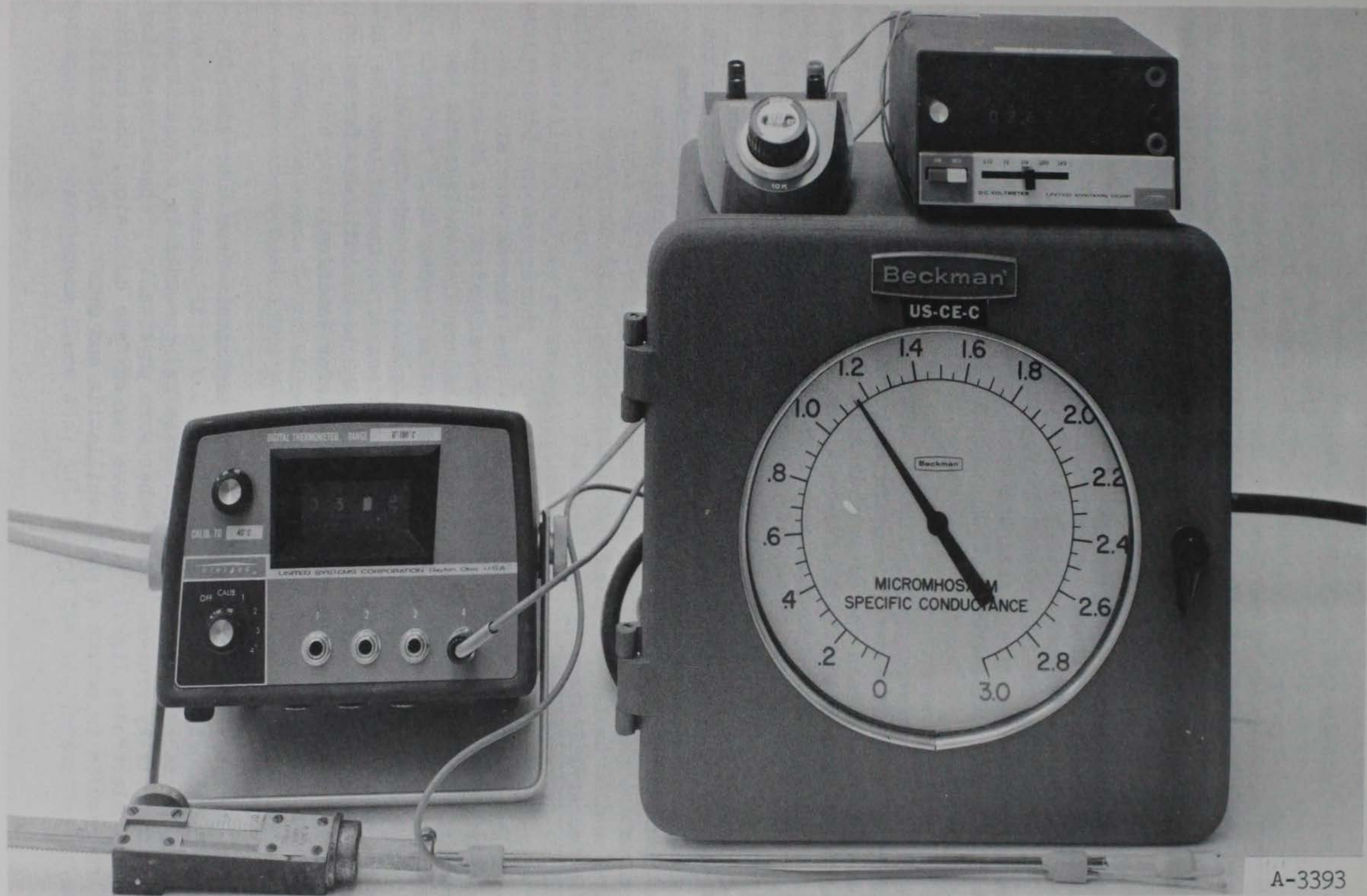
A-3393

Fig. 4. Conductivity-temperature probe assembly and readout

SECTION IV.  PROGRAM AND PROCEDURE OF TESTS

## A.  General

During preliminary tests it was noted that the vertical jets tended to
lean considerably in the same direction as flow in the diffuser section of
the outfall.  This leaning was caused by relatively high velocities in the
diffuser and was reduced by increasing the outfall diameter.  The final
prototype outfall diameters of 20, 20, and 30 in. for the 3-, 6-, and 9-in.
ports, respectively, minimized plume lean to the point that the height of
the jets was not significantly affected, though the plume center line still
deviated to the positive side (left side looking downstream) of the flume
axis.  While it was desirable to minimize plume lean in the model so that
the analysis would be more straightforward, this lean could be an asset in
a prototype situation where the longer plume arc length could increase
overall mixing.

Brine solutions were prepared identically for both jet geometry and
dilution tests.  Sufficient fine-grain salt was dissolved in about 120 ft$^3$
of fresh water to attain the desired density differential between the brine
effluent and the ambient fresh water.  A red food coloring was then added
in sufficient quantities to give even the diluted brine a discernible color
contrast with the ambient flow.  After repeated density checks with hydrom-
eters indicated that the salt had dissolved completely, the brine was
pumped through the appropriate Rotameter or venturi and into the outfall
and diffuser.  When visual observations indicated that a steady-state con-
dition had been reached, tests were initiated.  Ambient and brine flow
rates were checked frequently during tests to maintain steady-state
conditions.

## B.  Jet Geometry Tests

Either one or two movie cameras were used to photograph the brine plume
in the vertical plane through the periscope.  The cameras were aimed at
points 17 ft (prototype) above the flume floor, and at points 20 and 100 ft
downstream.  After a steady-state condition had been established in the
flume, the camera(s) were turned on for approximately 10 sec.  A visual
sketch of the plan view spreading of the brine was then made from above the
flume for about half the tests.  Flow conditions were changed, and the en-
tire procedure was repeated.  Table 1 shows the test conditions for which
jet geometry data were taken (see Appendix A for Notation).

## C.  Dilution Tests

Tests for downstream dilution were run separately from those for jet
geometry, although tests having identical flow conditions were given the
same number.  Each series of dilution tests was preceded by a recalibration
of the conductivity probes.  The probes were physically prepared by filing
the copper electrodes lightly to remove any surface corrosion, the buildup
of which results in output signal oscillation and drift.  The adjustable
bridge potentiometer was set to a value that would accommodate the expected

12

range of conductivity. Several (three or more) calibration solutions were prepared, the first of which was pure ambient fresh water and the others were fresh water with enough brine solution added to give a range of conductivity readings up to full scale. Each probe to be used was dipped into each solution, and the temperature and conductivity were recorded. Later, the solution densities were determined on a specific gravity balance, and the corresponding temperature was again recorded. The procedure for reducing these calibrations is discussed in Appendix B.

The objective of the far-field dilution testing was to quantify the three-dimensional mixing patterns for a given operating condition from the peak of the dense plume to the downstream point where the brine spread laterally to the walls of the flume. Accordingly, conductivity-temperature probes were positioned at a number of downstream stations and detailed vertical profiles of conductivity and temperature were taken at each location with one probe at a time. Each conductivity-temperature measurement consisted of the following steps: (1) chart recorder turned on, stopwatch and integrating circuit simultaneously started; (2) temperature recorded; (3) stopwatch and integrating circuit simultaneously stopped; (4) chart recorder turned off; (5) integrating circuit voltage divided by run time and multiplied by calibration factor to get time-averaged conductivity; (6) maximum and minimum conductivity read from recorder; (7) all instruments zeroed for the next test. The ambient freshwater conductivity was also recorded for each probe as it was being used.

The basic dilution testing was conducted using a 6-in. prototype port with a density difference of about 0.021 g/cc. A few spot checks were made using an 0.01 g/cc differential, and several tests were conducted with 3- and 9-in. ports at 0.021 g/cc. A multiple-port, 20-in.-diam outfall and diffuser, with four 6-in. ports spaced at 13 ft, was tested with a density differential of 0.021 g/cc, and a 20-in.-diam simple outfall discharging horizontally with flow rates equivalent to that of the four-port diffuser was tested for comparison.

A limited test using heated brine was conducted to determine whether or not the temperature differential itself was an important factor influencing mixing. Two large space heaters were placed next to a 55-gal drum in which a brine solution was prepared. A temperature probe was installed inside a 20-in.-diam diffuser at the 6-in. port. The brine density in the heated drum was adjusted to maintain approximately an 0.021 g/cc density differential at the port. Limited downstream conductivity-temperature measurements were made, the brine temperature ranging from 4.5 to 9.4°C above the ambient temperature during the brief test.

Flow rates were checked frequently, and a visual sketch of the lateral brine spread was made for each test. Table 2 shows the dilution tests conducted. Fig. 5 presents typical plume characteristics as determined in a given test.

13
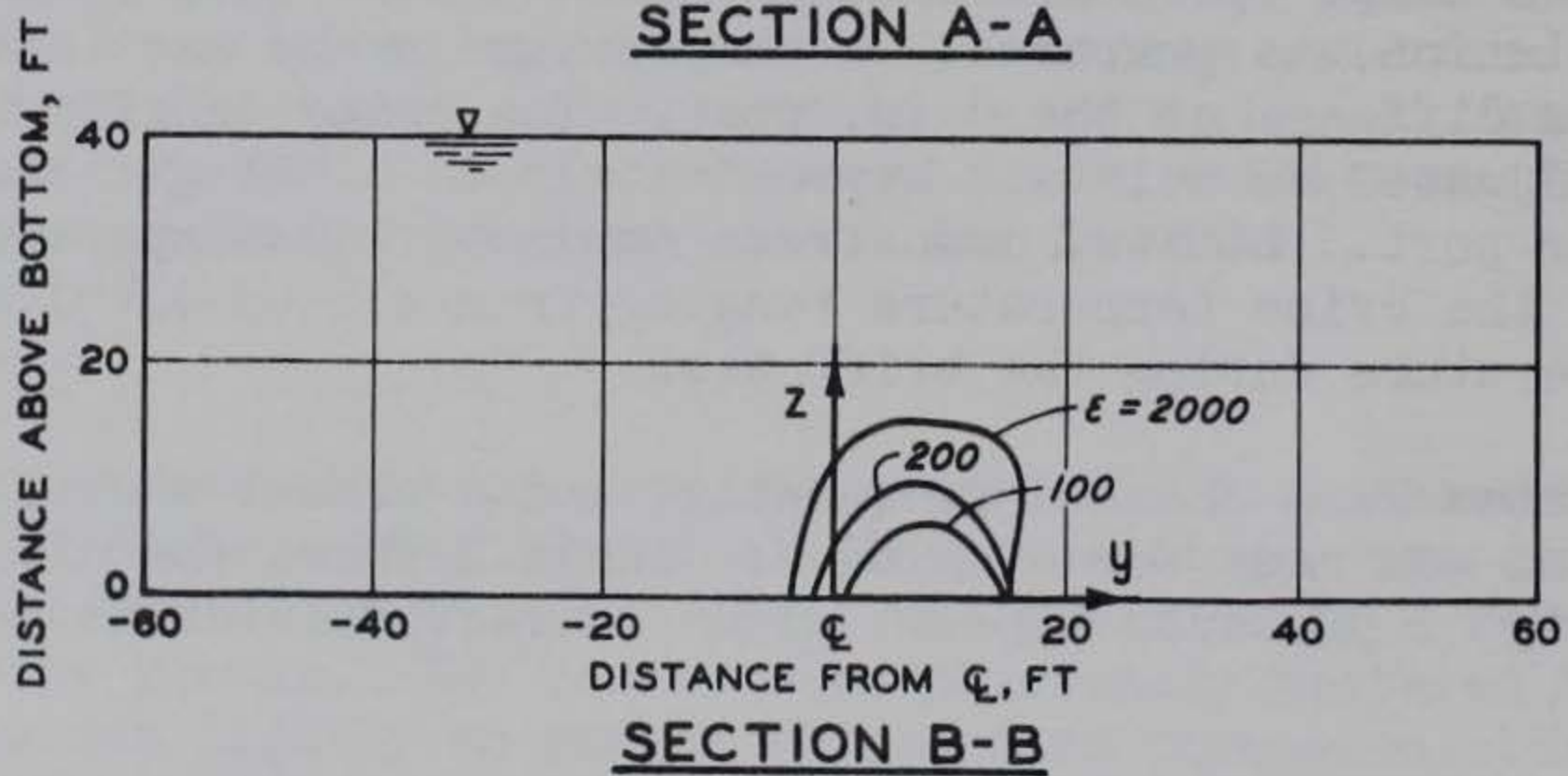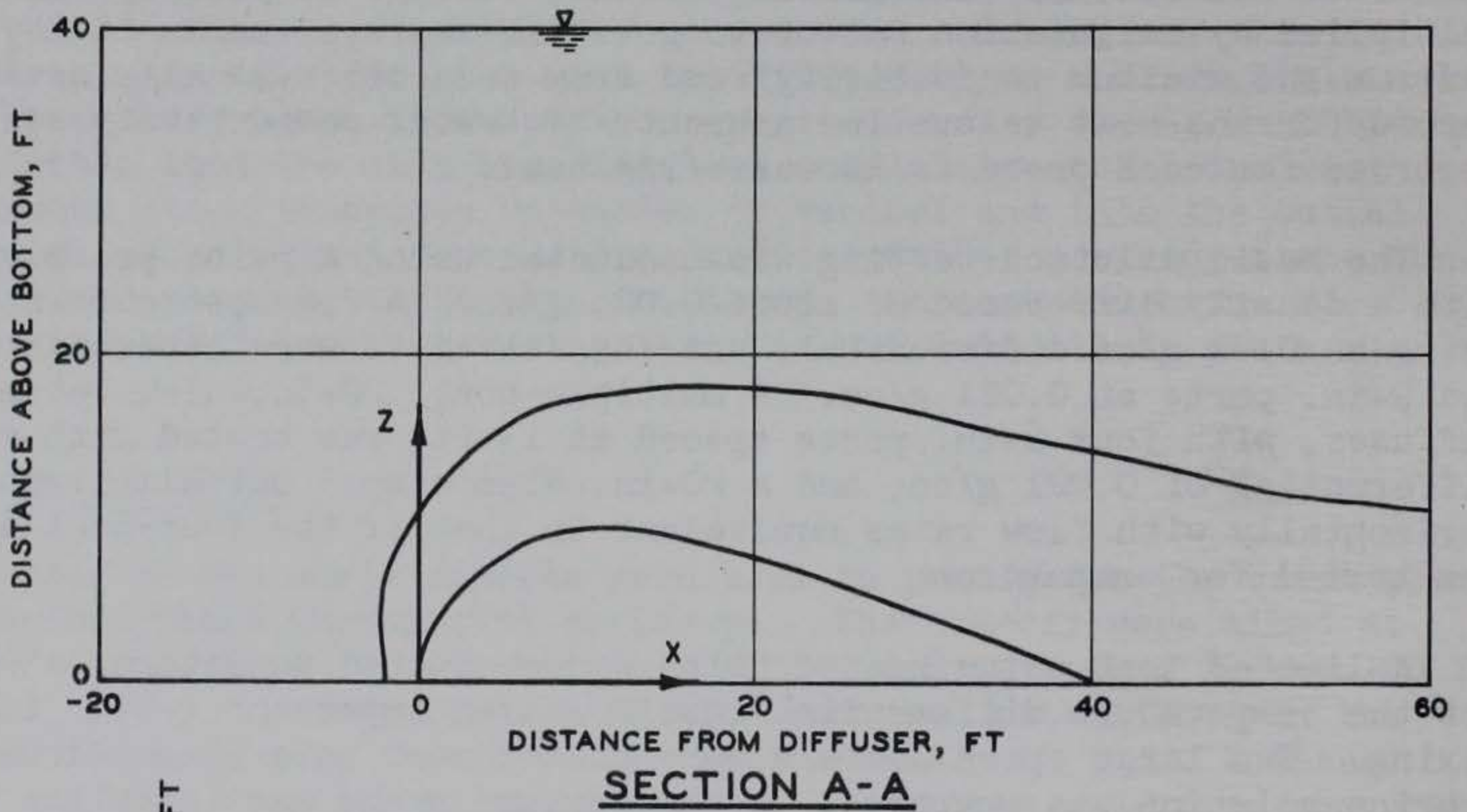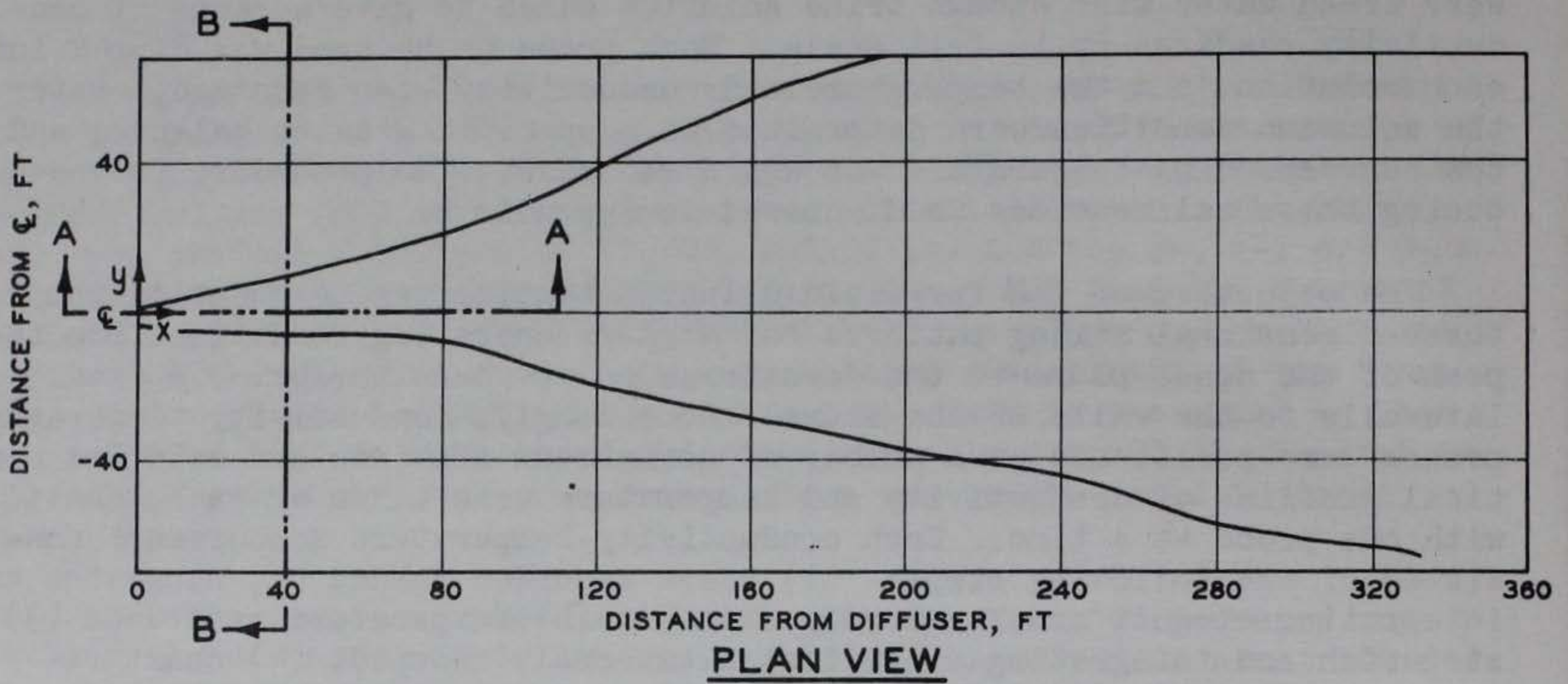
Fig. 5. Typical plume characteristics (test 639)

# SECTION V: DATA REDUCTION AND ANALYSIS

## A. Maximum Height of Jet

The movie of a grid of known dimensions photographed at the flume center line was projected onto graph paper and the distance of the projector from the paper adjusted so that the scale of jet tracings would be 1 in. to 10 ft prototype. The scale is exact only at the center of the frame; distortion increases toward the edges of the film. Movies of colored brine plumes were projected onto graph paper, and the projector was stopped periodically so that average tracings of the shape of a plume could be made as far downstream as the color contrast permitted. A typical profile is shown in fig. 5. Appendix C (under separate cover) contains the original tracings acquired in this manner, to a scale of one major division = 10 ft prototype. Due to distortion, the apparent plume origin does not coincide with the grid origin exactly.

From each plume tracing, $Z_m$, the maximum height of the upper boundary of the jet, was noted and recorded (see table 1). In cases where no distinct peak was evident, the height of the upper boundary directly above the point where the lower plume boundary peaked was taken as $Z_m$.

During testing, it was noted that for equivalent flow conditions, the maximum height of the plume increased as the port diameter was increased. This is explained as follows. Upon its discharge from a port, the plume consists essentially of a uniform, undiluted core of constant velocity that is eroded by turbulent mixing with the ambient fluid until the turbulence has progressed all the way to the center of the plume. The undisturbed central core is being decelerated only by a modified gravity force, while the outer turbulent regions are primarily being slowed by momentum exchange with the ambient fluid. Thus, the maximum height of a plume is related to the distance required for the turbulent erosion to spread into the central core, this distance being greater for a thick jet than for a thin one.

Keffer and Baines[2] found in studies of a turbulent neutrally buoyant air jet perpendicular to an ambient stream that a significant parameter was the ratio of the initial jet velocity to the free stream velocity. For a dense jet it is reasonable to expect that the density difference between the jet and the ambient fluid will affect the trajectory to some degree before the plume reaches a peak, and significantly thereafter. Studies conducted by Dow Chemical Company[1] determined that for dense jets discharging at various angles into a still fluid the normalized maximum jet height is a linear function of densimetric port Froude number. Therefore, in attempting to develop an equation for the prediction of the maximum jet height, it was assumed that

$$\frac{Z_m}{D_o} = f\left(\frac{V_o}{U}, \; \mathbb{F}_D, \; \frac{\Delta\rho_m}{\rho_f}\right) \tag{1}$$

15

where

$Z_m$ = maximum height of upper boundary of the plume

$D_o$ = port diameter

$U$ = free stream velocity

$V_o$ = initial port discharge velocity

$\mathbb{F}_D$ = densimetric port Froude number, $\dfrac{V_o}{\sqrt{\dfrac{\Delta \rho_m}{\rho_f} g D_o}}$

$\Delta \rho_m$ = initial density differential between brine and ambient fluid

$\rho_f$ = density of ambient fluid

Correlations of (1) $Z_m/D_o$ versus $\mathbb{F}_D$ for constant $V_o/U$, (2) $Z_m/D_o$ versus $V_o/U$ for constant $\mathbb{F}_D$, and (3) $Z_m/D_o$ versus $V_o/U$ for constant $\Delta \rho_m/\rho_f$ all yielded equations for $Z_m/D_o$ that satisfied most of the data but appeared to be invalid at the lower ambient velocities. This indicated that the separate effects of the dimensionless variables were being neither fully isolated nor accounted for over the entire range of flow conditions. This conclusion was confirmed by visual observations of erosion and dispersion of the jets. The dispersion in the near field appeared to be predominantly influenced by the turbulence of the jet itself or densimetric Froude number (though admittedly the pressure field and turbulence of the flowing fluid are pertinent to near-field jet dispersion), while the far-field dispersion can be primarily attributed to the relative intensity of turbulence in the far-field plume, or density current, and that of the ambient channel flow. This relative turbulence is considered to be related to the ratio of ambient to port velocities, $U/V_o$. Therefore, it was decided that analysis of data would be made in a manner such that correlation of the interrelations of $U/V_o$ and $\mathbb{F}_D$ would be included in an empirical coefficient much as the frictional and form drag components are represented by an empirically determined drag coefficient.

At a conference on the study, Professor R. O. Reid of Texas A&M University indicated that Fan[3] had found the product $(U/V_o)\mathbb{F}_D$ to be a significant parameter. Least-squares correlations of $Z_m/D_o$ versus $\mathbb{F}_D$ were made at WES for constant values of $(U/V_o)\mathbb{F}_D$, resulting in equations of the form

$$\frac{Z_m}{D_o} = C\mathbb{F}_D + B \tag{2}$$

where $B$ is a random intercept whose mean value is essentially zero and

16

$$C = \emptyset \left( \frac{U}{V_o} \mathbb{F}_D \right) \tag{3}$$

A plot of the predicted versus observed $Z_m/D_o$ values indicated that the prediction equation was valid over the entire range of variables. The scatter was improved somewhat by accounting for the outfall diameter, $D$, which as reproduced in the model had the effect of elevating the entire jet a small amount. Thus $Z_m/D_o$ was replaced by $(Z_m - D)/D_o$, and least-squares correlations of $(Z_m - D)/D_o$ versus $\mathbb{F}_D$ for constant $(U/V_o)\mathbb{F}_D$ were repeated, leading to the following equation:

$$\frac{Z_m - D}{D_o} = C\mathbb{F}_D \tag{4}$$

$$C = 3.4 \times 10^{-0.148(U/V_o)\mathbb{F}_D} \tag{5}$$

$$Z_m \leq H \tag{6}$$

Fig. 6 is a plot of actual versus predicted values of $(Z_m - D)/D_o$.

B. Lateral Spread of Jet

Superposition of single-port dilution results to predict multiple-port characteristics requires prediction of the lateral spread of the plume. As discussed in the previous section, visual sketches of the lateral spread of the dense effluent were made for approximately half of the jet geometry tests. From these sketches, $w$, the observed horizontal width of the plume irrespective of the plume center line, was measured and recorded along with $x$, the corresponding downstream distance from the diffuser. These selected sets of coordinates, the number of which is determined by the downstream length required for the brine to spread to the edges of the flume floor for each test, are given in table 3.

The lateral spread can generally be divided into two regions: (1) before the arcing plume has settled to the bottom, and (2) after this point, when spread is generally more rapid. For a single test, $w$ correlates linearly with $x$ for each region as defined above. The slopes and intercepts of these correlations were related to the ambient velocity, port velocity, etc.

In attempting to develop a method for prediction of the lateral spread, three general approaches were considered and are briefly described as follows:

(1) Compute the least-squares slopes and intercepts of individual
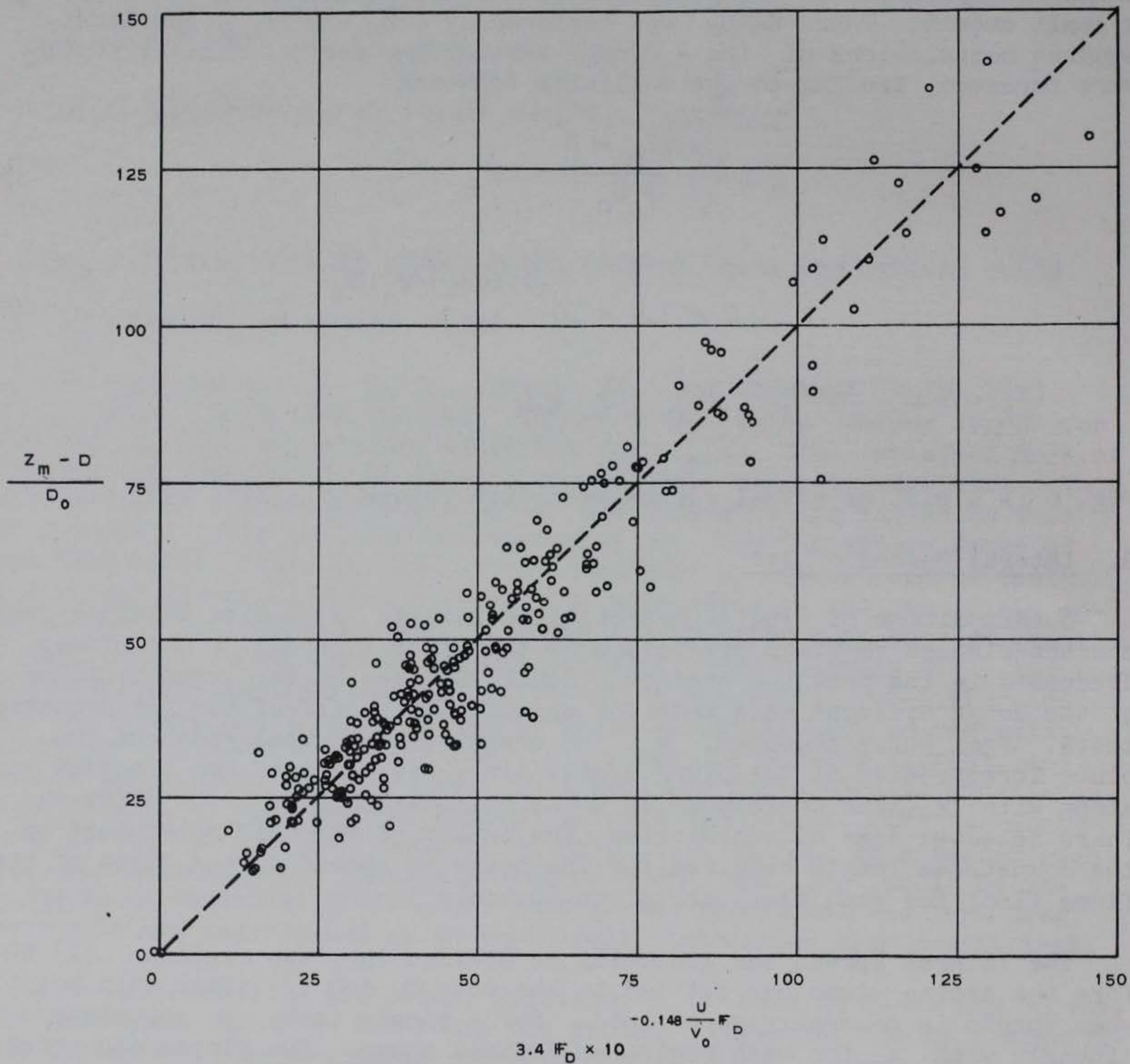
Fig. 6. Actual versus predicted values of dimensionless jet height according to equation 4

linear correlations of $w/D_O$ versus $x/D_O$ for each region. Determine their functional dependence on the relevant flow parameters.

(2) Normalize $w$ and $x$ by $D_O(V_O^2/U^2)$ as suggested by Keffer and Baines.[2] Relate $wU^2/D_O V_O^2$ to $xU^2/D_O V_O^2$ in terms of relevant flow parameters.

(3) Defining $x_O$ and $w_O$ as the downstream distance at which the plume falls to the bottom and its width at that point, respectively, determine $x_O$ and $w_O$ as functions of $F_D$, $Z_m/D_O$, and $(U/V_O)F_D$. Then correlate $x/x_O$ with $w/w_O$ in terms of other flow parameters for both regions.

Approach 1 above yielded fair estimates of the lateral spread, but with enough systematic deviations from a perfect prediction to warrant a different approach. The success with which a modified Froude number, $(U/V_O)F_D$, was used to predict the maximum jet height indicated that approach 3 was worthy of consideration.

Use of this approach first requires a means of predicting $x_O$ and $w_O$. For roughly 100 of the lateral spread sketches, $x_O$ could be approximated by the downstream distance at which the initial linear rate of spread changed to a more rapid rate. This point was often difficult to define, especially for the higher ambient velocities; all values thus determined were checked against the corresponding plume trajectory sketches (Appendix C) and a few unreasonable values revised. Values of $w_O$, the total width of the plume at $x_O$, were concurrently recorded.

Following the general approach of the maximum jet height correlations, $x_O/D_O$ was correlated with $F_D$ for constant values of $(U/V_O)F_D$. Individual log-log correlations were reasonably good, but their slopes and intercepts could not be correlated consistently with $(U/V_O)F_D$. A more successful correlation resulted from linear plots of $x_O/D_O$ and $Z_m/D_O$ for constant $(U/V_O)F_D$, where $Z_m/D_O$ has been assumed nearly equal to $(Z_m - D)/D_O$. Forcing these correlations to pass through the origin (assuming $x_O = 0$ when $Z_m = 0$), their slopes were found to be a logarithmic function of $(U/V_O)F_D$. An identical procedure was used for $w_O/D_O$, and the following empirical equations resulted:

$$\frac{x_O}{D_O} = 9.62 \, \log_{10}\left(2\, \frac{U}{V_O}\, F_D\right)\frac{Z_m}{D_O} \tag{7}$$

$$\frac{w_O}{D_O} = 1.51 \, \log_{10}\left(4.91\, \frac{U}{V_O}\, F_D\right)\frac{Z_m}{D_O} \tag{8}$$

Having developed a means of predicting $x_O$ and $w_O$, the relation between $x/x_O$ and $w/w_O$ could now be investigated. The coordinates of

19

total spread, as included in table 3, were divided by predicted values of $x_o$ and $w_o$ for each of the 187 tests for which sketches were made, and $x/x_o$ was plotted against $w/w_o$ for constant values of $(U/V_o)F_D$. Least-squares linear fits of these log-log correlations (which by definition passed through $x/x_o = 1.0$, $w/w_o = 1.0$) clearly indicated an increase in rates of spread when $x/x_o > 1$, as was suggested by qualitative observations. The rates of spread were found to be an exponential function of $(U/V_o)F_D$ for $x \leq x_o$, and a logarithmic function for $x > x_o$. Thus

$$\frac{w}{w_o} = \left(\frac{x}{x_o}\right)^R \tag{9}$$

where

$$R = 3.02 \times 10^{-0.26(U/V_o)F_D} \quad \text{for } x \leq x_o \tag{10}$$

and

$$R = 0.61 \log_{10}\left(4 \frac{U}{V_o} F_D\right) \quad \text{for } x > x_o \tag{11}$$

Fig. 7 is a plot of observed values of $w/w_o$ versus the values predicted using equations 7-11. Although there is a broad band of scatter due to errors in visually sketching the lateral spread and subjectively determining $x_o$ and $w_o$, the overall trend indicates a valid prediction over the entire spread regime.

C.  Dilution for Single-Port Tests

A convenient dimensionless representation of mixing is dilution, defined as

$$\epsilon = \Delta \rho_m / \Delta \rho$$

where

$\Delta \rho_m = \rho_b - \rho_f$

$\Delta \rho = \rho - \rho_f$

$\rho_b$ = initial brine density, g/cc

$\rho_f$ = ambient density, g/cc

$\rho$ = density at some point in the far-field mixing region, g/cc

20
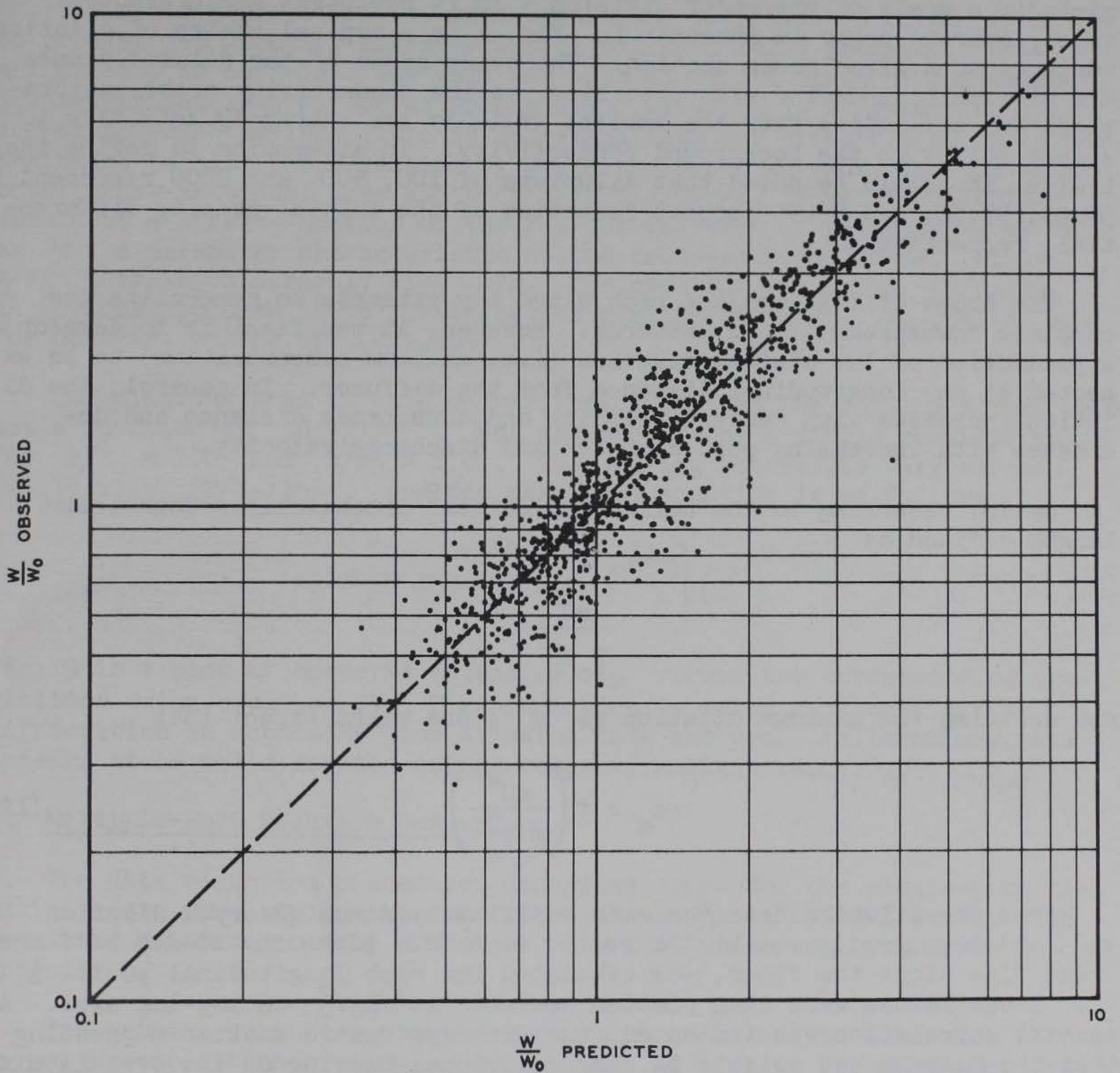
Fig. 7. Observed values of dimensionless plume width versus values
predicted by equations 7-11

As defined above, the dilution of pure unmixed brine is 1.0 and that of undisturbed ambient fluid is infinity. The FORTRAN program described in Appendix B was used to calibrate the conductivity probes and to compute dilution values corresponding to minimum, average, and maximum conductivity readings at a point. Table 2 is a list of dilution test conditions. Average dilution values have been plotted at each longitudinal station for each test, and contours of constant dilution have been sketched. The resulting plots to a scale of one major division = 20 ft prototype are presented under separate cover in Appendix D. Fig. 5 is a typical sketch of dilution contours at a given cross section. The outer edges of the diluted plumes are difficult to define with precision, as the conductivity probe calibrations for salinities near the ambient salinity are extremely sensitive to slight shifts in the background conductivity. In attempting to define the limits, it should be noted that dilutions of 100, 500, and 2000 represent a 99.00, 99.80, and 99.95 percent reduction of the initial density differential, respectively.

The scope of this project prohibited any attempts to generalize the complete downstream mixing patterns. However, it was feasible to develop a prediction of the minimum dilution (i.e. maximum concentration) to be expected at any longitudinal distance from the diffuser. In general, the dilution increases with ambient velocity and downstream distance and decreases with increasing port diameter and discharge velocity.

Again, referring to the Keffer and Baines[2] dimensionless downstream length defined as

$$\frac{xU^2}{D_o V_o^2}$$

and defining the minimum dilution as $\epsilon_m$ , one might expect that

$$\epsilon_m = f\left(\frac{xU^2}{D_o V_o^2}\right) \tag{12}$$

From the dilution data for each test, the minimum observed dilution $\epsilon_m$ , which generally was at the center of a free plume and at the bottom of brine flow along the floor, was tabulated for each longitudinal position $x$ . These values were then plotted against $xU^2/D_o V_o^2$ on log-log axes. A general correlation was indicated, but with systematic scatter suggesting that the maximum jet height $Z_m$ had additional bearing on the overall mixing. A second correlation using $\epsilon_m/(Z_m/D_o)$ in place of $\epsilon_m$ diminished the systematic scatter, and a final log-log plot of

$$\frac{\epsilon_m}{(Z_m/D_o)^2} \quad \text{versus} \quad \frac{xU^2}{D_o V_o^2} \tag{13}$$

22

displayed good overall correlation with random scatter (fig. 8). The data for ambient velocity of 0.1 knot tended to correlate separately from the data for all other ambient velocities. The scatter in fig. 8 is due to small errors in the calibration and data reduction procedure as well as to the likelihood of "missing" a true minimum dilution which fell between discrete vertical or horizontal sampling points.

The above correlation was made before the potential of using $(U/V_o)\mathbb{F}_D$ to predict jet geometry characteristics had been fully realized. Thus a new attempt to correlate the data was made along the lines of the maximum jet height and lateral spread approaches. Dilution is a measure of the degree to which ambient fluid is entrained into the brine plume. This entrainment is also the mechanism by which the plume spreads, increasing its total cross-sectional area and effective discharge. Thus the dilution should be a direct function of the rate of increase of plume area, as well as $w$, a parameter characteristic of the cross-sectional area. Since $w/w_o$ correlated directly with $x/x_o$ for constant values of $(U/V_o)\mathbb{F}_D$, an obvious approach is to correlate the minimum dilution, $\epsilon_m$, with $x/x_o$ for constant values of $(U/V_o)\mathbb{F}_D$.

Correlations made in this manner indicated that the log-log slopes were not a function of $(U/V_o)\mathbb{F}_D$, but appeared to be a single constant value for $x/x_o \leq 1.0$ and $x/x_o > 1.0$. The log-log intercepts vary exponentially with $(U/V_o)\mathbb{F}_D$, and the resulting equation is as follows:

$$\epsilon_m = \left[31.0 \times 10^{0.4(U/V_o)\mathbb{F}_D}\right]\left(\frac{x}{x_o}\right)^{0.68} \tag{14}$$

Fig. 9 is a plot of observed values of $\epsilon_m$ versus the corresponding predictions using equation 14. The prediction is quite good considering the difficulties in obtaining good dilution data and probe calibrations, and appears to be valid for the entire range of ambient velocity.

D. Multiple-Port Dilution Comparison

The data reduction procedures described above for the single-port dilution tests were applied to the five multiple-port diffuser tests. The resulting dilution contour plots are presented under separate cover in Appendix D.

The primary purpose of the multiple-port tests was to determine whether or not superposition of single-port results is a valid technique for prediction of multiple-port mixing. Accordingly, the single-port results of tests 655, 659, 671, and 675 were conceptually overlaid to simulate four identical plumes spaced at 13 ft o.c.; the dilution values at a single downstream station were calculated assuming linear superposition of the separate overlapping dilution contours. Fig. 10 is a plot of the calculated and observed contours; note that for tests 671 and 675 the comparison could not be made at identical downstream stations.

23
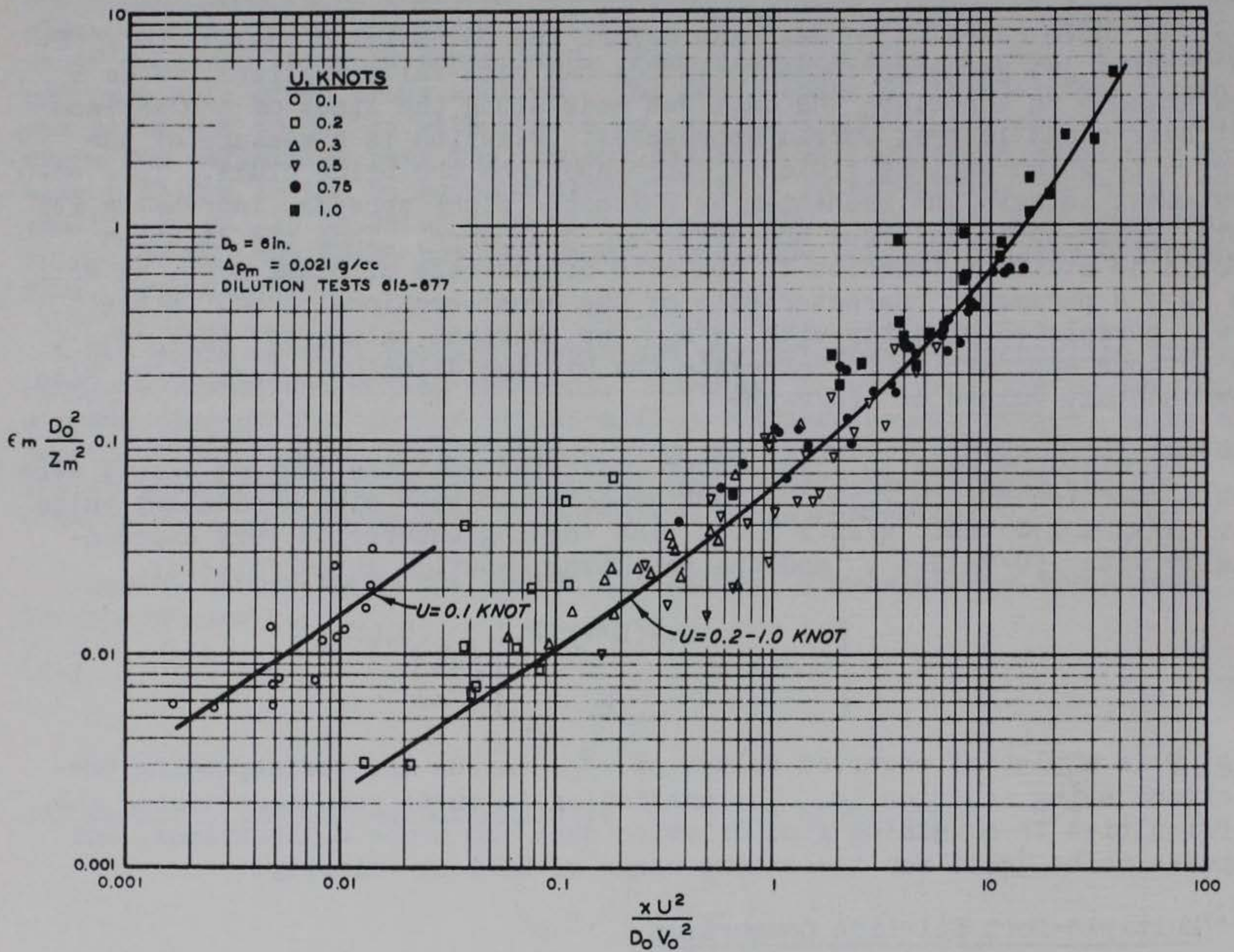
Fig. 8. Correlation of minimum dilution with dimensionless downstream distance
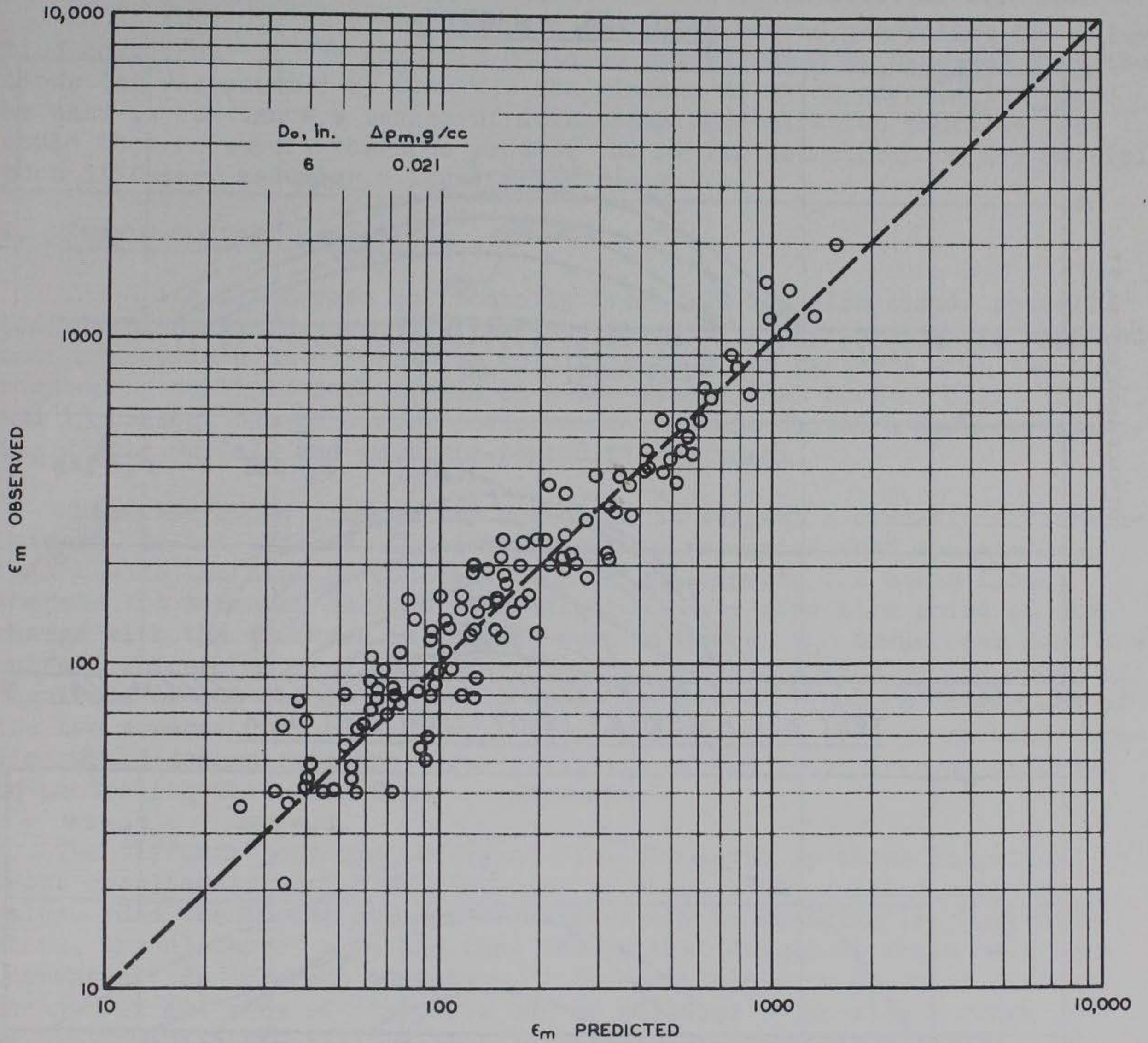
Fig. 9. Observed values of minimum dilution versus values predicted
by equation 14
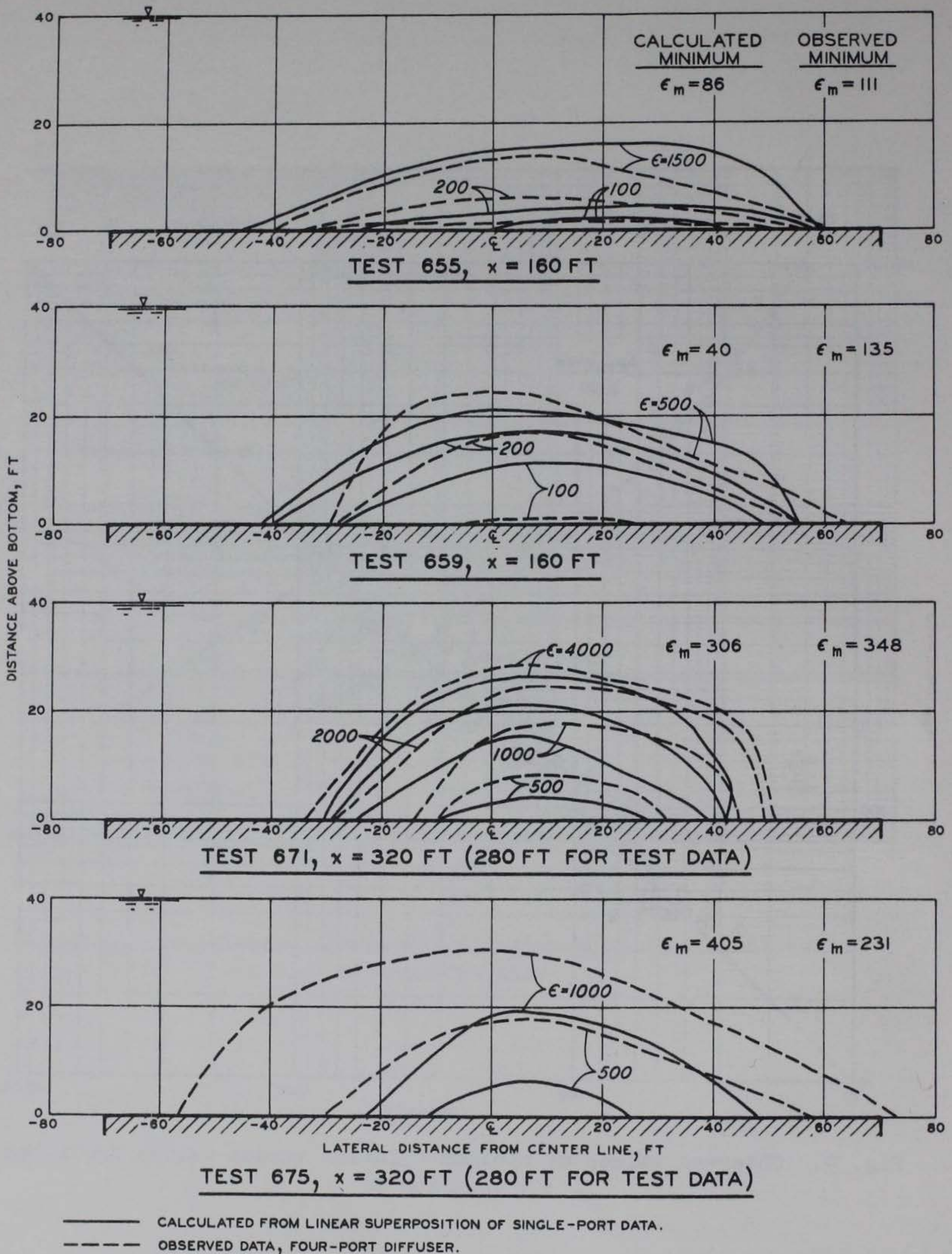
Fig. 10. Comparison of observed multiple-port dilution contours with superposition prediction (looking upstream)

The individual effects of the four separate plumes were essentially indiscernible downstream of the point where the jets merged. There appeared to be no hydrodynamic interaction between the plumes that might invalidate an assumption of linear superposition. Tests 4-655 and 4-659 agree quite well with the calculated predictions in terms of overall area of influence and degree of dilution. Tests 4-671 and 4-675 have been compared at $x = 320$ ft with superposition of corresponding plumes at $x = 280$ ft ; agreement is good for 4-671 but poorer for 4-675, possibly due to the sensitivity of the results to the probe calibrations. The superposition technique does appear adequate for prediction of downstream mixing patterns.

No attempt has been made as part of this study to generalize the dilution contours. If the contours could be approximated by Gaussian distributions (as was assumed by Crew [4]), the minimum dilution correlation could be used to construct a series of downstream concentration profiles that could then be superimposed to predict the mixing downstream of any multiple-port diffuser, assuming a level ocean floor.

## E.  Simple Outfall Comparison

The brine discharged horizontally from a 20-in.-diam simple outfall tended to remain in close proximity to the bottom. Therefore, it appeared most appropriate to compare the resulting dilution patterns with the corresponding multiple-port mixing on a two-dimensional basis. Figs. 11, 12, and 13 present the plan view contours of constant dilution for corresponding simple outfall and multiple-port diffuser tests.

While the above figures may not at first suggest a dramatic difference between the two schemes, it is important to recognize that the simple outfall places the highest concentrations directly onto the ocean floor; whereas, in terms of maximum concentrations, the effective point of discharge with the diffuser is located some distance $x_0$ downstream from the outfall where the brine has undergone an initial dilution of the order of magnitude of 100 before impinging upon the bottom. Thus, a comparison of the two schemes on the basis of bottom area affected by a given concentration would demonstrate the clear advantage of the multiple-port diffuser in protecting the ocean floor environment.

The diffuser port diameters and flow rate used in these comparison tests resulted in port Froude numbers of about 13.1, a relatively low value. Had the Froude numbers been increased by reducing the port diameters, the distance $x_0$ , and thus the initial dilution, would have been increased. An inherent advantage of the multiple-port diffuser is that the number and size of its ports can be adjusted to provide a range of initial dilutions.

## F.  Effect of Heated Brine

Fig. 14 is a comparison of the dilution contours for the heated brine test with those for test 657 for which all flow conditions except the temperature differential were equivalent. Agreement is quite good at $x = 40$ ft  and 80 ft, and acceptable at $x = 120$ ft  and 280 ft where low concentrations amplify the probe calibration error.

TEST 4 - 615

TEST 20 - 4 - 615

DISTANCE FROM DIFFUSER, FT

$\epsilon_m = 30$

$\epsilon_m = 40$

15

10

30

30

40 ℄ -40

40 ℄ -40
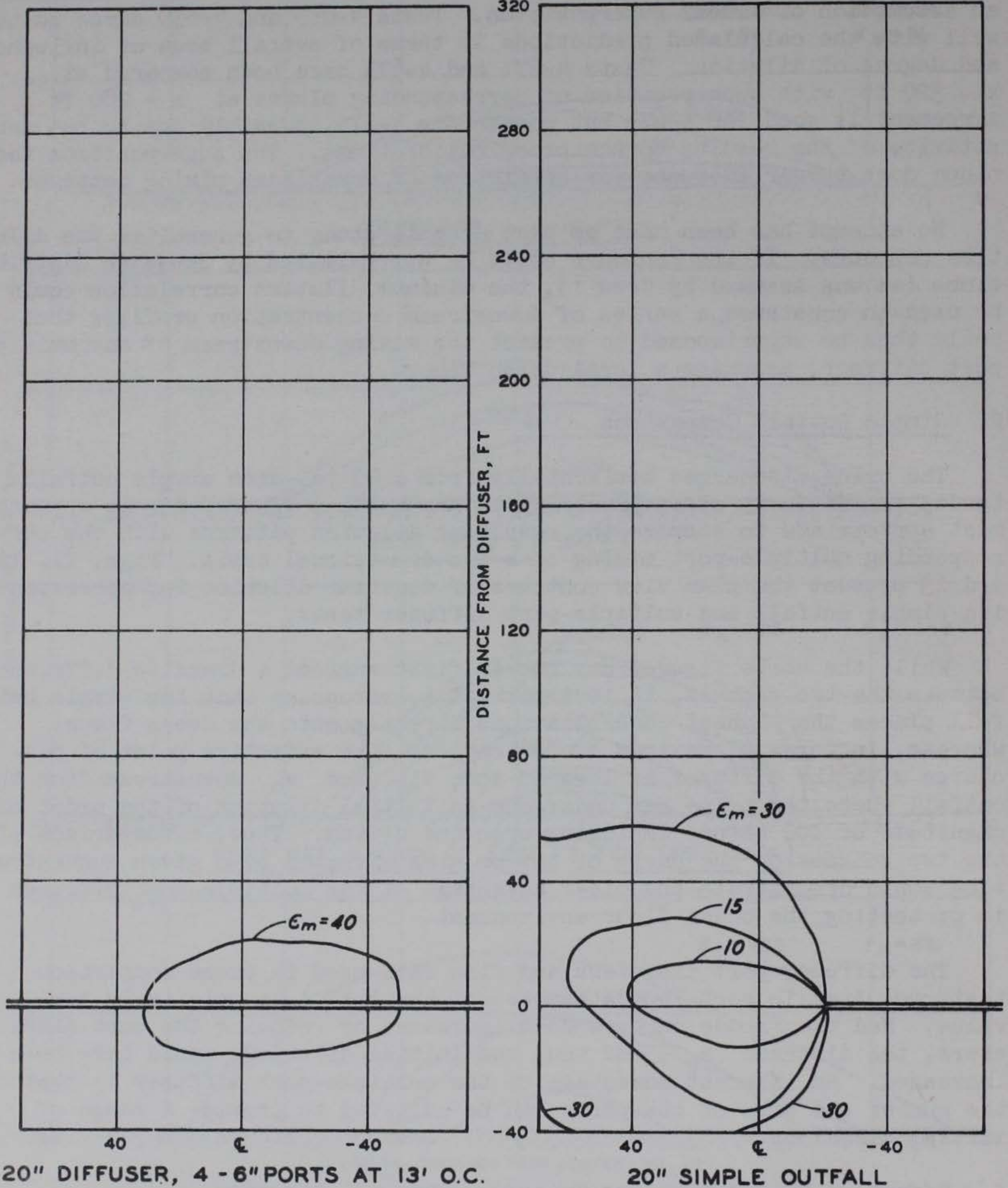
20" DIFFUSER, 4 - 6"PORTS AT 13' O.C.

20" SIMPLE OUTFALL

Fig. 11. Comparison of simple outfall and multiple-port diffuser;
U = 0.1 knot, brine flow = 5.01 cfs, and $\Delta\rho_m$ = 0.021 g/cc. Con-
tours of minimum observed average dilution

TEST 4 - 655

TEST 20 - 4 - 655

DISTANCE FROM DIFFUSER, FT

$\epsilon_m=120$

$\epsilon_m=200$

-100

-200

50-

20" DIFFUSER, 4 - 6" PORTS AT 13' O.C.
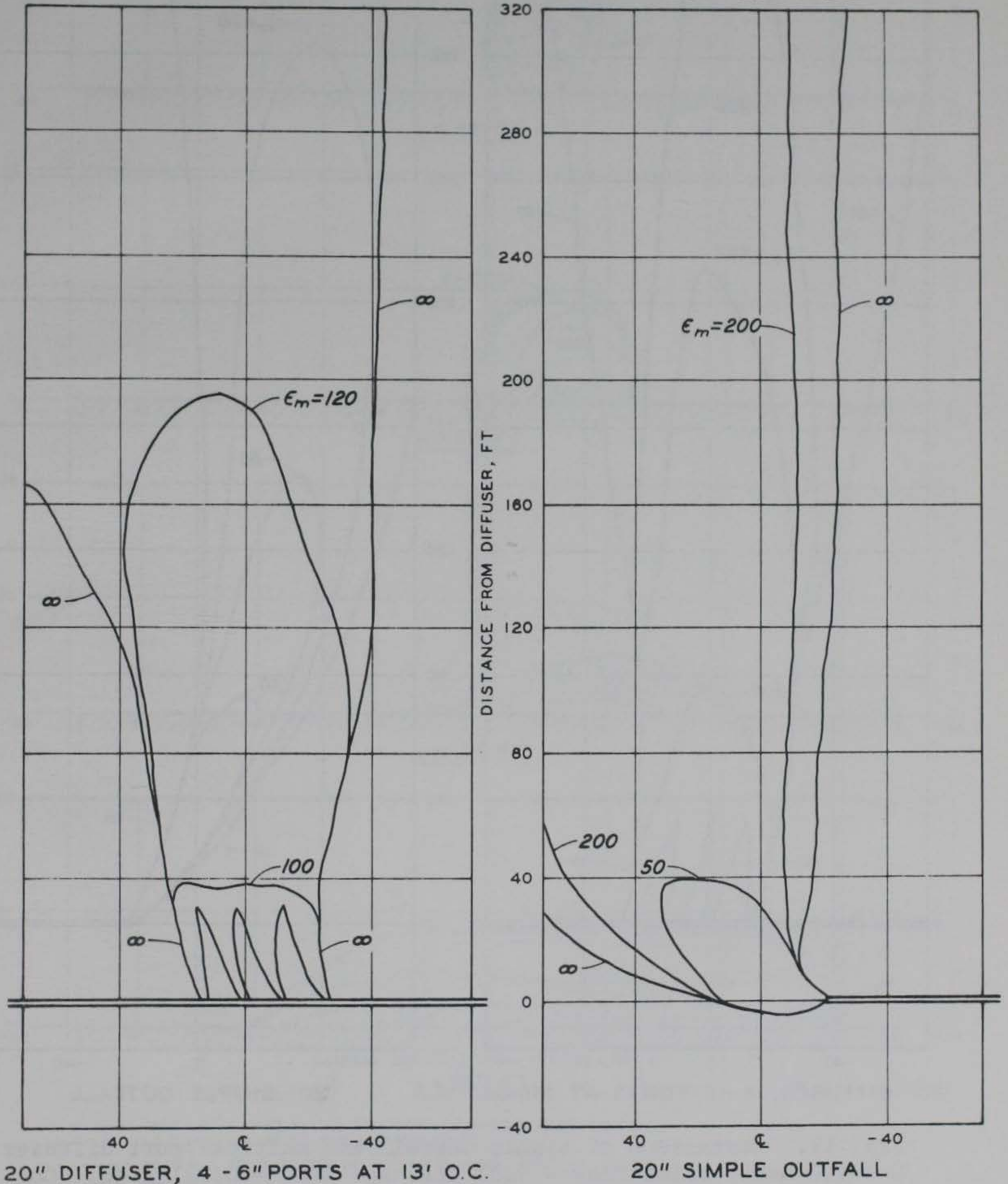
20" SIMPLE OUTFALL

Fig. 12. Comparison of simple outfall and multiple-port diffuser; U = 0.5 knot, brine flow = 5.01 cfs, and $\Delta\rho_m$ = 0.021 g/cc. Contours of minimum observed average dilution

29
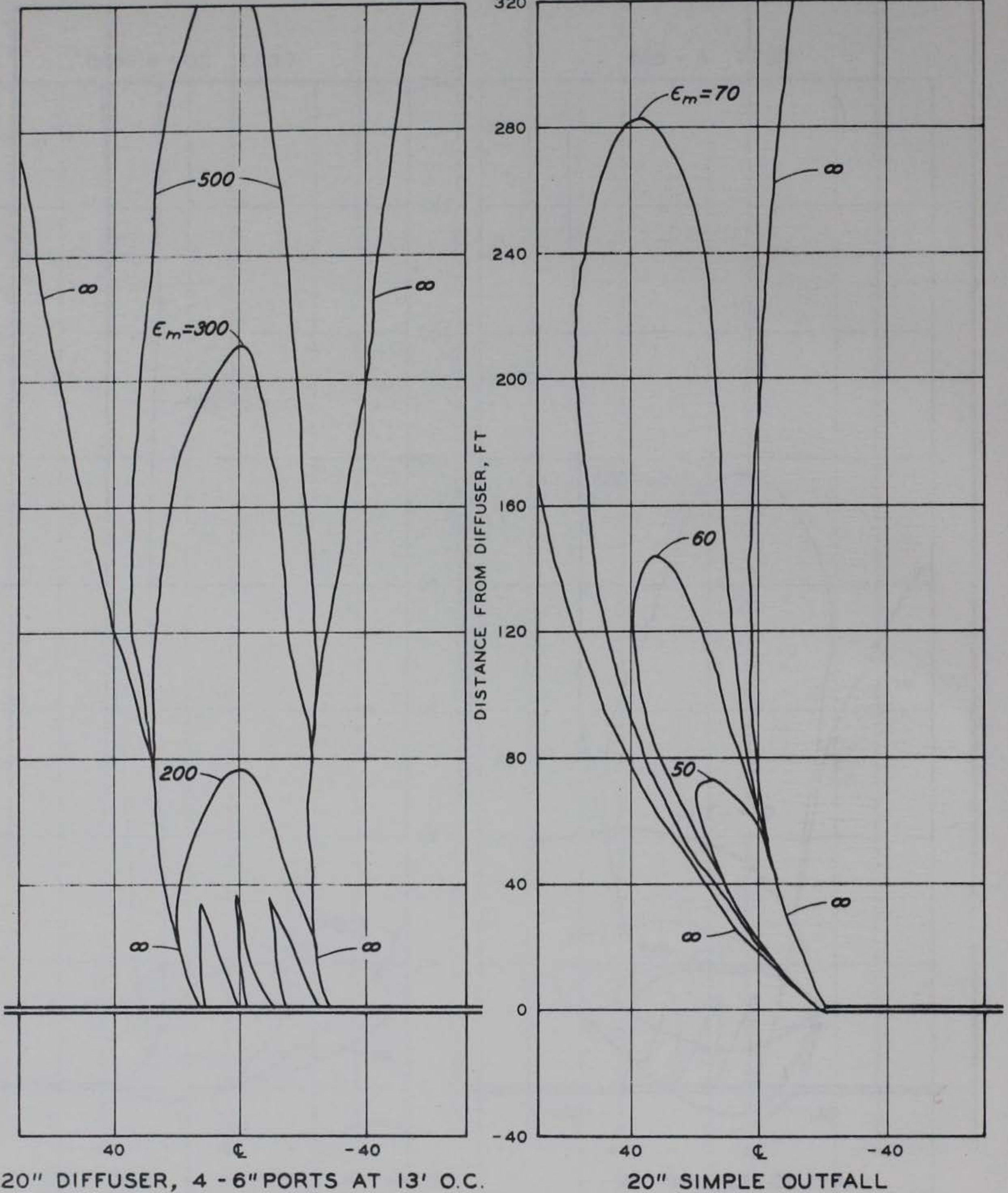
Fig. 13. Comparison of simple outfall and multiple-port diffuser; U = 1.0 knot, brine flow = 5.01 cfs, and $\Delta\rho_m$ = 0.021 g/cc. Contours of minimum observed average dilution
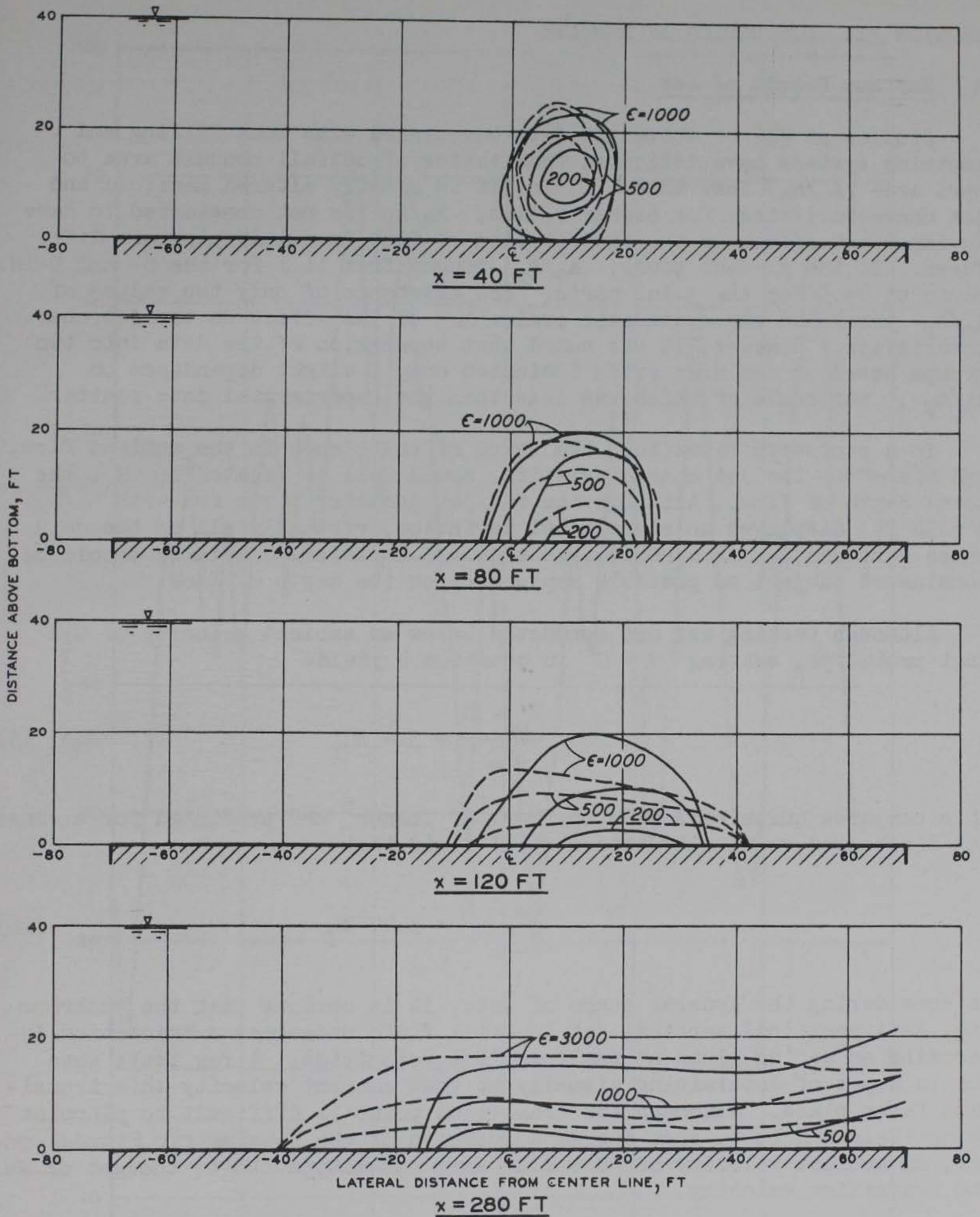
Fig. 14. Comparison of dilution contours for single 6-in. port for heated brine and test 657 (looking upstream); U = 0.5 knot, $\mathbb{F}_D = 18.7$, $\Delta\rho_m = 0.021$ g/cc

31

# SECTION VI: DISCUSSION OF RESULTS

## A. Maximum Height of Jet

Studies at WES of submerged jets associated with lock filling and emptying systems have indicated that ratios of outfall conduit area to port area $(A_o/A_p)$ less than 1.05 result in greatly altered manifold and jet characteristics; for higher ratios, $A_o/A_p$ is not considered to have an important effect on the distribution of flow in a multiple-port diffuser. In the present study, $A_o/A_p$ ranged from 11.1 for the 6- and 9-in. ports to 44.5 for the 3-in. ports. The existence of only two values of $A_o/A_p$ precluded any systematic evaluation of its effect on the jet characteristics. However, it was noted that separation of the data into two groups based on the area ratio indicated only a slight dependence on $A_o/A_p$, the scale of which was less than the experimental data scatter.

In a prototype situation, the level of turbulence in the ambient flow, and therefore the jet characteristics, could well be related to H , the total depth of flow. Although the few jet geometry tests run with H = 30 ft displayed no significant deviation, virtually all of the data taken here was for H = 40 ft , so that all empirical constants should be considered subject to possible dependence on the depth of flow.

Although testing was not conducted below an ambient velocity of 0.1 knot prototype, setting U = 0 in equation 4 yields

$$\frac{Z_m - D}{D_o} = 3.4 \; \mathbb{F}_D \tag{15}$$

This compares quite well with the work of Turner[5] who predicted for a dense jet discharged vertically into a still fluid that

$$\frac{Z_m - D}{D_o} = 3.47 \; \mathbb{F}_D \tag{16}$$

In considering the general shape of jets, it is obvious that the mushrooming, axisymmetrical vertical jet in still fluid undergoes a transition in becoming an arcing plume at small ambient velocities. A few tests were run in hopes of determining visually at what ambient velocity this transition takes place. Although the transition point is difficult to pinpoint objectively and is to some degree a function of the densimetric Froude number, an ambient velocity of U = 0.07 knot prototype can be thought of as the transition velocity.

## B. Dilution Contours

Fig. 15 is an example of the extreme fluctuations in conductivity at a point due to the turbulent jet mixing. The level of fluctuations decreased
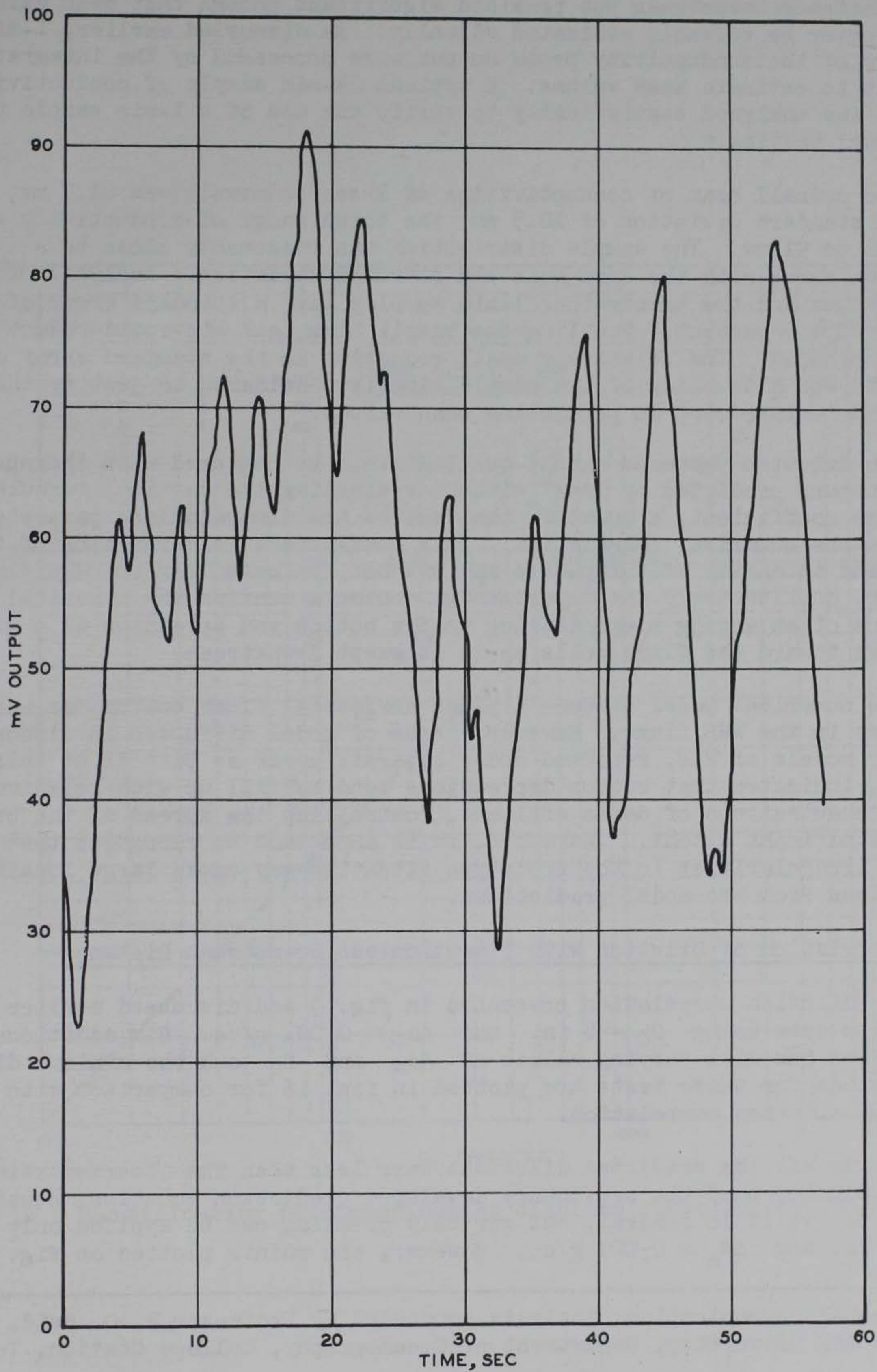
Fig. 15. Fluctuations in conductivity due to turbulent jet mixing

with distance downstream but remained significant enough that mean values could never be reliably estimated visually. As discussed earlier, 1-min samples of the conductivity probe output were processed by the integrating circuit to estimate mean values. A typical 24-min sample of conductivity output was analyzed statistically to verify the use of a 1-min sample time in actual testing.*

The overall mean of conductivities at 1-sec intervals was 61.7 mv, with a standard deviation of 10.5 mv; the total range of conductivity was from 26 to 91 mv. The sample distribution was reasonably close to a Gaussian curve with the same mean and standard deviation. Analysis of the mean values for the twenty-four 1-min samples gave a standard error of estimate of 4.5 percent. Doubling the sample time to 2 min would reduce this to 3.4 percent. The relatively small reduction in the standard error of estimate for a doubling of the sample time is considered to justify the use of a 1-min record in predicting mean values.

The dilution patterns cannot qualitatively be compared with the numerical contours predicted by Crew[4] without evaluating the vertical turbulence exchange coefficient, a quantity that scales the dimensionless parameters used in the numerical formulation. This coefficient is a function of the scale and intensity of turbulence and was not evaluated for the WES flume. However, qualitatively the experimental contours confirm the numerical predictions of an arcing plume falling to the bottom and spreading as a gravity wave toward the flume walls as it is swept downstream.

The numerical model assumed a plane horizontal flume bottom, as was the case in the WES flume. However, tests of model diffusers in distorted estuary models at WES, reported under separate cover as Part II of this report, indicated that bottom depressions tend to fill up with relatively high concentrations of dense effluent, controlling the spread of the brine to a significant extent. Therefore, it is important to recognize that bottom irregularities in the prototype situation may cause large localized deviations from the model predictions.

C. Correlation of Dilution with Dimensionless Downstream Distance

The dilution correlation presented in fig. 9 and discussed earlier was made with data using $D_o = 6$ in. and $\Delta\rho_m = 0.021$ g/cc. Six additional tests were run with varying values of $\Delta\rho_m$ and $D_o$ and the minimum dilution values for these tests are plotted in fig. 16 for comparison with the previous dilution correlation.

Nearly all the predicted dilutions were less than the observed values. This indicates that the previously developed prediction equation, equation 14, is not valid in general, but strictly speaking can be applied only when $D_o = 6$ in. and $\Delta\rho_m = 0.021$ g/cc. However, the points plotted on fig. 16

---

* Personal communication; analysis conducted by Professor R. O. Reid, Texas A&M University, Department of Oceanography, College Station, Tex.
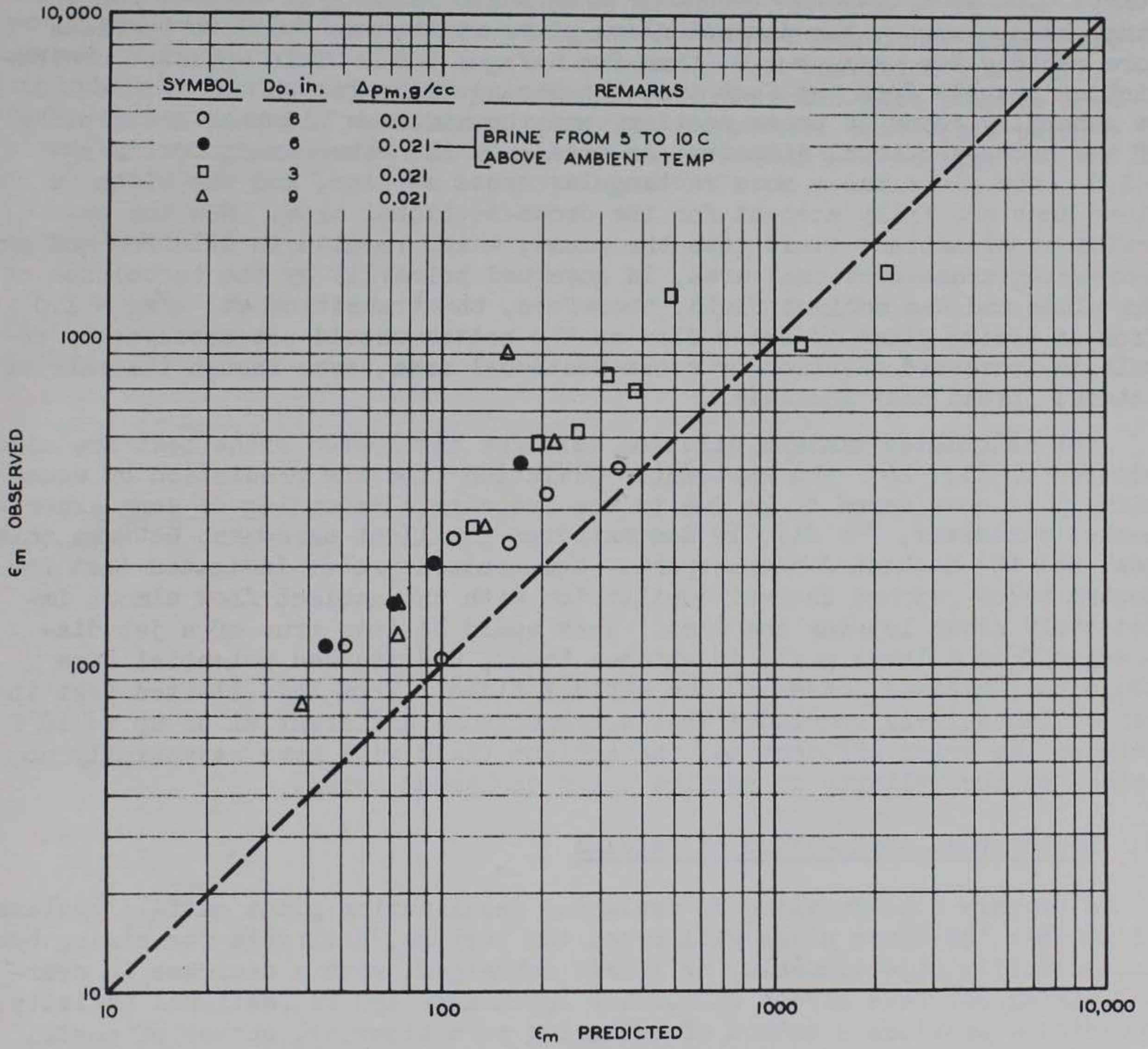
Fig. 16. Vertification of dimensionless dilution correlation, equation 14

do not fall appreciably outside the basic scatter of fig. 9, and the errors in prediction are conservative; that is, predicted dilutions may be too low. (Predicted concentrations may be too high.) This suggests that equation 14 still can be used in designing diffusers for which the concentration at some downstream point is not to exceed a specified maximum.

In developing equation 14, it was noted that, for any given value of $(U/V_o)\mathbb{F}_D$, the dilution is proportional to $(x/x_o)^{0.68}$, where the exponent 0.68 is a constant for both $x/x_o \leq 1.0$ and $x/x_o > 1.0$. On the other hand, $w/w_o$, the dimensionless plume width, was found to increase more rapidly for $x/x_o > 1.0$ than for $x/x_o \leq 1.0$. This apparent contradiction results from the fact that the arcing plume for which $x/x_o \leq 1.0$ is generally round in cross section, and the width $w$ is thus descriptive of the cross-sectional diameter, or area. On the other hand, for $x/x_o > 1.0$, the plume has a more rectangular cross section, and the width $w$ alone does not fully account for the cross-sectional area. Now the entrainment of ambient fluid into the plume, which results in dilution and an increasing cross-sectional area, is governed primarily by the turbulence of the plume and the ambient fluid; therefore, the transition at $x/x_o = 1.0$ from an arcing plume to dense flow on the bottom should not necessarily result in increased dilution or cross-sectional area, even though the rate of lateral spread does increase.

The calculated minimum dilution data for the heated brine test are also plotted on fig. 16. The systematic deviation from the prediction by equation 15 is considered to be due to the inaccurate recording of some experimental parameter, for fig. 14 demonstrates excellent agreement between this test and its nonheated counterpart. Temperature probes indicated that the heated brine reached thermal equilibrium with the ambient flow almost immediately after leaving the port. This would be less true of a jet discharged from a large port, in which a thick, undisturbed potential core would have minimum losses to the ambient fluid. From this limited test it can be tentatively concluded that a temperature differential of up to 10°C between the brine effluent and the ambient fluid will have essentially no effect on the validity of results using nonheated brine.

D. Recommended Application of Results

A primary consideration in designing desalination plant outfall systems is whether the dense plume will reach the surface, desirable for mixing but aesthetically objectionable, or remain submerged, with a decrease in overall mixing but less effect on surface appearance and recreational activity. Equation 4 provides a method of balancing port diameter, number of ports, total brine flow rate, and density differential with the ambient velocity to obtain a desired maximum jet height. Where the ambient velocity varies periodically, as in an estuary, the required rates of diversion of brine to holding tanks can be calculated for acceptable jet performance during slack-water periods.

Although generalized three-dimensional dilution patterns downstream of

a diffuser were not developed as part of this study, equation 14 does provide a means of predicting the maximum concentrations of effluent to be expected at some downstream distance from the diffuser. Thus the port diameter, number of ports, total brine flow rate, density differential, and maximum jet height can be balanced with the ambient velocity to meet established water-quality criteria downstream.

Equations 7-11 can be used to predict the lateral spread of dense plumes, which must be done before superposition of single-port results can be accomplished. As part of a proposed extended research effort, a computer program would be developed to compute three-dimensional mixing and geometry characteristics for any set of design and operation conditions, including unsteady ambient flow. Such a program would also compute specific combinations of design and operation parameters that would permit plant operation consistent with specific water-quality criteria.

# SECTION VII:  LITERATURE CITED

1.  Dow Chemical Co., "Conceptual Designs of Outfall Systems for Desalination Plants," Contract No. 14-01-0001-2109, Apr 1970, U. S. Department of Interior, Office of Saline Water, Washington, D. C.

2.  Keffer, J. F. and Baines, W. D., "The Round Turbulent Jet in a Cross-Wind," Journal of Fluid Mechanics, Vol 15, Part 4, Apr 1963, pp 481-496.

3.  Fan, L.-N., "Turbulent Buoyant Jets into Stratified or Flowing Ambient Fluids," Report No. KH-R-15, June 1967, California Institute of Technology, W. M. Keck Laboratory, Pasadena, Calif.

4.  Crew, H., "A Numerical Model of the Dispersion of a Dense Effluent in a Stream," A&M Project 716, Reference 70-10T, June 1970, Texas A&M University, Department of Oceanography and Meteorology, College Station, Tex.

5.  Turner, J. S., "Jets and Plumes with Negative or Reversing Buoyance," Journal of Fluid Mechanics, Vol 26, Part 4, Dec 1966, pp 779-792.

6.  Tilton, L. W. and Taylor, J. K., "Accurate Representation of the Refractivity and Density of Distilled Water as a Function of Temperature," Journal of Research of the National Bureau of Standards, Vol 18, Research Paper RP-971, Feb 1937, pp 205-214.

# SECTION VIII: SELECTED BIBLIOGRAPHY

Albertson, M. L., et al., "Diffusion of Submerged Jets," Transactions, American Society of Civil Engineers, Vol 115, 1950, pp 639-664.

Bradbury, L. J. S. and Wood, M. N., "The Static Pressure Distribution Around a Circular Jet Exhausting Normally from a Plane Wall into an Air-Stream," Technical Note No. Aero 2978, Aug 1964, British Royal Aircraft Establishment.

Callaghan, E. E. and Bowden, D. T., "Investigation of the Penetration of an Air Jet Directed Perpendicularly to an Air Stream," TN 1615, June 1948, National Advisory Committee for Aeronautics, Washington, D. C.

Carter, H. H., "A Preliminary Report on the Characteristics of a Heated Jet Discharged Horizontally into a Transverse Current; Part I, Constant Depth," Technical Report No. 61, Reference 69-14, Nov 1969, Johns Hopkins University, Chesapeake Bay Institute, Baltimore, Md.

Gordier, R., "Studies on Fluid Jets Discharging Normally into Moving Fluid," Technical Paper No. 28, Series B, Aug 1959, University of Minnesota, St. Anthony Falls Hydraulic Laboratory, Minneapolis, Minn.

Jordinson, R., "Flow in a Jet Directed Normal to the Wind," R&M 3074, Oct 1956, British Aeronautical Research Council.

Lee, C. C., "A Review of Research on the Interaction of a Jet with an External Stream," Technical Note R-184, Mar 1966, Brown Engineering Co., Inc., Huntsville, Ala.

Lee, S.-L., "Axisymmetrical Turbulent Swirling Natural-Convection Plume," Journal of Applied Mechanics, Vol 33, Series E, No. 3, Sept 1966, pp 647-667.

Liseth, P., "Mixing of Merging Buoyant Jets from a Manifold in Stagnant Receiving Water of Uniform Density," Technical Report HEL 23-1, Nov 1970, University of California at Berkeley, Hydraulic Engineering Laboratory, Berkeley, Calif.

McAllister, J. D., "A Momentum Theory for the Effects of Cross Flow on Impressible Turbulent Jets," Ph. D. dissertation, Aug 1968, University of Tennessee, Knoxville, Tenn.

Mosher, D. K., "An Experimental Investigation of a Turbulent Jet in a Cross Flow," Report 70-7, Dec 1970, Georgia Institute of Technology, School of Aerospace Engineering, Atlanta, Ga.

Pratte, B. C. and Baines, W. D., "Profiles of the Round Turbulent Jet in a Cross Flow," Journal, Hydraulics Division, American Society of Civil Engineers, Vol 93, No. HY6, Nov 1967, pp 53-64.

Pratte, B. C. and Keffer, J. F., "Swirling Turbulent Jet Flows; Part I: The Single Swirling Jet," UTME-TP 6901, Mar 1969, Department of Mechanical Engineering, University of Toronto, Toronto, Canada.

Ruggeri, R., Callaghan, E., and Bowden, D., "Penetration of Air Jets Issuing from Circular, Square, and Elliptical Orifices Directed Perpendicularly to an Air Stream," TN 2019, Feb 1950, National Advisory Committee for Aeronautics, Washington, D. C.

Stolzenbach, K. D. and Harleman, D. R. F., "An Analytical and Experimental Investigation of Surface Discharges of Heated Water," Report No. 135, Feb 1971, Massachusetts Institute of Technology, Ralph M. Parsons Laboratory for Water Resources and Hydrodynamics, Cambridge, Mass.

Wu, J. D., Mosher, D. K., and Wright, M. A., "Experimental and Analytical Investigations of Jets Exhausting into a Deflecting Stream," Journal of Aircraft, Vol 7, No. 1, Jan-Feb 1970.

Table 1

Jet Geometry Tests

| Test | $D_o$ in. | $D$ in. | $\rho_f$ g/cc | $\Delta\rho_m$ g/cc | $F_D$ | $U$ knots | $H$ ft | $Z_m$ ft |
|---|---|---|---|---|---|---|---|---|
| 301 | 3 | 20 | 0.9972 | 0.0180 | 18.8 | 0.10 | 40 | 14.4 |
| 302 | 3 | 20 | 0.9972 | 0.0180 | 24.5 | 0.10 | 40 | 21.0 |
| 303 | 3 | 20 | 0.9972 | 0.0180 | 29.8 | 0.10 | 40 | 25.6 |
| 304 | 3 | 20 | 0.9972 | 0.0180 | 35.7 | 0.10 | 40 | 30.0 |
| 305 | 3 | 20 | 0.9972 | 0.0180 | 41.4 | 0.10 | 40 | 36.0 |
| 306 | 3 | 20 | 0.9972 | 0.0180 | 46.8 | 0.10 | 40 | 40.0 |
| 307 | 3 | 20 | 0.9972 | 0.0180 | 18.8 | 0.21 | 40 | 11.0 |
| 308 | 3 | 20 | 0.9972 | 0.0180 | 24.5 | 0.21 | 40 | 15.6 |
| 309 | 3 | 20 | 0.9972 | 0.0180 | 29.8 | 0.21 | 40 | 21.8 |
| 310 | 3 | 20 | 0.9972 | 0.0180 | 35.7 | 0.21 | 40 | 25.5 |
| 311 | 3 | 20 | 0.9972 | 0.0180 | 41.4 | 0.21 | 40 | 28.8 |
| 312 | 3 | 20 | 0.9972 | 0.0180 | 46.8 | 0.21 | 40 | 32.2 |
| 313 | 3 | 20 | 0.9972 | 0.0180 | 52.4 | 0.21 | 40 | 37.0 |
| 314 | 3 | 20 | 0.9972 | 0.0182 | 18.4 | 0.31 | 40 | 12.9 |
| 315 | 3 | 20 | 0.9972 | 0.0182 | 24.1 | 0.31 | 40 | 13.6 |
| 316 | 3 | 20 | 0.9972 | 0.0182 | 29.9 | 0.31 | 40 | 14.9 |
| 317 | 3 | 20 | 0.9972 | 0.0182 | 35.3 | 0.31 | 40 | 21.0 |
| 318 | 3 | 20 | 0.9972 | 0.0182 | 41.0 | 0.31 | 40 | 23.1 |
| 319 | 3 | 20 | 0.9972 | 0.0182 | 46.4 | 0.31 | 40 | 28.3 |
| 320 | 3 | 20 | 0.9972 | 0.0182 | 51.9 | 0.31 | 40 | 29.1 |
| 321 | 3 | 20 | 0.9970 | 0.0184 | 18.5 | 0.44 | 40 | 7.9 |
| 322 | 3 | 20 | 0.9970 | 0.0184 | 24.1 | 0.44 | 40 | 10.3 |
| 323 | 3 | 20 | 0.9970 | 0.0184 | 29.7 | 0.44 | 40 | 15.1 |
| 324 | 3 | 20 | 0.9970 | 0.0184 | 35.1 | 0.44 | 40 | 17.0 |
| 325 | 3 | 20 | 0.9970 | 0.0184 | 41.0 | 0.44 | 40 | 20.4 |
| 326 | 3 | 20 | 0.9970 | 0.0184 | 46.2 | 0.44 | 40 | 24.2 |
| 327 | 3 | 20 | 0.9970 | 0.0184 | 52.0 | 0.44 | 40 | 23.3 |
| 328 | 3 | 20 | 0.9969 | 0.0185 | 18.5 | 0.48 | 40 | 8.7 |
| 329 | 3 | 20 | 0.9969 | 0.0185 | 24.1 | 0.48 | 40 | 13.1 |
| 330 | 3 | 20 | 0.9969 | 0.0185 | 29.7 | 0.48 | 40 | 13.6 |
| 331 | 3 | 20 | 0.9969 | 0.0185 | 35.1 | 0.48 | 40 | 17.2 |
| 332 | 3 | 20 | 0.9969 | 0.0185 | 41.0 | 0.48 | 40 | 17.5 |
| 333 | 3 | 20 | 0.9969 | 0.0185 | 46.2 | 0.48 | 40 | 21.2 |
| 334 | 3 | 20 | 0.9969 | 0.0185 | 52.0 | 0.48 | 40 | 25.9 |
| 335 | 3 | 20 | 0.9969 | 0.0182 | 18.4 | 0.75 | 40 | 7.5 |
| 336 | 3 | 20 | 0.9969 | 0.0182 | 24.1 | 0.75 | 40 | 9.2 |
| 337 | 3 | 20 | 0.9969 | 0.0182 | 29.9 | 0.75 | 40 | 8.8 |
| 338 | 3 | 20 | 0.9969 | 0.0182 | 35.3 | 0.74 | 40 | 12.0 |
| 339 | 3 | 20 | 0.9969 | 0.0182 | 41.0 | 0.75 | 40 | 13.0 |
| 340 | 3 | 20 | 0.9969 | 0.0182 | 46.4 | 0.75 | 40 | 15.9 |
| 341 | 3 | 20 | 0.9969 | 0.0182 | 51.9 | 0.75 | 40 | 17.8 |
| 342 | 3 | 20 | 0.9969 | 0.0177 | 18.9 | 1.00 | 40 | 5.5 |
| 343 | 3 | 20 | 0.9969 | 0.0177 | 24.6 | 1.00 | 40 | 8.8 |
| 344 | 3 | 20 | 0.9969 | 0.0177 | 30.2 | 1.00 | 40 | 6.9 |
| 345 | 3 | 20 | 0.9969 | 0.0177 | 35.7 | 1.00 | 40 | 9.2 |
| 346 | 3 | 20 | 0.9969 | 0.0177 | 41.8 | 1.00 | 40 | 9.8 |
| 347 | 3 | 20 | 0.9969 | 0.0177 | 47.0 | 1.00 | 40 | 7.5 |
| 348 | 3 | 20 | 0.9969 | 0.0177 | 52.0 | 1.00 | 40 | 10.0 |
| 350 | 3 | 20 | 0.9978 | 0.0105 | 25.0 | 0.10 | 40 | 20.7 |
| 351 | 3 | 20 | 0.9978 | 0.0105 | 40.3 | 0.10 | 40 | 33.1 |
| 352 | 3 | 20 | 0.9978 | 0.0105 | 55.3 | 0.10 | 40 | 40.0 |
| 353 | 3 | 20 | 0.9978 | 0.0105 | 70.0 | 0.10 | 40 | 40.0 |
| 354 | 3 | 20 | 0.9978 | 0.0105 | 25.0 | 0.31 | 40 | 9.8 |
| 355 | 3 | 20 | 0.9978 | 0.0105 | 40.3 | 0.31 | 40 | 18.8 |

(Continued)                                    (1 of 7 sheets)

41

Table 1 (Continued)

| Test | $D_o$ in. | $D$ in. | $\rho_f$ g/cc | $\Delta\rho_m$ g/cc | $F_D$ | $U$ knots | $H$ ft | $Z_m$ ft |
|------|-----------|---------|---------------|---------------------|-------|-----------|--------|----------|
| 356 | 3 | 20 | 0.9978 | 0.0105 | 55.3 | 0.31 | 40 | 25.0 |
| 357 | 3 | 20 | 0.9978 | 0.0105 | 70.0 | 0.31 | 40 | 30.2 |
| 358 | 3 | 20 | 0.9978 | 0.0105 | 25.0 | 0.50 | 40 | 8.5 |
| 359 | 3 | 20 | 0.9978 | 0.0105 | 40.3 | 0.50 | 40 | 11.4 |
| 360 | 3 | 20 | 0.9978 | 0.0105 | 55.3 | 0.50 | 40 | 19.0 |
| 361 | 3 | 20 | 0.9978 | 0.0105 | 70.0 | 0.50 | 40 | 23.0 |
| 362 | 3 | 20 | 0.9978 | 0.0105 | 25.0 | 0.75 | 40 | 5.0 |
| 363 | 3 | 20 | 0.9978 | 0.0105 | 40.3 | 0.75 | 40 | 7.0 |
| 364 | 3 | 20 | 0.9978 | 0.0105 | 55.3 | 0.75 | 40 | 9.0 |
| 365 | 3 | 20 | 0.9978 | 0.0105 | 70.0 | 0.75 | 40 | 12.0 |
| 366 | 3 | 20 | 1.0002 | 0.0263 | 15.6 | 0.10 | 40 | 9.8 |
| 367 | 3 | 20 | 1.0002 | 0.0263 | 25.3 | 0.10 | 40 | 16.8 |
| 368 | 3 | 20 | 1.0002 | 0.0263 | 34.7 | 0.10 | 40 | 20.5 |
| 369 | 3 | 20 | 1.0002 | 0.0263 | 44.0 | 0.10 | 40 | 31.0 |
| 370 | 3 | 20 | 1.0002 | 0.0157 | 20.0 | 0.10 | 40 | 11.2 |
| 371 | 3 | 20 | 1.0002 | 0.0157 | 32.3 | 0.10 | 40 | 22.7 |
| 372 | 3 | 20 | 1.0002 | 0.0157 | 44.3 | 0.10 | 40 | 32.8 |
| 373 | 3 | 20 | 1.0002 | 0.0157 | 56.2 | 0.10 | 40 | 40.0 |
| 374 | 3 | 20 | 1.0002 | 0.0157 | 20.0 | 0.30 | 40 | 9.0 |
| 375 | 3 | 20 | 1.0002 | 0.0157 | 32.3 | 0.30 | 40 | 17.0 |
| 376 | 3 | 20 | 1.0002 | 0.0157 | 44.3 | 0.30 | 40 | 23.0 |
| 377 | 3 | 20 | 1.0002 | 0.0157 | 56.2 | 0.30 | 40 | 30.2 |
| 378 | 3 | 20 | 1.0002 | 0.0263 | 15.6 | 0.30 | 40 | 6.7 |
| 379 | 3 | 20 | 1.0002 | 0.0263 | 25.3 | 0.30 | 40 | 11.0 |
| 380 | 3 | 20 | 1.0002 | 0.0263 | 34.7 | 0.30 | 40 | 20.0 |
| 381 | 3 | 20 | 1.0002 | 0.0263 | 44.0 | 0.30 | 40 | 24.0 |
| 382 | 3 | 20 | 1.0002 | 0.0263 | 15.6 | 0.50 | 40 | 6.2 |
| 383 | 3 | 20 | 1.0002 | 0.0263 | 25.3 | 0.50 | 40 | 11.5 |
| 384 | 3 | 20 | 1.0002 | 0.0263 | 34.7 | 0.50 | 40 | 14.4 |
| 385 | 3 | 20 | 1.0002 | 0.0263 | 44.0 | 0.50 | 40 | 20.0 |
| 386 | 3 | 20 | 1.0002 | 0.0157 | 20.0 | 0.50 | 40 | 9.6 |
| 387 | 3 | 20 | 1.0002 | 0.0157 | 32.3 | 0.50 | 40 | 15.0 |
| 388 | 3 | 20 | 1.0002 | 0.0157 | 44.3 | 0.50 | 40 | 20.2 |
| 389 | 3 | 20 | 1.0002 | 0.0157 | 56.2 | 0.50 | 40 | 23.4 |
| 390 | 3 | 20 | 1.0002 | 0.0157 | 20.0 | 0.75 | 40 | 8.6 |
| 391 | 3 | 20 | 1.0002 | 0.0157 | 32.3 | 0.75 | 40 | 11.2 |
| 392 | 3 | 20 | 1.0002 | 0.0157 | 44.3 | 0.75 | 40 | 12.0 |
| 393 | 3 | 20 | 1.0002 | 0.0157 | 56.2 | 0.75 | 40 | 16.0 |
| 394 | 3 | 20 | 1.0002 | 0.0263 | 15.6 | 0.75 | 40 | 6.8 |
| 395 | 3 | 20 | 1.0002 | 0.0263 | 25.3 | 0.75 | 40 | 9.0 |
| 396 | 3 | 20 | 1.0002 | 0.0263 | 34.7 | 0.75 | 40 | 10.0 |
| 397 | 3 | 20 | 1.0002 | 0.0263 | 44.0 | 0.75 | 40 | 13.0 |
| 398 | 3 | 20 | 1.0002 | 0.0263 | 15.6 | 1.00 | 40 | 5.0 |
| 399 | 3 | 20 | 1.0002 | 0.0263 | 25.3 | 1.00 | 40 | 8.5 |
| 400 | 3 | 20 | 1.0002 | 0.0263 | 34.7 | 1.00 | 40 | 10.0 |
| 401 | 3 | 20 | 1.0002 | 0.0263 | 44.0 | 1.00 | 40 | 10.3 |
| 402 | 3 | 20 | 1.0002 | 0.0157 | 20.0 | 1.00 | 40 | 5.2 |
| 403 | 3 | 20 | 1.0002 | 0.0157 | 32.3 | 1.00 | 40 | 8.6 |
| 404 | 3 | 20 | 1.0002 | 0.0157 | 44.3 | 1.00 | 40 | 10.0 |
| 405 | 3 | 20 | 1.0002 | 0.0157 | 56.2 | 1.00 | 40 | 14.2 |
| 406 | 3 | 20 | 1.0007 | 0.0045 | 37.0 | 0.10 | 40 | 21.2 |
| 407 | 3 | 20 | 1.0007 | 0.0045 | 58.0 | 0.10 | 40 | 34.0 |
| 408 | 3 | 20 | 1.0007 | 0.0045 | 79.6 | 0.10 | 40 | 40.0 |
| 409 | 3 | 20 | 1.0007 | 0.0045 | 37.0 | 0.30 | 40 | 12.0 |

(Continued)  (2 of 7 sheets)

Table 1 (Continued)

| Test | $D_o$ in. | $D$ in. | $\rho_f$ g/cc | $\Delta\rho_m$ g/cc | $F_D$ | $U$ knots | $H$ ft | $Z_m$ ft |
|------|------|------|--------|--------|-------|-------|------|-------|
| 410 | 3 | 20 | 1.0007 | 0.0045 | 58.0 | 0.30 | 40 | 21.3 |
| 411 | 3 | 20 | 1.0007 | 0.0045 | 79.6 | 0.30 | 40 | 27.2 |
| 412 | 3 | 20 | 1.0007 | 0.0045 | 100.3 | 0.30 | 40 | 31.6 |
| 413 | 3 | 20 | 1.0007 | 0.0045 | 37.0 | 0.50 | 40 | 7.8 |
| 414 | 3 | 20 | 1.0007 | 0.0045 | 58.0 | 0.50 | 40 | 13.7 |
| 415 | 3 | 20 | 1.0007 | 0.0045 | 79.6 | 0.50 | 40 | 15.8 |
| 416 | 3 | 20 | 1.0007 | 0.0045 | 100.3 | 0.50 | 40 | 21.0 |
| 601 | 6 | 10 | 0.9968 | 0.0192 | 12.5 | 0.10 | 40 | 21.2 |
| 602 | 6 | 10 | 0.9968 | 0.0192 | 15.9 | 0.10 | 40 | 29.5 |
| 603 | 6 | 10 | 0.9968 | 0.0192 | 20.0 | 0.10 | 40 | 34.5 |
| 604 | 6 | 10 | 0.9980 | 0.0192 | 24.8 | 0.10 | 40 | 40.0 |
| 605 | 6 | 10 | 0.9968 | 0.0192 | 27.3 | 0.10 | 40 | 40.0 |
| 606 | 6 | 10 | 0.9968 | 0.0192 | 29.2 | 0.10 | 40 | 40.0 |
| 607 | 6 | 10 | 0.9970 | 0.0189 | 12.4 | 0.32 | 40 | 16.6 |
| 608 | 6 | 10 | 0.9970 | 0.0189 | 16.0 | 0.32 | 40 | 23.6 |
| 609 | 6 | 10 | 0.9970 | 0.0189 | 24.9 | 0.32 | 40 | 26.5 |
| 610 | 6 | 10 | 0.9970 | 0.0189 | 29.2 | 0.32 | 40 | 40.0 |
| 611 | 6 | 10 | 0.9970 | 0.0189 | 13.8 | 0.50 | 40 | 16.2 |
| 612 | 6 | 10 | 0.9970 | 0.0189 | 20.0 | 0.50 | 40 | 18.0 |
| 613 | 6 | 10 | 0.9970 | 0.0189 | 27.4 | 0.50 | 40 | 25.1 |
| 614 | 6 | 10 | 0.9970 | 0.0189 | 34.8 | 0.50 | 40 | 38.2 |
| 615 | 6 | 20 | 0.9968 | 0.0190 | 13.7 | 0.10 | 40 | 27.6 |
| 616 | 6 | 20 | 0.9968 | 0.0190 | 17.1 | 0.10 | 40 | 29.2 |
| 617 | 6 | 20 | 0.9968 | 0.0190 | 19.5 | 0.10 | 40 | 36.1 |
| 618 | 6 | 20 | 0.9968 | 0.0190 | 22.3 | 0.10 | 40 | 39.3 |
| 619 | 6 | 20 | 0.9968 | 0.0190 | 25.8 | 0.10 | 40 | 40.0 |
| 620 | 6 | 20 | 0.9968 | 0.0190 | 28.9 | 0.10 | 40 | 40.0 |
| 621 | 6 | 20 | 0.9968 | 0.0190 | 33.6 | 0.10 | 40 | 40.0 |
| 622 | 6 | 20 | 0.9968 | 0.0190 | 37.5 | 0.10 | 40 | 40.0 |
| 623 | 6 | 20 | 0.9968 | 0.0187 | 13.7 | 0.21 | 40 | 20.0 |
| 624 | 6 | 20 | 0.9968 | 0.0187 | 17.1 | 0.21 | 40 | 25.8 |
| 625 | 6 | 20 | 0.9968 | 0.0187 | 19.5 | 0.21 | 40 | 31.2 |
| 626 | 6 | 20 | 0.9968 | 0.0187 | 22.3 | 0.21 | 40 | 32.9 |
| 627 | 6 | 20 | 0.9968 | 0.0187 | 25.8 | 0.21 | 40 | 40.0 |
| 628 | 6 | 20 | 0.9968 | 0.0187 | 28.9 | 0.21 | 40 | 40.0 |
| 629 | 6 | 20 | 0.9968 | 0.0187 | 33.6 | 0.21 | 40 | 40.0 |
| 630 | 6 | 20 | 0.9968 | 0.0187 | 37.5 | 0.21 | 40 | 40.0 |
| 631 | 6 | 20 | 0.9968 | 0.0189 | 13.7 | 0.31 | 40 | 21.2 |
| 632 | 6 | 20 | 0.9968 | 0.0189 | 17.1 | 0.31 | 40 | 21.8 |
| 633 | 6 | 20 | 0.9968 | 0.0189 | 19.5 | 0.31 | 40 | 25.3 |
| 634 | 6 | 20 | 0.9968 | 0.0189 | 22.3 | 0.31 | 40 | 33.8 |
| 635 | 6 | 20 | 0.9968 | 0.0189 | 25.8 | 0.31 | 40 | 37.9 |
| 636 | 6 | 20 | 0.9968 | 0.0189 | 28.9 | 0.31 | 40 | 40.0 |
| 637 | 6 | 20 | 0.9968 | 0.0189 | 33.6 | 0.31 | 40 | 40.0 |
| 638 | 6 | 20 | 0.9968 | 0.0189 | 37.5 | 0.31 | 40 | 40.0 |
| 639 | 6 | 20 | 0.9968 | 0.0185 | 13.8 | 0.44 | 40 | 18.0 |
| 640 | 6 | 20 | 0.9968 | 0.0185 | 17.2 | 0.44 | 40 | 19.6 |
| 641 | 6 | 20 | 0.9968 | 0.0185 | 19.6 | 0.44 | 40 | 21.8 |
| 642 | 6 | 20 | 0.9968 | 0.0185 | 22.7 | 0.44 | 40 | 26.1 |
| 643 | 6 | 20 | 0.9968 | 0.0185 | 26.0 | 0.44 | 40 | 29.8 |
| 644 | 6 | 20 | 0.9968 | 0.0185 | 29.3 | 0.44 | 40 | 33.8 |
| 645 | 6 | 20 | 0.9968 | 0.0185 | 34.0 | 0.44 | 40 | 40.0 |
| 646 | 6 | 20 | 0.9968 | 0.0185 | 37.8 | 0.44 | 40 | 40.0 |
| 647 | 6 | 20 | 0.9966 | 0.0190 | 13.7 | 0.48 | 40 | 14.3 |

(Continued)

(3 of 7 sheets)

Table 1 (Continued)

| Test | $D_o$ in. | $D$ in. | $\rho_f$ g/cc | $\Delta\rho_m$ g/cc | $F_D$ | $U$ knots | $H$ ft | $Z_m$ ft |
|------|------|-----|--------|--------|------|------|----|------|
| 648 | 6 | 20 | 0.9966 | 0.0190 | 17.1 | 0.48 | 40 | 17,2 |
| 649 | 6 | 20 | 0.9966 | 0.0190 | 19.5 | 0.48 | 40 | 21,0 |
| 650 | 6 | 20 | 0.9966 | 0.0190 | 22.3 | 0.48 | 40 | 22,5 |
| 651 | 6 | 20 | 0.9966 | 0.0190 | 25.8 | 0.48 | 40 | 25,9 |
| 652 | 6 | 20 | 0.9966 | 0.0190 | 28.9 | 0.48 | 40 | 32,8 |
| 653 | 6 | 20 | 0.9966 | 0.0190 | 33.6 | 0.48 | 40 | 34,0 |
| 654 | 6 | 20 | 0.9966 | 0.0190 | 37.5 | 0.48 | 40 | 40,0 |
| 655 | 6 | 20 | 0.9968 | 0.0182 | 13.9 | 0.50 | 40 | 14,0 |
| 656 | 6 | 20 | 0.9968 | 0.0182 | 17.3 | 0.50 | 40 | 17,0 |
| 657 | 6 | 20 | 0.9968 | 0.0182 | 19.9 | 0.50 | 40 | 20,0 |
| 658 | 6 | 20 | 0.9968 | 0.0182 | 22.8 | 0.50 | 40 | 24,1 |
| 659 | 6 | 20 | 0.9968 | 0.0182 | 26.2 | 0.50 | 40 | 28,2 |
| 660 | 6 | 20 | 0.9968 | 0.0182 | 29.5 | 0.50 | 40 | 30,5 |
| 661 | 6 | 20 | 0.9968 | 0.0182 | 34.1 | 0.50 | 40 | 40,0 |
| 662 | 6 | 20 | 0.9968 | 0.0182 | 38.1 | 0.50 | 40 | 40,0 |
| 663 | 6 | 20 | 0.9965 | 0.0200 | 13.3 | 0.75 | 40 | 13,2 |
| 664 | 6 | 0 | 0.9965 | 0.0200 | 16.7 | 0.75 | 40 | 14,0 |
| 665 | 6 | 20 | 0.9965 | 0.0200 | 19,0 | 0.75 | 40 | 16,6 |
| 666 | 6 | 20 | 0.9965 | 0.0200 | 21.7 | 0.75 | 40 | 20,2 |
| 667 | 6 | 20 | 0.9965 | 0.0200 | 25.0 | 0.75 | 40 | 23,0 |
| 668 | 6 | 20 | 0.9965 | 0.0200 | 28.1 | 0.75 | 40 | 22,9 |
| 669 | 6 | 20 | 0.9965 | 0.0200 | 32.7 | 0.75 | 40 | 23,9 |
| 670 | 6 | 20 | 0.9965 | 0.0200 | 36.3 | 0.75 | 40 | 23,9 |
| 671 | 6 | 20 | 0.9965 | 0.0198 | 13.3 | 1.00 | 40 | 9,9 |
| 672 | 6 | 20 | 0.9965 | 0.0198 | 16.7 | 1.00 | 40 | 14,9 |
| 673 | 6 | 20 | 0.9965 | 0.0198 | 19.0 | 1.00 | 40 | 15,9 |
| 674 | 6 | 20 | 0.9965 | 0.0198 | 21.7 | 1.00 | 40 | 17,8 |
| 675 | 6 | 20 | 0.9965 | 0.0198 | 25.0 | 1.00 | 40 | 23,0 |
| 676 | 6 | 20 | 0.9965 | 0.0198 | 28.1 | 1.00 | 40 | 24,6 |
| 677 | 6 | 20 | 0.9965 | 0.0198 | 32.7 | 1.00 | 40 | 27,8 |
| 678 | 6 | 20 | 0.9965 | 0.0198 | 36.3 | 1.00 | 40 | 28,2 |
| 680 | 6 | 20 | 0.9983 | 0.0100 | 18.4 | 0.10 | 40 | 30,5 |
| 681 | 6 | 20 | 0.9983 | 0.0100 | 26.3 | 0.10 | 40 | 40,0 |
| 682 | 6 | 20 | 0.9983 | 0.0100 | 18.4 | 0.21 | 40 | 24,6 |
| 683 | 6 | 20 | 0.9983 | 0.0100 | 26.3 | 0.21 | 40 | 40,0 |
| 684 | 6 | 20 | 0.9983 | 0.0100 | 35.2 | 0.21 | 40 | 40,0 |
| 685 | 6 | 20 | 0.9983 | 0.0100 | 18.4 | 0.31 | 40 | 22,1 |
| 686 | 6 | 20 | 0.9983 | 0.0100 | 26.3 | 0.31 | 40 | 28,1 |
| 687 | 6 | 20 | 0.9983 | 0.0100 | 35.2 | 0.31 | 40 | 40,0 |
| 688 | 6 | 20 | 0.9983 | 0.0100 | 45.8 | 0.31 | 40 | 40,0 |
| 689 | 6 | 20 | 0.9983 | 0.0100 | 18.4 | 0.44 | 40 | 13,8 |
| 690 | 6 | 20 | 0.9983 | 0.0100 | 26.3 | 0.44 | 40 | 20,9 |
| 691 | 6 | 20 | 0.9983 | 0.0100 | 35.2 | 0.44 | 40 | 30,3 |
| 692 | 6 | 20 | 0.9983 | 0.0100 | 45.8 | 0.44 | 40 | 40,0 |
| 693 | 6 | 20 | 0.9983 | 0.0100 | 18.4 | 0.50 | 40 | 15,7 |
| 694 | 6 | 20 | 0.9983 | 0.0100 | 26.3 | 0.50 | 40 | 21,0 |
| 695 | 6 | 20 | 0.9983 | 0.0100 | 35.2 | 0.50 | 40 | 28,0 |
| 696 | 6 | 20 | 0.9983 | 0.0100 | 45.8 | 0.50 | 40 | 40,0 |
| 697 | 6 | 20 | 0.9983 | 0.0100 | 18.4 | 0.75 | 40 | 11,9 |
| 698 | 6 | 20 | 0.9983 | 0.0100 | 26.3 | 0.75 | 40 | 12,0 |
| 699 | 6 | 20 | 0.9983 | 0.0100 | 35.2 | 0.75 | 40 | 19,4 |
| 700 | 6 | 20 | 0.9983 | 0.0100 | 45.8 | 0.75 | 40 | 25,7 |
| 701 | 6 | 20 | 0.9983 | 0.0100 | 18.4 | 1.00 | 40 | 8,0 |
| 702 | 6 | 20 | 0.9983 | 0.0100 | 26.3 | 1.00 | 40 | 12,0 |

(Continued)                                    (4 of 7 sheets)

Table 1 (Continued)

| Test | $D_o$ in. | $D$ in. | $\rho_f$ g/cc | $\Delta\rho_m$ g/cc | $\mathbb{F}_D$ | $U$ knots | $H$ ft | $Z_m$ ft |
|------|------|------|--------|--------|------|------|----|------|
| 703 | 6 | 20 | 0.9983 | 0.0100 | 35.2 | 1.00 | 40 | 17.1 |
| 704 | 6 | 20 | 0.9983 | 0.0100 | 45.8 | 1.00 | 40 | 27.5 |
| 705 | 6 | 20 | 1.0002 | 0.0263 | 11.4 | 0.10 | 40 | 15.5 |
| 706 | 6 | 20 | 1.0002 | 0.0263 | 16.4 | 0.10 | 40 | 18.3 |
| 707 | 6 | 20 | 1.0002 | 0.0263 | 21.7 | 0.10 | 40 | 32.7 |
| 708 | 6 | 20 | 1.0002 | 0.0263 | 28.3 | 0.10 | 40 | 40.0 |
| 709 | 6 | 20 | 1.0020 | 0.0155 | 14.9 | 0.10 | 40 | 18.9 |
| 710 | 6 | 20 | 1.0020 | 0.0155 | 21.5 | 0.10 | 40 | 28.2 |
| 711 | 6 | 20 | 1.0020 | 0.0155 | 28.5 | 0.10 | 40 | 40.0 |
| 712 | 6 | 20 | 1.0002 | 0.0155 | 14.9 | 0.20 | 40 | 19.7 |
| 713 | 6 | 20 | 1.0002 | 0.0155 | 21.5 | 0.20 | 40 | 29.2 |
| 714 | 6 | 20 | 1.0002 | 0.0155 | 28.5 | 0.20 | 40 | 40.0 |
| 715 | 6 | 20 | 1.0002 | 0.0263 | 11.4 | 0.20 | 40 | 40.0 |
| 716 | 6 | 20 | 1.0002 | 0.0263 | 16.4 | 0.20 | 40 | 24.3 |
| 717 | 6 | 20 | 1.0002 | 0.0263 | 21.7 | 0.20 | 40 | 33.3 |
| 718 | 6 | 20 | 1.0002 | 0.0263 | 28.3 | 0.20 | 40 | 40.0 |
| 719 | 6 | 20 | 1.0002 | 0.0263 | 11.4 | 0.30 | 40 | 13.3 |
| 720 | 6 | 20 | 1.0002 | 0.0263 | 16.4 | 0.30 | 40 | 22.2 |
| 721 | 6 | 20 | 1.0002 | 0.0263 | 21.7 | 0.30 | 40 | 31.0 |
| 722 | 6 | 20 | 1.0002 | 0.0263 | 28.3 | 0.30 | 40 | 40.0 |
| 723 | 6 | 20 | 1.0002 | 0.0155 | 14.9 | 0.30 | 40 | 19.5 |
| 724 | 6 | 20 | 1.0002 | 0.0155 | 21.5 | 0.30 | 40 | 27.3 |
| 725 | 6 | 20 | 1.0002 | 0.0155 | 28.5 | 0.30 | 40 | 32.6 |
| 726 | 6 | 20 | 1.0002 | 0.0155 | 37.0 | 0.30 | 40 | 40.0 |
| 727 | 6 | 20 | 1.0002 | 0.0155 | 14.9 | 0.50 | 40 | 14.5 |
| 728 | 6 | 20 | 1.0002 | 0.0155 | 21.5 | 0.50 | 40 | 20.7 |
| 729 | 6 | 20 | 1.0002 | 0.0155 | 28.5 | 0.50 | 40 | 25.5 |
| 730 | 6 | 20 | 1.0002 | 0.0155 | 37.0 | 0.50 | 40 | 30.8 |
| 731 | 6 | 20 | 1.0002 | 0.0263 | 11.4 | 0.50 | 40 | 12.0 |
| 732 | 6 | 20 | 1.0002 | 0.0263 | 16.4 | 0.50 | 40 | 18.2 |
| 733 | 6 | 20 | 1.0002 | 0.0263 | 21.7 | 0.50 | 40 | 25.0 |
| 734 | 6 | 20 | 1.0002 | 0.0263 | 28.3 | 0.50 | 40 | 31.2 |
| 735 | 6 | 20 | 1.0002 | 0.0263 | 11.4 | 0.75 | 40 | 10.0 |
| 736 | 6 | 20 | 1.0002 | 0.0263 | 16.4 | 0.75 | 40 | 14.0 |
| 737 | 6 | 20 | 1.0002 | 0.0263 | 21.7 | 0.75 | 40 | 17.0 |
| 738 | 6 | 20 | 1.0002 | 0.0263 | 28.3 | 0.75 | 40 | 21.3 |
| 739 | 6 | 20 | 1.0002 | 0.0153 | 14.9 | 0.75 | 40 | 12.9 |
| 740 | 6 | 20 | 1.0002 | 0.0153 | 21.5 | 0.75 | 40 | 16.6 |
| 741 | 6 | 20 | 1.0002 | 0.0153 | 28.5 | 0.75 | 40 | 20.4 |
| 742 | 6 | 20 | 1.0002 | 0.0153 | 37.0 | 0.75 | 40 | 22.7 |
| 743 | 6 | 20 | 1.0002 | 0.0153 | 14.9 | 1.00 | 40 | 17.4 |
| 744 | 6 | 20 | 1.0002 | 0.0153 | 21.5 | 1.00 | 40 | 18.5 |
| 745 | 6 | 20 | 1.0002 | 0.0153 | 28.5 | 1.00 | 40 | 20.0 |
| 746 | 6 | 20 | 1.0002 | 0.0153 | 37.0 | 1.00 | 40 | 21.5 |
| 747 | 6 | 20 | 1.0002 | 0.0263 | 11.4 | 1.00 | 40 | 9.6 |
| 748 | 6 | 20 | 1.0002 | 0.0263 | 16.4 | 1.00 | 40 | 14.5 |
| 749 | 6 | 20 | 1.0002 | 0.0263 | 21.7 | 1.00 | 40 | 18.5 |
| 750 | 6 | 20 | 1.0002 | 0.0263 | 28.3 | 1.00 | 40 | 21.6 |
| 751 | 6 | 20 | 1.0005 | 0.0046 | 25.5 | 0.10 | 40 | 40.0 |
| 752 | 6 | 20 | 1.0005 | 0.0046 | 38.3 | 0.10 | 40 | 40.0 |
| 753 | 6 | 20 | 1.0005 | 0.0046 | 26.5 | 0.30 | 40 | 20.0 |
| 754 | 6 | 20 | 1.0005 | 0.0046 | 38.3 | 0.30 | 40 | 30.3 |
| 755 | 6 | 20 | 1.0005 | 0.0046 | 50.8 | 0.30 | 40 | 40.0 |
| 756 | 6 | 20 | 1.0005 | 0.0046 | 65.7 | 0.30 | 40 | 40.0 |

(Continued)        (5 of 7 sheets)

Table 1 (Continued)

| Test | $D_o$ in. | $D$ in. | $\rho_f$ g/cc | $\Delta\rho_m$ g/cc | $F_D$ | $U$ knots | $H$ ft | $Z_m$ ft |
|------|-----------|---------|---------------|---------------------|-------|-----------|--------|----------|
| 757 | 6 | 20 | 1.0005 | 0.0046 | 26.5 | 0.50 | 40 | 18.6 |
| 758 | 6 | 20 | 1.0005 | 0.0046 | 38.3 | 0.50 | 40 | 19.8 |
| 759 | 6 | 20 | 1.0005 | 0.0046 | 50.8 | 0.50 | 40 | 28.6 |
| 760 | 6 | 20 | 1.0005 | 0.0046 | 65.7 | 0.50 | 40 | 30.8 |
| 761 | 6 | 20 | 1.0005 | 0.0046 | 26.5 | 0.75 | 40 | 12.2 |
| 762 | 6 | 20 | 1.0005 | 0.0046 | 38.3 | 0.75 | 40 | 15.0 |
| 763 | 6 | 20 | 1.0005 | 0.0046 | 50.8 | 0.75 | 40 | 20.2 |
| 764 | 6 | 20 | 1.0005 | 0.0046 | 65.7 | 0.75 | 40 | 23.0 |
| 765 | 6 | 20 | 1.0005 | 0.0046 | 26.5 | 1.00 | 40 | 11.3 |
| 766 | 6 | 20 | 1.0005 | 0.0046 | 50.8 | 1.00 | 40 | 16.4 |
| 901 | 9 | 30 | 0.9967 | 0.0198 | 11.9 | 0.10 | 40 | 33.1 |
| 902 | 9 | 30 | 0.9967 | 0.0198 | 15.1 | 0.10 | 40 | 40.0 |
| 903 | 9 | 30 | 0.9967 | 0.0198 | 18.0 | 0.10 | 40 | 40.0 |
| 904 | 9 | 30 | 0.9967 | 0.0198 | 21.1 | 0.10 | 40 | 40.0 |
| 905 | 9 | 30 | 0.9967 | 0.0198 | 23.5 | 0.10 | 40 | 40.0 |
| 906 | 9 | 30 | 0.9967 | 0.0198 | 26.4 | 0.10 | 40 | 40.0 |
| 907 | 9 | 30 | 0.9967 | 0.0198 | 29.0 | 0.10 | 40 | 40.0 |
| 908 | 9 | 30 | 0.9967 | 0.0196 | 11.9 | 0.21 | 40 | 31.0 |
| 909 | 9 | 30 | 0.9967 | 0.0196 | 15.1 | 0.21 | 40 | 37.3 |
| 910 | 9 | 30 | 0.9967 | 0.0196 | 18.0 | 0.21 | 40 | 40.0 |
| 911 | 9 | 30 | 0.9967 | 0.0196 | 21.1 | 0.21 | 40 | 40.0 |
| 912 | 9 | 30 | 0.9967 | 0.0196 | 23.5 | 0.21 | 40 | 40.0 |
| 913 | 9 | 30 | 0.9967 | 0.0196 | 26.4 | 0.21 | 40 | 40.0 |
| 914 | 9 | 30 | 0.9967 | 0.0196 | 29.0 | 0.21 | 40 | 40.0 |
| 915 | 9 | 30 | 0.9967 | 0.0196 | 11.9 | 0.31 | 40 | 29.8 |
| 916 | 9 | 30 | 0.9967 | 0.0196 | 15.1 | 0.31 | 40 | 37.8 |
| 917 | 9 | 30 | 0.9967 | 0.0196 | 18.0 | 0.31 | 40 | 40.0 |
| 918 | 9 | 30 | 0.9967 | 0.0196 | 21.1 | 0.31 | 40 | 40.0 |
| 919 | 9 | 30 | 0.9967 | 0.0196 | 23.5 | 0.31 | 40 | 40.0 |
| 920 | 9 | 30 | 0.9967 | 0.0196 | 26.4 | 0.31 | 40 | 40.0 |
| 921 | 9 | 30 | 0.9967 | 0.0196 | 29.0 | 0.31 | 40 | 40.0 |
| 922 | 9 | 30 | 0.9963 | 0.0203 | 11.8 | 0.44 | 40 | 26.0 |
| 923 | 9 | 30 | 0.9963 | 0.0203 | 15.0 | 0.44 | 40 | 29.7 |
| 924 | 9 | 30 | 0.9963 | 0.0203 | 17.9 | 0.44 | 40 | 38.8 |
| 925 | 9 | 30 | 0.9963 | 0.0203 | 21.0 | 0.44 | 40 | 40.0 |
| 926 | 9 | 30 | 0.9963 | 0.0203 | 23.3 | 0.44 | 40 | 40.0 |
| 927 | 9 | 30 | 0.9963 | 0.0203 | 26.2 | 0.44 | 40 | 40.0 |
| 928 | 9 | 30 | 0.9963 | 0.0203 | 28.7 | 0.44 | 40 | 40.0 |
| 930 | 9 | 30 | 0.9966 | 0.0199 | 11.9 | 0.48 | 40 | 24.6 |
| 931 | 9 | 30 | 0.9966 | 0.0199 | 15.1 | 0.48 | 40 | 28.2 |
| 932 | 9 | 30 | 0.9966 | 0.0199 | 18.0 | 0.48 | 40 | 35.0 |
| 933 | 9 | 30 | 0.9966 | 0.0199 | 21.1 | 0.48 | 40 | 40.0 |
| 934 | 9 | 30 | 0.9966 | 0.0199 | 23.5 | 0.48 | 40 | 40.0 |
| 935 | 9 | 30 | 0.9966 | 0.0199 | 26.4 | 0.48 | 40 | 40.0 |
| 936 | 9 | 30 | 0.9966 | 0.0199 | 29.0 | 0.48 | 40 | 40.0 |
| 937 | 9 | 30 | 0.9967 | 0.0197 | 11.9 | 0.50 | 40 | 25.1 |
| 938 | 9 | 30 | 0.9967 | 0.0197 | 15.1 | 0.50 | 40 | 29.9 |
| 939 | 9 | 30 | 0.9967 | 0.0197 | 18.0 | 0.50 | 40 | 36.2 |
| 940 | 9 | 30 | 0.9967 | 0.0197 | 21.1 | 0.50 | 40 | 40.0 |
| 941 | 9 | 30 | 0.9967 | 0.0197 | 23.5 | 0.50 | 40 | 40.0 |
| 942 | 9 | 30 | 0.9997 | 0.0197 | 26.4 | 0.50 | 40 | 40.0 |
| 943 | 9 | 30 | 0.9967 | 0.0197 | 29.0 | 0.50 | 40 | 40.0 |
| 944 | 9 | 30 | 0.9968 | 0.0196 | 11.9 | 0.75 | 40 | 21.1 |
| 945 | 9 | 30 | 0.9968 | 0.0196 | 15.1 | 0.75 | 40 | 22.0 |

(Continued)                    (6 of 7 sheets)

Table 1 (Concluded)

| Test | $D_o$ in. | $D$ in. | $\rho_f$ g/cc | $\Delta\rho_m$ g/cc | $F_D$ | $U$ knots | $H$ ft | $Z_m$ ft |
|------|------|------|--------|--------|------|-------|------|------|
| 946 | 9 | 30 | 0.9968 | 0.0196 | 18.0 | 0.75 | 40 | 26.7 |
| 947 | 9 | 30 | 0.9968 | 0.0196 | 21.1 | 0.75 | 40 | 28.0 |
| 948 | 9 | 30 | 0.9968 | 0.0196 | 23.5 | 0.75 | 40 | 30.3 |
| 949 | 9 | 30 | 0.9968 | 0.0196 | 26.4 | 0.75 | 40 | 32.8 |
| 950 | 9 | 30 | 0.9968 | 0.0196 | 29.0 | 0.75 | 40 | 40.0 |
| 951 | 9 | 30 | 0.9967 | 0.0197 | 11.9 | 1.00 | 40 | 17.8 |
| 952 | 9 | 30 | 0.9967 | 0.0197 | 15.1 | 1.00 | 40 | 22.0 |
| 953 | 9 | 30 | 0.9967 | 0.0197 | 18.0 | 1.00 | 40 | 23.0 |
| 954 | 9 | 30 | 0.9967 | 0.0197 | 21.1 | 1.00 | 40 | 27.0 |
| 955 | 9 | 30 | 0.9967 | 0.0197 | 23.5 | 1.00 | 40 | 27.2 |
| 956 | 9 | 30 | 0.9967 | 0.0197 | 26.4 | 1.00 | 40 | 32.3 |
| 957 | 9 | 30 | 0.9967 | 0.0197 | 29.0 | 1.00 | 40 | 37.0 |
| 960 | 9 | 30 | 0.9983 | 0.0100 | 16.6 | 0.10 | 40 | 40.0 |
| 961 | 9 | 30 | 0.9983 | 0.0100 | 16.6 | 0.31 | 40 | 33.0 |
| 962 | 9 | 30 | 0.9983 | 0.0100 | 25.2 | 0.31 | 40 | 40.0 |
| 963 | 9 | 30 | 0.9983 | 0.0100 | 16.6 | 0.50 | 40 | 23.0 |
| 964 | 9 | 30 | 0.9983 | 0.0100 | 25.2 | 0.50 | 40 | 40.0 |
| 965 | 9 | 30 | 0.9983 | 0.0100 | 33.0 | 0.50 | 40 | 40.0 |
| 966 | 9 | 30 | 0.9983 | 0.0100 | 40.8 | 0.50 | 40 | 40.0 |
| 967 | 9 | 30 | 0.9983 | 0.0100 | 16.6 | 0.75 | 40 | 22.0 |
| 968 | 9 | 30 | 0.9983 | 0.0100 | 25.2 | 0.75 | 40 | 22.0 |
| 969 | 9 | 30 | 0.9983 | 0.0100 | 33.0 | 0.75 | 40 | 31.0 |
| 970 | 9 | 30 | 0.9983 | 0.0100 | 40.8 | 0.75 | 40 | 40.0 |
| 971 | 9 | 30 | 0.9982 | 0.0103 | 16.6 | 1.00 | 40 | 20.0 |
| 972 | 9 | 30 | 0.9982 | 0.0103 | 25.2 | 1.00 | 40 | 25.3 |
| 973 | 9 | 30 | 0.9982 | 0.0103 | 33.0 | 1.00 | 40 | 27.6 |
| 974 | 9 | 30 | 0.9982 | 0.0103 | 40.8 | 1.00 | 40 | 36.2 |
| 975 | 9 | 30 | 0.9982 | 0.0103 | 16.6 | 0.75 | 30 | 22.0 |
| 976 | 9 | 30 | 0.9982 | 0.0103 | 25.2 | 0.75 | 30 | 29.0 |
| 977 | 9 | 30 | 0.9982 | 0.0103 | 21.1 | 0.75 | 30 | 22.0 |
| 978 | 9 | 30 | 0.9982 | 0.0103 | 16.6 | 0.50 | 30 | 25.8 |
| 979 | 9 | 30 | 0.9982 | 0.0103 | 21.1 | 0.50 | 30 | 30.0 |
| 980 | 9 | 30 | 0.9982 | 0.0103 | 16.6 | 0.50 | 30 | 30.0 |

(7 of 7 sheets)

**Table 2**

Dilution Tests

| Test | D_c in. | D in. | Δρ_m g/cc | F_D | U knots | H ft | Minimum Observed Dilution (Dimensionless) at Indicated Distance Downstream from Diffuser (ft) | | | | | | | | | | | | | | | | | | | | |
|---|---|---|---|---|---|---|---|---|---|---|---|---|---|---|---|---|---|---|---|---|---|---|---|---|---|---|---|
| | | | | | | | 5 | 10 | 15 | 20 | 30 | 40 | 50 | 60 | 80 | 100 | 120 | 160 | 200 | 220 | 240 | 280 | 320 | 400 | 440 | 480 | 500 |
| 420 | 3 | 20 | 0.021 | 36.3 | 0.5 | 40 | | | | | | 252 | | | 489 | | 532 | 792 | 703 | | | | 1380 | | | | |
| 421 | 3 | 20 | 0.022 | 36.3 | 1.0 | 40 | | | | | | | | | 980 | | | | 1619 | | | | 3388 | | | | |
| 615 | 6 | 20 | 0.021 | 13.1 | 0.1 | 40 | 40 | 80 | 95 | | | | | | | | | | | | | | | | | | |
| 617 | 6 | 20 | 0.021 | 18.9 | 0.1 | 40 | | 37 | | 63 | 108 | | | | | | | | | | | | | | | | |
| 619 | 6 | 20 | 0.021 | 25.0 | 0.1 | 40 | | 36 | | 49 | 48 | 83 | | | | | | | | | | | | | | | |
| 621 | 6 | 20 | 0.021 | 32.2 | 0.1 | 40 | | 37 | | | 37 | | | 75 | 103 | | | | | | | | | | | | |
| 623 | 6 | 20 | 0.021 | 13.2 | 0.2 | 40 | | 64 | | | 83 | | | | | 108 | | | | | | | | | | | |
| 625 | 6 | 20 | 0.021 | 18.3 | 0.2 | 40 | | | | 42 | | 78 | | | | 81 | | | | | | | | | | | |
| 627 | 6 | 20 | 0.021 | 25.1 | 0.2 | 40 | | | | 21 | | 44 | | | | | 55 | | | | | | | | | | |
| 629 | 6 | 20 | 0.021 | 32.6 | 0.2 | 40 | | | | 20 | | | | | | 41 | 68 | | | | | | | | | | |
| 631 | 6 | 20 | 0.021 | 13.0 | 0.3 | 40 | | | | | | 64 | | | 124 | | 190 | 215 | | | | | | | | | |
| 633 | 6 | 20 | 0.021 | 19.0 | 0.3 | 40 | | | | | | 56 | | | 85 | | 95 | 153 | | | | | | | | | |
| 635 | 6 | 20 | 0.021 | 25.2 | 0.3 | 40 | | | | | | 66 | | | 87 | | 137 | 131 | | | 197 | | | | | | |
| 637 | 6 | 20 | 0.021 | 32.9 | 0.3 | 40 | | | | | | 77 | | | 102 | | 158 | 160 | | | 200 | | | | | | |
| 639 | 6 | 20 | 0.021 | 13.2 | 0.44 | 40 | | | | | | 70 | | | | 142 | | 156 | | | | | | | | | |
| 641 | 6 | 20 | 0.021 | 19.0 | 0.44 | 40 | | | | | | 72 | | | | 148 | | 182 | | | | | | | | | |
| 643 | 6 | 20 | 0.021 | 24.7 | 0.44 | 40 | | | | | | 40 | | | | 59 | | 78 | | | | | | | | | |
| 645 | 6 | 20 | 0.021 | 32.7 | 0.44 | 40 | | | | | | 44 | | | | 75 | | 86 | | 90 | | | | | | | |
| 655 | 6 | 20 | 0.021 | 13.3 | 0.5 | 40 | | | | | | 80 | | | 124 | | 121 | 215 | 182 | | 212 | | | | | | |
| 657 | 6 | 20 | 0.021 | 16.7 | 0.5 | 40 | | | | | | 71 | | | 148 | | 138 | 134 | 177 | | | 188 | | | | | |
| 659 | 6 | 20 | 0.021 | 24.6 | 0.5 | 40 | | | | | | 85 | | | 172 | | 132 | 148 | 170 | | 168 | | | | | | |
| 661 | 6 | 20 | 0.021 | 32.1 | 0.5 | 40 | | | | | | 64 | | | 115 | | 94 | 137 | | | 177 | | | | 358 | | |
| 663 | 6 | 20 | 0.021 | 13.1 | 0.75 | 40 | | | | | | 157 | | | 197 | | 219 | 285 | 426 | | 436 | 442 | | | | | |
| 665 | 6 | 20 | 0.021 | 18.6 | 0.75 | 40 | | | | | | 125 | | | 240 | | | 302 | | | 408 | | 460 | | 660 | | |
| 667 | 6 | 20 | 0.021 | 24.2 | 0.75 | 40 | | | | | | 128 | | | 143 | | | 209 | | | 387 | | 460 | | | 542 | 603 |
| 669 | 6 | 20 | 0.021 | 31.7 | 0.75 | 40 | | | | | | 95 | | | 178 | | | 218 | | | 296 | | 396 | 396 | | | 572 |
| 671 | 6 | 20 | 0.021 | 12.9 | 1.0 | 40 | | | | | | 337 | | | 365 | | | 680 | | | 1060 | | 1020 | 2000 | | | |
| 673 | 6 | 20 | 0.021 | 18.3 | 1.0 | 40 | | | | | | 250 | | | 365 | | | 570 | | | 840 | | 1170 | 1420 | | | |
| 675 | 6 | 20 | 0.021 | 24.6 | 1.0 | 40 | | | | | | 237 | | | 382 | | | 570 | | | 715 | | 900 | | 1520 | | |
| 677 | 6 | 20 | 0.021 | 32.1 | 1.0 | 40 | | | | | | 178 | | | 363 | | | 700 | | | 940 | | 980 | | | 1780 | |
| 686 | 6 | 20 | 0.011 | 26.8 | 0.3 | 40 | | | | | | 116 | | | | | 241 | | | | | | | | | | |
| 694 | 6 | 20 | 0.011 | 26.8 | 0.5 | 40 | | | | | | 105 | | | 238 | | 336 | | | | 401 | | | | | | |
| 936 | 9 | 30 | 0.021 | 11.5 | 0.5 | 40 | | | | | | 76 | | | | 124 | | 207 | | | | | 909 | | | | |
| 950 | 9 | 30 | 0.022 | 11.5 | 1.0 | 40 | | | | | | | | | | | | 264 | | | | | 490 | | | | |
| 4-615* | 6 | 20 | 0.021 | 13.1 | 0.1 | 40 | 33 | | | | | | | | | | | | | | | | | | | | |
| 4-655* | 6 | 20 | 0.021 | 13.1 | 0.5 | 40 | | | | | | 150 | | | | | | 111 | | | | | | | | | |
| 4-659* | 6 | 20 | 0.021 | 24.8 | 0.5 | 40 | | | | | | 81 | | | | | | 128 | | | | | | | | | |
| 4-671* | 6 | 20 | 0.021 | 13.1 | 1.0 | 40 | | | | | | | | | 207 | | | | | | 348 | | | | | | |
| 4-675* | 6 | 20 | 0.021 | 24.8 | 1.0 | 40 | | | | | | | | | 184 | | | | | | 231 | | | | | | |
| Heated** | 6 | 20 | 0.021 | 18.8 | 0.5 | 40 | | | | | | 113 | | | 157 | | 210 | | | | 422 | | | | | | |
| Outfall 1† | -- | 20 | 0.021 | -- | 0.1 | 40 | | | | | | | | | | | | | | | | | | | | |
| Outfall 2† | -- | 20 | 0.021 | -- | 0.5 | 40 | | | | | | | | | | | | | | | | | | | | |
| Outfall 3† | -- | 20 | 0.021 | -- | 1.0 | 40 | | | | | | | | | | | | | | | | | | | | |

* 4 ports at 13 ft c.c.
** Heated brine.
† Q_b = 5.91 cfs.

48

## Table 3

### Lateral Spread Coordinates

| Test | Coordinates of Lateral Spread of Brine, ft | | | | | | | | | | | | | | | | | | |
|---|---|---|---|---|---|---|---|---|---|---|---|---|---|---|---|---|---|---|---|
| | x | w | x | w | x | w | x | w | x | w | x | w | x | w | x | w | x | w | x | w |
| 307 | 40 | 33 | 80 | 82 | 100 | 103 | | | | | | | | | | | | | | |
| 308 | 40 | 30 | 80 | 72 | 120 | 106 | | | | | | | | | | | | | | |
| 309 | 40 | 26 | 80 | 52 | 120 | 91 | 140 | 112 | | | | | | | | | | | | |
| 310 | 40 | 23 | 80 | 48 | 120 | 86 | 60 | 32 | 150 | 113 | | | | | | | | | | |
| 311 | 40 | 15 | 80 | 38 | 120 | 106 | | | | | | | | | | | | | | |
| 312 | 20 | 22 | 80 | 36 | 120 | 76 | 140 | 104 | | | | | | | | | | | | |
| 313 | 40 | 25 | 80 | 23 | 120 | 40 | 155 | 101 | | | | | | | | | | | | |
| 314 | 40 | 20 | 60 | 33 | 80 | 38 | 100 | 47 | 140 | 64 | 180 | 87 | | | | | | | | |
| 315 | 40 | 11 | 60 | 23 | 80 | 36 | 100 | 50 | 140 | 71 | 180 | 87 | | | | | | | | |
| 316 | 40 | 15 | 60 | 25 | 80 | 47 | 100 | 57 | 140 | 73 | 180 | 97 | | | | | | | | |
| 317 | 40 | 17 | 60 | 20 | 80 | 23 | 100 | 31 | 140 | 70 | 180 | 87 | | | | | | | | |
| 318 | 40 | 16 | 60 | 22 | 80 | 27 | 100 | 32 | 140 | 52 | 180 | 78 | 220 | 97 | 260 | 107 | | | | |
| 319 | 46 | 25 | 60 | 29 | 80 | 35 | 100 | 37 | 140 | 49 | 180 | 76 | 220 | 98 | | | | | | |
| 320 | 40 | 23 | 60 | 30 | 80 | 37 | 100 | 38 | 140 | 41 | 180 | 62 | 220 | 96 | | | | | | |
| 321 | 40 | 8 | 80 | 26 | 120 | 32 | 160 | 35 | 200 | 42 | 240 | 54 | 280 | 62 | | | | | | |
| 322 | 40 | 14 | 80 | 24 | 120 | 25 | 160 | 44 | 200 | 49 | 240 | 51 | 280 | 60 | 320 | 65 | | | | |
| 323 | 40 | 16 | 80 | 20 | 120 | 27 | 160 | 35 | 200 | 48 | 240 | 70 | 280 | 72 | 320 | 75 | | | | |
| 324 | 40 | 17 | 80 | 19 | 120 | 36 | 160 | 36 | 200 | 42 | 240 | 60 | 280 | 67 | 320 | 80 | | | | |
| 325 | 40 | 16 | 80 | 25 | 120 | 30 | 160 | 29 | 200 | 49 | 240 | 60 | 280 | 66 | 320 | 72 | | | | |
| 326 | 40 | 19 | 80 | 21 | 120 | 26 | 160 | 35 | 200 | 40 | 240 | 53 | 280 | 65 | 320 | 80 | | | | |
| 327 | 40 | 20 | 80 | 29 | 120 | 28 | 160 | 33 | 200 | 44 | 240 | 41 | 280 | 59 | 320 | 72 | | | | |
| 328 | 40 | 9 | 80 | 27 | 120 | 28 | 160 | 25 | 200 | 23 | 240 | 30 | 280 | 40 | 320 | 44 | | | | |
| 329 | 40 | 12 | 80 | 21 | 120 | 28 | 160 | 36 | 200 | 36 | 240 | 49 | 280 | 49 | 320 | 54 | | | | |
| 330 | 40 | 10 | 80 | 24 | 120 | 24 | 160 | 34 | 200 | 41 | 240 | 46 | 280 | 60 | 320 | 60 | | | | |
| 331 | 40 | 19 | 80 | 23 | 120 | 26 | 160 | 29 | 200 | 25 | 240 | 46 | 280 | 48 | 320 | 72 | | | | |
| 333 | 40 | 17 | 80 | 25 | 120 | 33 | 160 | 37 | 200 | 43 | 240 | 48 | 280 | 57 | 320 | 64 | | | | |
| 334 | 40 | 18 | 80 | 21 | 120 | 25 | 160 | 34 | 200 | 51 | 240 | 48 | 280 | 48 | 320 | 52 | | | | |
| 335 | 40 | 6 | 80 | 7 | 120 | 13 | 160 | 15 | 120 | 24 | 240 | 23 | | | | | | | | |
| 336 | 40 | 7 | 80 | 10 | 120 | 20 | 160 | 19 | 200 | 16 | 240 | 22 | 280 | 40 | | | | | | |
| 337 | 40 | 9 | 80 | 18 | 120 | 28 | 160 | 25 | 200 | 25 | 240 | 35 | 280 | 37 | | | | | | |
| 338 | 40 | 6 | 80 | 8 | 120 | 13 | 160 | 15 | 200 | 19 | 240 | 20 | 280 | 23 | | | | | | |
| 339 | 40 | 12 | 80 | 22 | 120 | 25 | 160 | 30 | 200 | 30 | 240 | 34 | 280 | 35 | 320 | 40 | | | | |
| 340 | 40 | 11 | 80 | 16 | 120 | 24 | 160 | 29 | 200 | 31 | 240 | 33 | 280 | 35 | 320 | 32 | | | | |
| 341 | 40 | 15 | 80 | 17 | 120 | 29 | 160 | 31 | 200 | 33 | 240 | 34 | 280 | 40 | 320 | 44 | | | | |
| 342 | 40 | 8 | 80 | 12 | 120 | 18 | 160 | 20 | 200 | 18 | 240 | 17 | 280 | 20 | | | | | | |
| 343 | 40 | 8 | 80 | 11 | 120 | 17 | 160 | 22 | 200 | 24 | 240 | 31 | | | | | | | | |
| 344 | 40 | 8 | 80 | 13 | 120 | 24 | 160 | 21 | 200 | 21 | | | | | | | | | | |
| 345 | 40 | 10 | 80 | 14 | 120 | 25 | 160 | 27 | 200 | 25 | | | | | | | | | | |
| 346 | 40 | 11 | 80 | 13 | 120 | 15 | 160 | 21 | 200 | 23 | 240 | 20 | 280 | 22 | | | | | | |
| 347 | 40 | 15 | 80 | 23 | 120 | 35 | 160 | 35 | 200 | 36 | | | | | | | | | | |
| 348 | 40 | 15 | 80 | 20 | 120 | 25 | 160 | 33 | 200 | 32 | | | | | | | | | | |
| 355 | 40 | 17 | 80 | 24 | 120 | 30 | | | | | | | | | | | | | | |
| 356 | 40 | 18 | 80 | 26 | 120 | 30 | | | | | | | | | | | | | | |
| 357 | 40 | 24 | 80 | 26 | 120 | 24 | | | | | | | | | | | | | | |
| 358 | 40 | 12 | 80 | 14 | 120 | 17 | | | | | | | | | | | | | | |
| 359 | 40 | 17 | 80 | 24 | 120 | 27 | | | | | | | | | | | | | | |
| 360 | 40 | 19 | 80 | 22 | 120 | 27 | | | | | | | | | | | | | | |
| 362 | 40 | 12 | 80 | 18 | | | | | | | | | | | | | | | | |
| 363 | 40 | 15 | 80 | 23 | | | | | | | | | | | | | | | | |
| 364 | 40 | 17 | 80 | 21 | 120 | 27 | | | | | | | | | | | | | | |
| 623 | 40 | 59 | 60 | 110 | | | | | | | | | | | | | | | | |
| 624 | 40 | 59 | 60 | 110 | | | | | | | | | | | | | | | | |
| 625 | 40 | 20 | 70 | 114 | | | | | | | | | | | | | | | | |
| 626 | 40 | 19 | 70 | 100 | | | | | | | | | | | | | | | | |

(Continued)

(1 of 4 sheets)

Table 3 (Continued)

| Test | x | w | x | w | x | w | x | w | x | w | x | w | x | w | x | w | x | w |
|---|---|---|---|---|---|---|---|---|---|---|---|---|---|---|---|---|---|---|
| 627 | 40 | 20 | 80 | 25 | 100 | 118 | | | | | | | | | | | | |
| 628 | 40 | 36 | 80 | 38 | 120 | 118 | | | | | | | | | | | | |
| 631 | 40 | 20 | 60 | 26 | | | | | | | | | | | | | | |
| 632 | 40 | 19 | 60 | 33 | 80 | 62 | | | | | | | | | | | | |
| 633 | 40 | 32 | 60 | 45 | 80 | 61 | 100 | 71 | 140 | 104 | | | | | | | | |
| 634 | 40 | 23 | 60 | 28 | 80 | 35 | 100 | 59 | 140 | 105 | | | | | | | | |
| 635 | 40 | 24 | 60 | 31 | 80 | 36 | 100 | 55 | 140 | 95 | 160 | 109 | | | | | | |
| 636 | 40 | 28 | 60 | 33 | 80 | 34 | 100 | 32 | 140 | 54 | 180 | 95 | | | | | | |
| 637 | 40 | 28 | 60 | 28 | 80 | 30 | 100 | 27 | 140 | 50 | 180 | 93 | | | | | | |
| 638 | 40 | 31 | 60 | 39 | 80 | 42 | 100 | 38 | 140 | 50 | 180 | 70 | 220 | 96 | | | | |
| 639 | 40 | 17 | 80 | 27 | 120 | 62 | 160 | 86 | | | | | | | | | | |
| 640 | 40 | 20 | 80 | 26 | 120 | 60 | 160 | 82 | 200 | 97 | | | | | | | | |
| 641 | 40 | 16 | 80 | 30 | 120 | 52 | 160 | 87 | 200 | 102 | | | | | | | | |
| 642 | 40 | 15 | 80 | 27 | 120 | 53 | 160 | 78 | 200 | 94 | | | | | | | | |
| 643 | 40 | 17 | 80 | 26 | 120 | 51 | 160 | 74 | 200 | 95 | | | | | | | | |
| 644 | 40 | 20 | 80 | 26 | 120 | 47 | 160 | 76 | 200 | 91 | | | | | | | | |
| 645 | 40 | 22 | 80 | 33 | 120 | 40 | 160 | 47 | 200 | 77 | 230 | 92 | | | | | | |
| 646 | 40 | 14 | 80 | 22 | 120 | 33 | 160 | 54 | 200 | 73 | 240 | 97 | | | | | | |
| 647 | 40 | 18 | 80 | 27 | 120 | 53 | 160 | 68 | 200 | 87 | 240 | 100 | | | | | | |
| 648 | 40 | 17 | 80 | 26 | 120 | 45 | 160 | 63 | 200 | 91 | | | | | | | | |
| 649 | 40 | 11 | 80 | 25 | 120 | 49 | 160 | 65 | 200 | 82 | 240 | 99 | | | | | | |
| 650 | 40 | 17 | 80 | 28 | 120 | 45 | 160 | 65 | 200 | 75 | 240 | 92 | | | | | | |
| 651 | 40 | 24 | 80 | 27 | 120 | 50 | 160 | 57 | 200 | 82 | | | | | | | | |
| 652 | 40 | 26 | 80 | 30 | 120 | 33 | 160 | 50 | 200 | 74 | 240 | 90 | | | | | | |
| 653 | 40 | 23 | 80 | 36 | 120 | 42 | 160 | 60 | 200 | 78 | 240 | 84 | | | | | | |
| 654 | 40 | 30 | 80 | 36 | 120 | 42 | 160 | 46 | 200 | 60 | 240 | 70 | 280 | 84 | | | | |
| 655 | 40 | 17 | 60 | 20 | 80 | 30 | 100 | 43 | 140 | 56 | 180 | 65 | 220 | 80 | | | | |
| 656 | 40 | 18 | 60 | 21 | 80 | 26 | 100 | 33 | 140 | 50 | 180 | 70 | 220 | 85 | | | | |
| 657 | 40 | 21 | 60 | 23 | 80 | 26 | 100 | 36 | 140 | 56 | 180 | 70 | 220 | 81 | | | | |
| 658 | 40 | 21 | 60 | 25 | 80 | 30 | 100 | 35 | 140 | 50 | 180 | 64 | 220 | 80 | | | | |
| 659 | 40 | 26 | 60 | 29 | 80 | 30 | 100 | 35 | 140 | 46 | 180 | 70 | 220 | 83 | | | | |
| 660 | 40 | 25 | 60 | 30 | 80 | 34 | 100 | 35 | 140 | 42 | 180 | 57 | 220 | 75 | 260 | 90 | | |
| 661 | 40 | 21 | 60 | 24 | 80 | 28 | 100 | 36 | 140 | 51 | 180 | 60 | 220 | 74 | | | | |
| 662 | 40 | 26 | 60 | 29 | 80 | 29 | 100 | 28 | 140 | 34 | 180 | 49 | 220 | 63 | 260 | 72 | 300 | 92 |
| 663 | 40 | 17 | 60 | 24 | 80 | 26 | 100 | 32 | 140 | 40 | 180 | 45 | 220 | 47 | 260 | 55 | 300 | 65 |
| 664 | 40 | 19 | 60 | 22 | 80 | 26 | 100 | 26 | 140 | 28 | 180 | 34 | 220 | 40 | 260 | 45 | 300 | 48 |
| 665 | 40 | 23 | 60 | 22 | 80 | 25 | 100 | 27 | 140 | 34 | 180 | 43 | 220 | 53 | 260 | 65 | 300 | 70 |
| 666 | 40 | 25 | 60 | 26 | 80 | 27 | 100 | 32 | 140 | 36 | 180 | 43 | 220 | 52 | 260 | 58 | 300 | 67 |
| 667 | 40 | 15 | 60 | 19 | 80 | 25 | 100 | 29 | 140 | 42 | 180 | 49 | 220 | 51 | 260 | 53 | 300 | 65 |
| 668 | 40 | 20 | 60 | 21 | 80 | 26 | 100 | 34 | 140 | 42 | 180 | 46 | 220 | 52 | 260 | 55 | 300 | 63 |
| 669 | 40 | 20 | 60 | 23 | 80 | 27 | 100 | 29 | 140 | 34 | 180 | 44 | 220 | 56 | 260 | 60 | 300 | 69 |
| 670 | 40 | 19 | 60 | 23 | 80 | 27 | 100 | 28 | 140 | 35 | 180 | 44 | 220 | 46 | 260 | 48 | 300 | 62 |
| 671 | 40 | 12 | 80 | 17 | 120 | 22 | 160 | 22 | 200 | 24 | 240 | 27 | 260 | 26 | 320 | 28 | | |
| 672 | 40 | 14 | 80 | 17 | 120 | 21 | 160 | 25 | 200 | 30 | 240 | 30 | 280 | 35 | 320 | 33 | | |
| 673 | 40 | 21 | 80 | 28 | 120 | 33 | 160 | 39 | 200 | 41 | 240 | 41 | 260 | 40 | 320 | 42 | | |
| 674 | 40 | 15 | 80 | 22 | 120 | 30 | 160 | 38 | 200 | 40 | 240 | 40 | 280 | 39 | 320 | 40 | | |
| 675 | 40 | 10 | 80 | 15 | 120 | 22 | 160 | 31 | 200 | 41 | 240 | 44 | 280 | 47 | | | | |
| 676 | 40 | 13 | 80 | 20 | 120 | 30 | 160 | 45 | 200 | 46 | 240 | 55 | 280 | 58 | 320 | 60 | | |
| 677 | 40 | 23 | 80 | 37 | 120 | 42 | 160 | 42 | 200 | 46 | 240 | 49 | 280 | 53 | 320 | 50 | | |
| 678 | 40 | 16 | 80 | 24 | 120 | 30 | 160 | 36 | 200 | 40 | 240 | 38 | 280 | 37 | 320 | 38 | | |
| 682 | 40 | 29 | 80 | 67 | 120 | 111 | | | | | | | | | | | | |
| 683 | 40 | 22 | 80 | 33 | 120 | 78 | 140 | 98 | | | | | | | | | | |
| 684 | 40 | 32 | 80 | 37 | 120 | 45 | 160 | 67 | 200 | 110 | 225 | 125 | | | | | | |
| 685 | 40 | 21 | 80 | 32 | 120 | 56 | 160 | 85 | | | | | | | | | | |

(Continued)

Table 3 (Continued)

| Test | Coordinates of Lateral Spread of Brine, ft | | | | | | | | | | | | | | | | | |
| --- | --- | --- | --- | --- | --- | --- | --- | --- | --- | --- | --- | --- | --- | --- | --- | --- | --- | --- |
| | x | w | x | w | x | w | x | w | x | w | x | w | x | w | x | w | x | w |
| 686 | 40 | 19 | 80 | 28 | 120 | 54 | 160 | 80 | | | | | | | | | | |
| 687 | 40 | 20 | 80 | 27 | 120 | 32 | 160 | 46 | 200 | 86 | | | | | | | | |
| 688 | 40 | 27 | 80 | 40 | 120 | 45 | 160 | 49 | 200 | 63 | | | | | | | | |
| 689 | 40 | 20 | 80 | 26 | 120 | 38 | 160 | 52 | 200 | 65 | 240 | 81 | | | | | | |
| 690 | 40 | 19 | 80 | 27 | 120 | 35 | 160 | 54 | 240 | 75 | | | | | | | | |
| 691 | 40 | 17 | 80 | 26 | 120 | 30 | 160 | 53 | 200 | 67 | 240 | 86 | | | | | | |
| 692 | 40 | 21 | 80 | 37 | 120 | 39 | 160 | 40 | 200 | 42 | 240 | 44 | 280 | 47 | 320 | 57 | | |
| 693 | 40 | 18 | 80 | 26 | 120 | 37 | 160 | 47 | 200 | 58 | 240 | 67 | 260 | 76 | | | | |
| 694 | 40 | 18 | 80 | 26 | 120 | 37 | 160 | 56 | 200 | 70 | 240 | 81 | | | | | | |
| 695 | 40 | 23 | 80 | 33 | 120 | 37 | 160 | 48 | 200 | 58 | 240 | 72 | 280 | 82 | | | | |
| 696 | 40 | 24 | 80 | 29 | 120 | 28 | 160 | 31 | 200 | 35 | 240 | 40 | 280 | 44 | | | | |
| 697 | 40 | 13 | 80 | 20 | 120 | 22 | 160 | 27 | 200 | 32 | 240 | 39 | 280 | 45 | | | | |
| 698 | 40 | 18 | 80 | 27 | 120 | 30 | 160 | 34 | 200 | 37 | 240 | 47 | 260 | 54 | 320 | 56 | | |
| 699 | 40 | 15 | 80 | 24 | 120 | 27 | 160 | 27 | 200 | 34 | 240 | 45 | 280 | 52 | 320 | 51 | | |
| 700 | 40 | 19 | 80 | 30 | 120 | 31 | 160 | 36 | 200 | 40 | 240 | 47 | 280 | 52 | 320 | 53 | | |
| 701 | 40 | 15 | 80 | 23 | 120 | 25 | | | | | | | | | | | | |
| 702 | 40 | 18 | 80 | 25 | 120 | 28 | 160 | 26 | 200 | 26 | | | | | | | | |
| 703 | 40 | 13 | 80 | 19 | 120 | 23 | | | | | | | | | | | | |
| 704 | 40 | 21 | 80 | 26 | 120 | 25 | 160 | 30 | 200 | 34 | 240 | 36 | 280 | 38 | | | | |
| 909 | 40 | 20 | | | | | | | | | | | | | | | | |
| 910 | 40 | 20 | | | | | | | | | | | | | | | | |
| 915 | 40 | 28 | 60 | 50 | 80 | 90 | | | | | | | | | | | | |
| 916 | 40 | 24 | 60 | 46 | 80 | 73 | | | | | | | | | | | | |
| 917 | 40 | 29 | 60 | 29 | 80 | 34 | | | | | | | | | | | | |
| 918 | 40 | 39 | 60 | 40 | 80 | 42 | 100 | 49 | 120 | 68 | 140 | 98 | 160 | 132 | | | | |
| 922 | 40 | 23 | 80 | 38 | 120 | 63 | 160 | 102 | | | | | | | | | | |
| 923 | 40 | 16 | 80 | 26 | 120 | 63 | 160 | 64 | 195 | 104 | | | | | | | | |
| 924 | 40 | 18 | 80 | 26 | 120 | 36 | 160 | 70 | 200 | 96 | | | | | | | | |
| 925 | 40 | 20 | 80 | 35 | 120 | 40 | 160 | 63 | 200 | 95 | 240 | 116 | | | | | | |
| 926 | 40 | 29 | 80 | 39 | 120 | 40 | 160 | 45 | 200 | 70 | 240 | 101 | | | | | | |
| 927 | 40 | 39 | 80 | 43 | 120 | 47 | 160 | 49 | 200 | 70 | 240 | 99 | 280 | 119 | | | | |
| 928 | 40 | 46 | 80 | 64 | 120 | 80 | 160 | 78 | 200 | 83 | 240 | 114 | | | | | | |
| 930 | 40 | 21 | 80 | 30 | 120 | 56 | 160 | 74 | 200 | 93 | | | | | | | | |
| 931 | 40 | 22 | 80 | 26 | 120 | 36 | 160 | 66 | 200 | 83 | | | | | | | | |
| 932 | 40 | 20 | 80 | 32 | 120 | 38 | 160 | 56 | 200 | 75 | 240 | 96 | | | | | | |
| 933 | 40 | 18 | 80 | 35 | 120 | 37 | 160 | 43 | 200 | 67 | 240 | 80 | 280 | 96 | | | | |
| 934 | 40 | 33 | 80 | 45 | 120 | 45 | 160 | 47 | 200 | 68 | 240 | 89 | 260 | 101 | | | | |
| 935 | 40 | 32 | 80 | 48 | 120 | 48 | 160 | 49 | 200 | 67 | 240 | 95 | 280 | 112 | | | | |
| 936 | 60 | 29 | 80 | 31 | 100 | 45 | 140 | 66 | 180 | 91 | | | | | | | | |
| 937 | 60 | 25 | 80 | 30 | 100 | 36 | 140 | 61 | 180 | 82 | | | | | | | | |
| 938 | 60 | 25 | 80 | 28 | 100 | 30 | 140 | 41 | 180 | 59 | 220 | 80 | | | | | | |
| 939 | 60 | 26 | 80 | 28 | 100 | 27 | 140 | 39 | 180 | 66 | 220 | 91 | | | | | | |
| 940 | 60 | 32 | 80 | 37 | 100 | 39 | 140 | 39 | 180 | 49 | 220 | 72 | 260 | 85 | 300 | 101 | | |
| 941 | 60 | 36 | 80 | 40 | 100 | 41 | 140 | 43 | 180 | 48 | 220 | 62 | 260 | 88 | | | | |
| 942 | 60 | 36 | 80 | 42 | 100 | 46 | 140 | 55 | 180 | 71 | 220 | 80 | 260 | 80 | 300 | 82 | | |
| 943 | 40 | 19 | 60 | 24 | 80 | 25 | 100 | 32 | 140 | 32 | 180 | 42 | 220 | 54 | 260 | 63 | 300 | 67 |
| 944 | 40 | 23 | 60 | 26 | 80 | 26 | 100 | 27 | 140 | 36 | 180 | 57 | 220 | 68 | 260 | 73 | 300 | 77 |
| 945 | 40 | 21 | 60 | 26 | 80 | 31 | 100 | 33 | 140 | 43 | 180 | 56 | 220 | 69 | 260 | 78 | 300 | 83 |
| 946 | 40 | 19 | 60 | 24 | 80 | 28 | 100 | 31 | 140 | 38 | 180 | 53 | 220 | 63 | 260 | 71 | 300 | 82 |
| 947 | 40 | 24 | 60 | 27 | 80 | 30 | 100 | 33 | 140 | 50 | 180 | 58 | 220 | 69 | 260 | 78 | 300 | 88 |
| 948 | 40 | 25 | 60 | 32 | 80 | 37 | 100 | 37 | 140 | 40 | 180 | 44 | 220 | 48 | 260 | 62 | 300 | 87 |
| 949 | 40 | 26 | 60 | 32 | 80 | 37 | 100 | 40 | 140 | 45 | 180 | 45 | 220 | 45 | 260 | 43 | 300 | 49 |
| 950 | 40 | 17 | 80 | 22 | 120 | 24 | 160 | 30 | 200 | 38 | 240 | 47 | 280 | 51 | 320 | 54 | | |
| 951 | 40 | 12 | 80 | 17 | 120 | 25 | 160 | 36 | 200 | 45 | 240 | 43 | 280 | 46 | 320 | 48 | | |

(Continued)　　　　　(3 of 4 sheets)

Table 3 (Concluded)

| Test | | | | | | | Coordinates of Lateral Spread of Brine, ft | | | | | | | | | |
|------|---|---|---|---|---|---|---|---|---|---|---|---|---|---|---|---|
| | x | w | x | w | x | w | x | w | x | w | x | w | x | w | x | w |
| 952 | 40 | 25 | 80 | 29 | 120 | 32 | 160 | 42 | 200 | 48 | 240 | 50 | 280 | 50 | | |
| 953 | 40 | 23 | 80 | 31 | 120 | 35 | 160 | 38 | 200 | 41 | 240 | 42 | 280 | 42 | 320 | 39 |
| 954 | 40 | 24 | 80 | 28 | 120 | 40 | 160 | 32 | 200 | 47 | 240 | 45 | 280 | 47 | 320 | 47 |
| 955 | 40 | 26 | 80 | 33 | 120 | 33 | 160 | 38 | 200 | 42 | 240 | 43 | 280 | 45 | 320 | 47 |
| 956 | 40 | 21 | 80 | 35 | 120 | 33 | 160 | 36 | 200 | 36 | 240 | 38 | 280 | 44 | 320 | 47 |
| 961 | 40 | 19 | 80 | 30 | 120 | 47 | 160 | 81 | | | | | | | | |
| 962 | 40 | 35 | 80 | 40 | 120 | 40 | 160 | 43 | | | | | | | | |
| 963 | 40 | 16 | 80 | 25 | 120 | 40 | 160 | 60 | 200 | 73 | | | | | | |
| 964 | 40 | 23 | 80 | 31 | 120 | 35 | 160 | 43 | 200 | 63 | 240 | 82 | | | | |
| 965 | 40 | 25 | 80 | 31 | 120 | 37 | 160 | 45 | 200 | 49 | 240 | 53 | 280 | 52 | | |
| 966 | 40 | 29 | 80 | 41 | 120 | 56 | 160 | 67 | 200 | 73 | 240 | 77 | 280 | 76 | | |
| 967 | 40 | 16 | 80 | 25 | 120 | 34 | 160 | 42 | 200 | 46 | | | | | | |
| 968 | 40 | 20 | 80 | 28 | 120 | 41 | 160 | 42 | 200 | 45 | 240 | 51 | | | | |
| 969 | 40 | 22 | 80 | 27 | 120 | 28 | 160 | 33 | 200 | 40 | 240 | 51 | | | | |
| 970 | 40 | 18 | 80 | 34 | 120 | 40 | 160 | 40 | 200 | 43 | 240 | 50 | 280 | 55 | | |
| 971 | 40 | 13 | 80 | 19 | 120 | 23 | 160 | 30 | | | | | | | | |
| 972 | 40 | 21 | 80 | 26 | 120 | 29 | 160 | 28 | 200 | 34 | 240 | 40 | 280 | 45 | | |
| 973 | 40 | 24 | 80 | 25 | 120 | 32 | 160 | 34 | 200 | 40 | 240 | 45 | 280 | 50 | 320 | 53 |
| 974 | 40 | 20 | 80 | 24 | 180 | 27 | 160 | 34 | 200 | 48 | 240 | 57 | 280 | 54 | | |
| 975 | 40 | 18 | 80 | 22 | 120 | 25 | 160 | 35 | 200 | 39 | 240 | 42 | 280 | 41 | | |
| 976 | 40 | 19 | 80 | 25 | 120 | 29 | 160 | 38 | 200 | 39 | 240 | 41 | 280 | 42 | | |
| 977 | 40 | 17 | 80 | 22 | 120 | 24 | 160 | 29 | 200 | 31 | 240 | 37 | 280 | 42 | | |
| 978 | 40 | 19 | 80 | 24 | 120 | 30 | 160 | 33 | 200 | 43 | 240 | 65 | 280 | 70 | | |
| 979 | 40 | 22 | 80 | 28 | 120 | 28 | 160 | 30 | 200 | 36 | 240 | 50 | 280 | 53 | 320 | 55 |

(4 of 4 sheets)

# APPENDIX A: NOTATION

$A_o$     Cross-sectional area of outfall, $ft^2$

$A_p$     Cross-sectional area of port, $ft^2$

$B$     Dimensionless intercept

$B_{T_2}$     Calibration intercept at temperature $T_2$ , g/cc

$B_{T_3}$     Calibration intercept at temperature $T_3$ , g/cc

$C$     Dimensionless coefficient

$C_o$     Conductivity meter voltage for a salt solution, mv

$D$     Outfall diameter, ft or in.

$D_o$     Port diameter, ft or in.

$\mathbb{F}_D$     Densimetric port Froude number, $V_o / \sqrt{\dfrac{\Delta \rho_m}{\rho_f} g D_o}$

$g$     Gravitational acceleration, $ft/sec^2$

$H$     Ambient flow depth, ft

$Q_b$     Brine discharge, cfs

$R$     Exponent, see equation 9

$\mathbb{R}_c$     Channel Reynolds number

$\mathbb{R}_p$     Port Reynolds number

$T$     Temperature, C

$T_a, T_b$     Temperatures of brine solutions, C

$T_1$     Temperature when solution densities are checked, C

$T_2$     Temperature when probes are calibrated, C

$T_3$     Temperature at which data are taken, C

$U$     Ambient flow velocity, fps

$V_o$     Average port velocity, fps

$w$     Plume width, ft

$w_o$     Total plume width at $x_o$ , ft

$x$     Distance downstream from port center line, ft

$x_o$     Downstream distance from port at which plume falls to bottom, ft

$y$     Distance parallel to diffuser in reference to center of a given port, ft

$z$     Elevation above bottom, ft

| | |
|---|---|
| $Z_m$ | Maximum height of upper boundary of jet above bottom, ft |
| $\Delta\rho$ | Far-field effluent density minus ambient fluid density, g/cc |
| $\Delta\rho_m$ | Initial effluent density minus ambient fluid density, g/cc |
| $\epsilon$ | $\Delta\rho_m/\Delta\rho$ = dilution |
| $\epsilon_m$ | Minimum observed dilution |
| $\nu$ | Kinematic viscosity of water, $ft^2/sec$ |
| $\rho$ | Density, g/cc |
| $\rho_a, \rho_b$ | Densities of brine solutions, g/cc |
| $\rho_f$ | Ambient fluid density, g/cc |
| $\rho_{s1}$ | Solution density at temperature $T_1$ , g/cc |
| $\rho_{s2}$ | Solution density at temperature $T_2$ , g/cc |
| $\rho_1, \rho_2, \rho_3$ | Densities of distilled water at temperatures $T_1, T_2, T_3$ , g/cc |
| $\emptyset$ | Indicates functional relation |
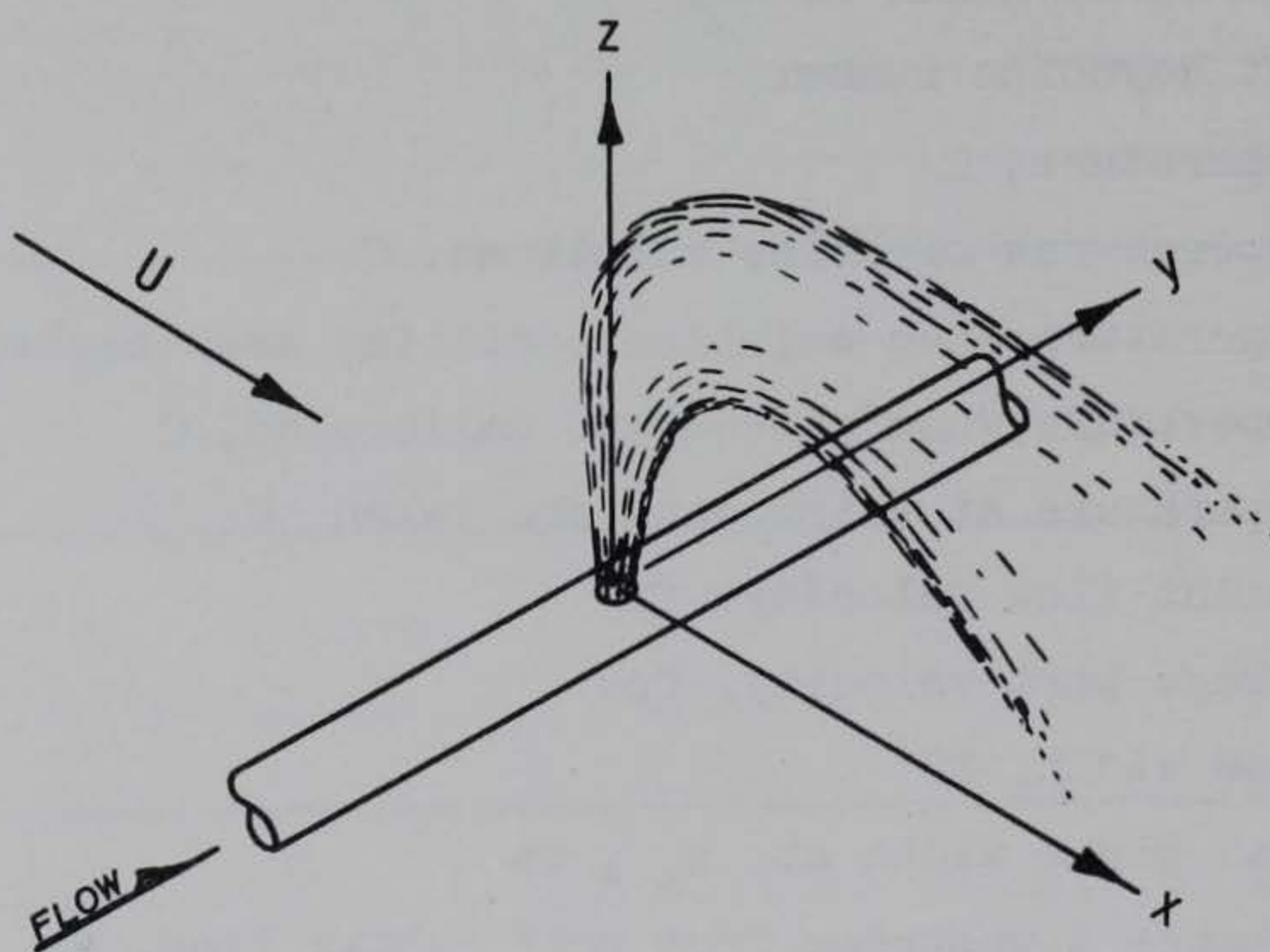


Definition of coordinate system

# APPENDIX B:  CONDUCTIVITY PROBE CALIBRATION AND DATA REDUCTION

Density is assumed to vary as a function of temperature and salinity only, and conductivity is assumed to vary only with salinity over the small range of temperatures encountered in the testing.  At a given temperature, density varies linearly with conductivity (salinity); and at a different temperature, the linear variation has the same slope but is displaced by the difference in the density of distilled water at the two temperatures. An equivalent statement is that the nonlinear temperature-density relation for distilled water is linearly displaced upward by small changes in density due to salinity.  Fig. B1 illustrates these relations.

In practice, the temperature of the calibrating solutions differed from one to another; the temperature at which the solutions were checked for density was different from that at which the probes were calibrated; and temperatures during actual testing were still different.  In a FORTRAN program written to reduce the calibrations and compute dilutions, the following equation for the density of distilled water is used to make temperature adjustments:[6*]

$$\rho = 1 - \left[ \frac{(T - 3.9863)^2}{508,929.2} \cdot \frac{T + 288.9414}{T + 68.12963} \right] \tag{B1}$$

where

$\rho$ = density, g/cc

$T$ = temperature, C

Letting

$\rho_{s1}$ = solution density at temperature $T_1$

$\rho_{s2}$ = solution density at temperature $T_2$

$\rho_1$ = density of distilled water at temperature $T_1$

$\rho_2$ = density of distilled water at temperature $T_2$

$T_1$ = temperature when solution densities are checked

$T_2$ = temperature when probes are calibrated

the solution densities are converted to density at the calibration temperature by the following equation:

---

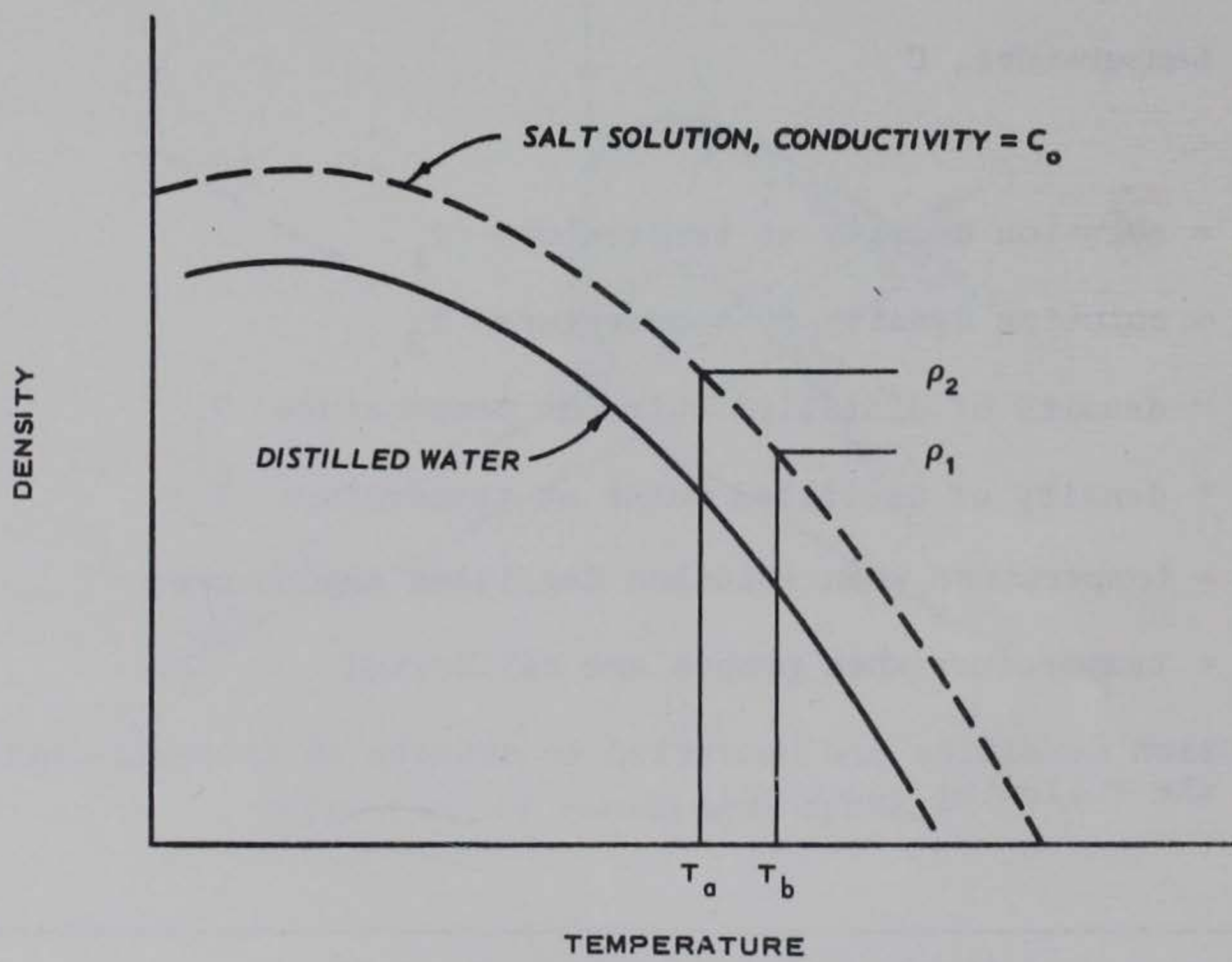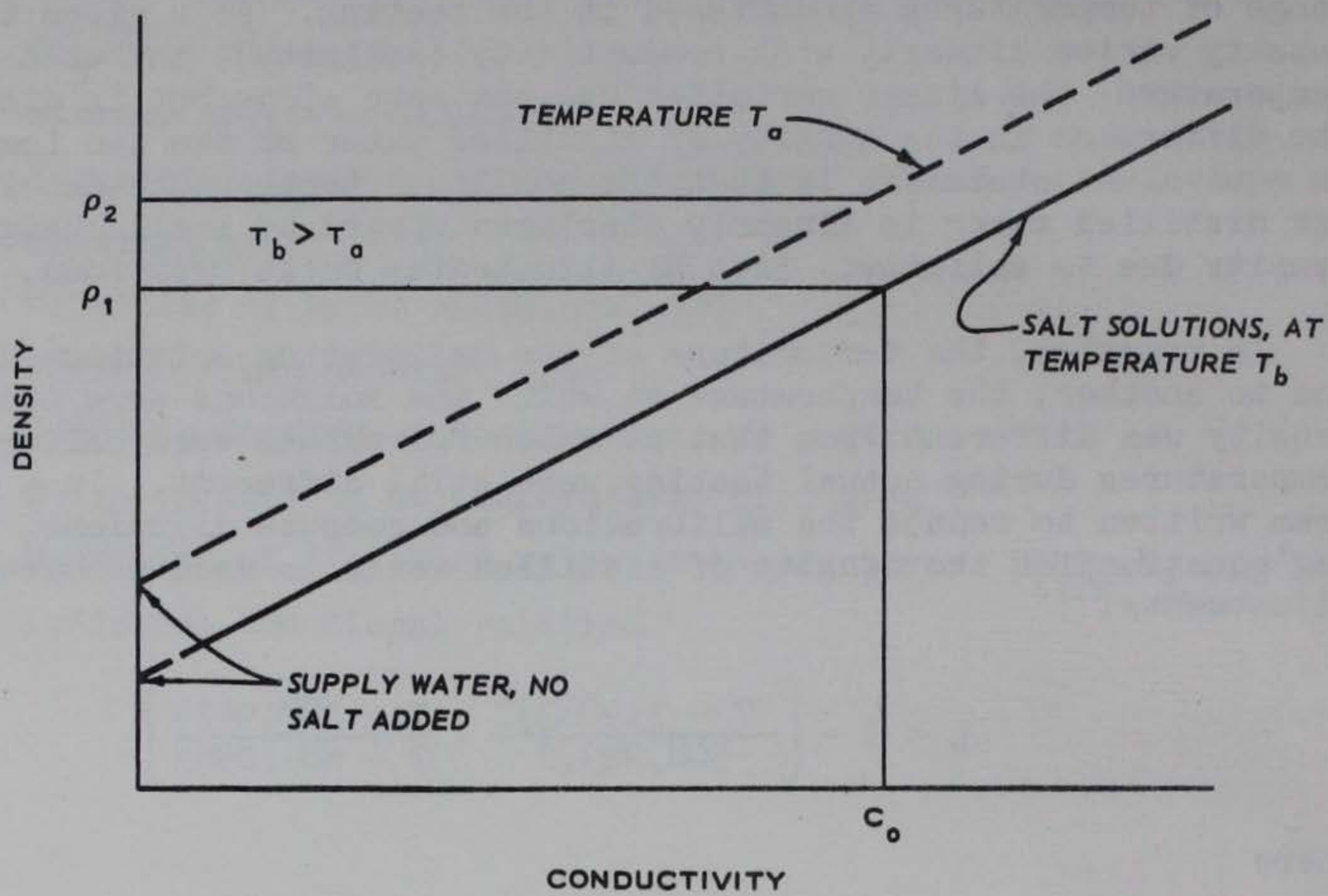*  See Literature Cited at end of main text, p 38.

Fig. Bl. Conductivity-temperature-density relations

$$\rho_{s2} = \rho_{s1} + (\rho_1 - \rho_2) \tag{B2}$$

At the calibration temperature $T_2$, linear calibrations of density versus conductivity can be constructed for each probe. A least-squares slope is computed and the intercept calculated by forcing the calibration to pass through the first calibration point, which in practice was "fresh" water; this procedure was necessary to ensure that calibration error was minimized at the sensitive lower ranges of conductivity. These intercepts, representing the density of water having zero conductivity (but denser than distilled water due to suspended solids, etc.), are functions only of temperature. Thus the calibrations of temperature $T_2$ are adjusted to temperature $T_3$ by

$$B_{T_3} = B_{T_2} + (\rho_2 - \rho_3) \tag{B3}$$

where

$B_{T_2}$ = calibration intercept at temperature $T_2$

$B_{T_3}$ = calibration intercept at temperature $T_3$

$\rho_3$ = density of distilled water at temperature $T_3$

$T_3$ = temperature at which data are taken

In reducing the raw data, the FORTRAN program first processes the calibration data as described above to yield basic linear calibrations. The raw data input consists of grouped conductivities and temperatures, along with a "background" conductivity that represents the approximate fresh-water conductivity during the test for each probe. Although the density of the background remains essentially constant at a given temperature, its conductivity may shift slightly from its calibration value due to small changes in background salinity. Therefore, each conductivity reading is slightly adjusted by an amount equal to the background shift between the time of calibration and time of test so that calibrations are continuously updated.

For a given data point, the calibration for that probe is shifted to the data temperature $T_3$, and a density is computed. In computing dilution, the initial density difference $\Delta\rho_m$ is calculated from hydrometer readings for the brine and ambient fluid, adjusted to the same temperature. The diluted density difference $\Delta\rho$ is the difference between the density as computed from the temperature-conductivity data and the density of the ambient fluid, adjusted to the data temperature. Dilution is then calculated by

$$\epsilon = \frac{\Delta\rho_m}{\Delta\rho} \tag{B4}$$